UPPER LIMB MOVEMENT IN VIRTUAL AND REAL-WORLD ENVIRONMENTS

by

KATHERINE ANNE SPITZLEY

A DISSERTATION

Presented to the Department of Human Physiology
and the Division of Graduate Studies of the University of Oregon
in partial fulfillment of the requirements
for the degree of
Doctor of Philosophy

September 2023

DISSERTATION APPROVAL PAGE

Student: Katherine Anne Spitzley

Title: Upper Limb Movement in Virtual and Real-World Environments

This dissertation has been accepted and approved in partial fulfillment of the requirements for the Doctor of Philosophy degree in the Department of Human Physiology by:

Andrew Karduna, PhD	Chairperson
Michael Hahn, PhD	Core Member
Michelle Marneweck, PhD	Core Member
Paul Dassonville, PhD	Institutional Representative

and

Krista Chronister	Vice Provost for Graduate Studies

Original approval signatures are on file with the University of Oregon Division of Graduate Studies.

Degree awarded September 2023

DISSERTATION ABSTRACT

Katherine A. Spitzley

Doctor of Philosophy

Department of Human Physiology

September 2023

Title: Upper Limb Movement in Virtual and Real-World Environments

In recent years, virtual reality (VR) systems have experienced significant technological advancements, resulting in increased accessibility and improved product quality. Early VR systems were limited by low visual quality, large size, and high cost, but advancements in technology have propelled VR into the mainstream. As VR becomes increasingly prevalent, it is vital to understand its effects on the human sensorimotor system, particularly with vulnerable populations. The upper limb is within the field of view of current VR headsets and is the main point of contact between the user and virtual environment. It is therefore an essential component of the relationship between user and system.

This dissertation is organized into five sections, each contributing to the overarching objective of understanding upper limb movement in real and virtual environments. Chapter I serves as an introduction, providing essential background information and an overview of subsequent chapters. Chapters II and III are dedicated to validating the HTC VIVE tracker as a tool for collecting both static and dynamic data. This establishes the foundation for subsequent studies, which use the tracker to estimate body segment position and orientation. Chapter IV investigates the impact of visuoproprioceptive congruency on upper limb joint position matching within a VR

environment, highlighting the pivotal role of vision in the planning and execution of movements. Continuing the exploration of upper limb movements, Chapter V identifies kinematic and kinetic disparities between visually guided reaching movements conducted in VR and the real world (RW). Building upon the findings from Chapter V, Chapter VI investigates the translation of these differences when individuals switch between VR and RW environments. Collectively, these studies contribute to the broader knowledge base of motor control, informing the design and implementation of effective protocols and applications in both real and virtual settings.

This dissertation includes previously published and unpublished co-authored material.

CURRICULUM VITAE

NAME OF AUTHOR: Katherine A. Spitzley

GRADUATE AND UNDERGRADUATE SCHOOLS ATTENDED:

University of Oregon, Eugene, OR
California State University Long Beach, Long Beach, CA

DEGREES AWARDED:

Doctor of Philosophy, Human Physiology, 2023, University of Oregon, Eugene
Master of Science, Human Physiology, 2019, University of Oregon, Eugene
Bachelor of Science, Kinesiology, 2016, California State University Long Beach

AREAS OF SPECIAL INTEREST:

Virtual reality
Sensorimotor processing
Upper limb movement

PROFESSIONAL EXPERIENCE:

Director, Slocum Research and Education Foundation, Slocum Orthopedics, 2023-present

Grant Writing and Project Management Consultant, MPTX Inc., 2021-present

Graduate Research Assistant, University of Oregon, Department of Human Physiology, Orthopaedic Biomechanics Lab, 2016-2022

Graduate Teaching Assistant, University of Oregon, Department of Human Physiology, 2016-2022

Teaching Associate, CSU Long Beach, Department of Kinesiology, 2016

Laboratory Assistant, CSU Long Beach, Department of Kinesiology, Movement Science Lab, 2015-2016

GRANTS, AWARDS, AND HONORS:

Graduate Teaching Award, Department of Human Physiology, University of Oregon, 2022

Betty Foster McCue Scholarship, University of Oregon, 2021

Dissertation Research Fellowship, Graduate School, University of Oregon, 2020

Eugene and Clarissa Evonuk Memorial Graduate Fellowship, 2020

Hill Fund Gradaute Award, College of Arts and Sciences, University of Oregon, 2020

Harvey E Lee Graduate Scholarship, University of Oregon, 2020

De Luca Foundation Summer Research Award, Delsys Inc., 2020

Microsoft MR Academic Seeding Program, Microsoft Corporation, 2020

Ursula Moshburger Endowed Scholarship, Department of Human Physiology, University of Oregon, 2019 & 2020

Research and Travel Award, Graduate School, University of Oregon, 2019

Johnston Schlsp Scholarship, University of Oregon, 2018

Peter O'Day Fellowship in Biological Sciences, "The Effect of Hand Dominance on Propriocepive Response to Changes in Visual Stimuli", University of Oregon, 2018

Student Presentation Award, International Shoulder Group, International Society of Biomechanics, 2018

CSU Program for Education and Research in Biotechnology, "Pilates as an Osteogenic Exercise", CSU Long Beach, 2016

Student Research Funding, "Joint and Bone Loading when Jumping on a Pilates Reformer", Associated Students Inc., CSU Long Beach, 2016

PUBLICATIONS:

Spitzley, K., Karduna, A., Feasibility of using a fully immersive virtual reality system for kinematic data collection. J. Biomech. 2019. 87, 172–176

Spitzley, K., Karduna, A. (2021): Joint position sense accuracy is influenced by visuoproprioceptive congruency in virtual reality. Journal of Motor Behavior, DOI: 10.1080/00222895.2021.1916425

ACKNOWLEDGMENTS

Thank you to my advisor and friend Dr. Andy Karduna for providing guidance in innumerable categories. Your patience, enthusiasm, and flexibility make you the epitome of leading by example and creating an easy and enjoyable working environment, you have contributed more to my life over the last seven years than I could have hoped for. Dr. Mike Hahn, thank you for always being open to a chat, your smiling face and honesty give me something to look forward to and rely upon. Dr. Michelle Marneweck, thank you for jumping right on board with your interest and support for this project. Dr. Paul Dassonville, thank you for your insights as this project pivoted multiple, multiple times. Dr. Adrianne Huxtable, thank you for being an open and willing mentor, your feedback and guidance has given me direction and improved my technical expertise immensely. Dr. Jim Becker, thank you for seeing my value as a scientist and spending the last 10 years convincing others of the same. My life would be markedly different without your encouragement and trust.

Thank you to all the members of the Orthopaedic Biomechanics Lab over the years. To all those who came before me, thank you for setting me up for success by creating an excellent scientific and social foundation in the lab. Dr. Jennie Cooper, thank you for stimulating me intellectually in ways that exceeded a graduate curriculum and for making me laugh every day. Zach Hoffman, Sam Perlman, Taylor Brewster, Riley Huntington, Kasra Mirarabshahi, Kieley Trempy and all the undergraduate research assistants throughout the years, thank you for making this work possible and being kind, patient, and supportive individuals throughout. Motoki Sakurai and Taylor Wilson, thank

you for bringing life and happiness back to the lab after a long lockdown lull. I am almost sad to be leaving now with such a wonderful team in the lab! Take care of Andy.

Most of all, thank you to my family. Ben, thank you for consistently showing me that passions are as important as professions. Mom, thank you for teaching me how to listen and take extremely diligent notes. Dad, thank you for teaching me how to ask questions and solve problems on my own using creative strategies of (over) engineering. Michael, thank you for being my sounding board, editor, advisor, cheering section, and source of fun and lightheartedness throughout our years in school together. It is very fun and inspiring to have a live-in example of how one can excel in their professional and personal lives while exuding humility, grace, and kindness toward the world. You are an amazing scientist and human being. Thank you each for your encouragement and enthusiasm. Having a loving and reliable family to turn to in happiness and sadness is the most valuable gift in the world.

Lastly, I would like to acknowledge funding support from the Department of Human Physiology, the College of Arts and Sciences, University of Oregon, Eugene and Clarissa Evonuk, Microsoft Corporation, and the De Luca Foundation which contributed to the completion of this work.

This work is dedicated to my family.

TABLE OF CONTENTS

Chapter Page

LIST OF FIGURES

LIST OF TABLES

Table Page

CHAPTER I

GENERAL INTRODUCTION

1. Background

1.1 Virtual Reality Systems

Since the ideation of virtual spaces, the objective has been to create a sensory experience that parallels the fidelity of the real world. Room-scale projectors, glasses, headsets, audio immersion, and sensor-containing suits have each been used to advance this goal. To date, the level of immersion has been scaled into three main categories: 1) virtual reality (VR) where the user is fully immersed in the virtual experience, 2) mixed reality (MR) where the user experiences a combination of virtual and real-world inputs, and 3) augmented reality (AR) where the user experiences the real-world through a lens which can overlay additional information. Together these experiences are referred to as extended realities (XR).

In recent years, VR, MR, and AR systems have undergone substantial technological updates and reductions in cost. The result has been a proliferation of these systems throughout many industries including military, clinical, scientific, and education (Wohlgenannt et al., 2020). Of these, VR has seen the widest expansion. This is reflected in VR global markets projections of an increase from USD 7.3 billion in 2018 to USD 120.5 billion in 2026 (Wohlgenannt et al., 2020). The uptick in consumption parallels a leap in access and product quality. Though VR was first developed by Ivan Sutherland in the 1960s (**Fig. 1.1**), the low quality of visual information, prohibitive size, and high cost of these systems limited their use cases (Sutherland, 1968). It was not until the 2010s that

companies including HTC VIVE, Oculus, and PlayStation released systems that were portable, inexpensive, and high enough fidelity of information to break into the mainstream.

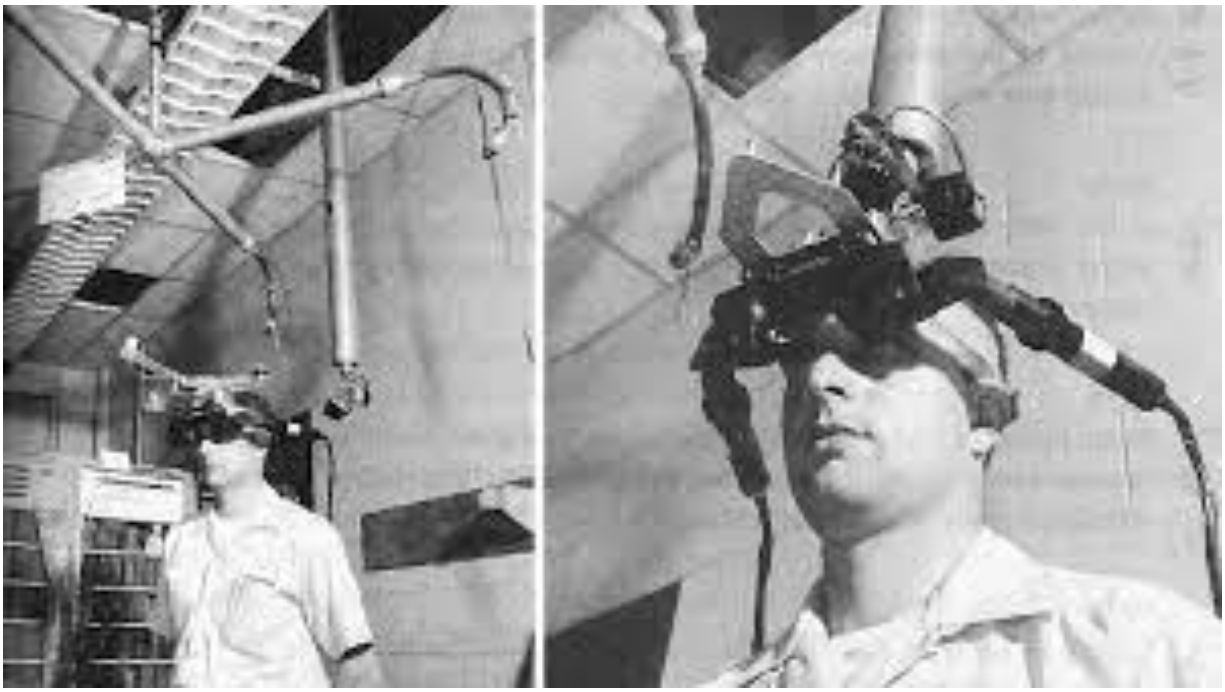

Figure 1.1. Figures 3 and 4 from Ivan Sutherland's A head-mounted three-dimensional display. This apparatus, named The Sword of Damocles was developed by Ivan Sutherland in 1968 and is largely regarded as the first virtual reality system (Sutherland, 1968).

Key results from the recent technological updates in virtual spaces are the decrease or elimination of sensory conflict-related illness along with an increase in presence, interactivity, and immersion for the user (Cipresso et al., 2018; Harris et al., 2020; Wohlgenannt et al., 2020). Each of these improvements moves the user further toward experiencing a seamless replication of real-world sensory experiences. The largest steps toward this goal have been improvements in the fidelity of visual information and the comfort and portability of wearable devices. The most sophisticated systems available to the public in the year 2023 consist of a lightweight stand-alone headset that can

perform hand tracking without the need for a controller. While the markerless tracking technology and storage capacity of these systems leave room for improvement, this is a huge leap from the room-scale systems that require multiple cameras and on-body sensors to perform at a similar level (Cruz-Neira et al., 1992). Therefore, it is not surprising in the least that use cases and consumption of these systems have skyrocketed in parallel.

1.2 Perceiving the Virtual and Real-Worlds

Even with the advances in VR technology, differences between virtual and real worlds exist in many forms and to varying degrees. In the visual space, differences such as objects disobeying laws of physics or the natural world showing unrealistic color (ex. a pink sky) are blatantly noticeable to the user and likely to affect the way that they interact with the virtual world (Cortes et al., 2018; Wright, 2014). These are obvious disruptions to the user's expectation of a 'normal' sensory experience and are easily manipulatable by the developer of the virtual environment. Possibly even more impactful than differences between external worlds, are observations that the user is making about their own form. Growing evidence shows that embodiment, or the parallels that the user perceives between their body and the form that they take within the virtual world, is essential to performance within the virtual space (Bourdin et al., 2019; Kilteni et al., 2012; Nierula et al., 2019). Even if every effort is taken to eliminate obvious differences between internal and external environments and parallel the real world perfectly, there are innate differences that cannot be overcome with current technology.

Because the virtual world is created digitally and transmitted to the user though screens, headphones, and other electronic devices, the fidelity of this world will inevitably be restricted by the technical specifications of the equipment it is delivered through. Specifications such as equipment weight, frame rates, pixel-aspect ratios, frequency response spectrums, and force feedback may influence the user's perception of the sensory experience. While many of these specifications also exist within the organic sensory systems and central nervous system of the user, they are at the same time highly adaptable, and the user is highly adapted to them (Ernst and Banks, 2002; Helms Tillery and Sainburg, 2012; Van Der Kooij et al., 2013; Wolpert et al., 2011). Using external, digital technology to provide sensory information imposes a level of novelty to the nervous system that must be overcome or adapted to.

Novelty in the nervous system is generally met with greater demand from the system and a redirection of information processing (Wenk et al., 2021). Due in part to altered requirements, these processes are slower, more energy consuming, and require a larger proportion of available attention to complete. For example, a simplified explanation of visual processing describes two streams of visual information through the brain, one for object identification and one for contextualization (Shomstein, 2012). When a visual stimulus is well known to the user, they can draw from a large experiential repository for both identification and contextualization. However, if a visual stimulus is either unknown to the user or is behaving in an unexpected way, past experiences provide less useful information for these functions (Bruno et al., 2008). In this case, more effort is required to identify and contextualize the visual information. Another novelty is the stereoscopic presentation of visual depth cues in VR. Depth perception relies on a

number of monocular and binocular visual cues, and the disruption or disagreement within these cues may lead users to process the signals differently in virtual and naturalistic environments (Goodale and Westwood, 2004; Harris et al., 2019; Verhoef et al., 2016).

1.3 Sensory Integration for Movement Control

The capture and processing of sensory information is critical in our ability to respond to external environments. To use sensory information for movement control, the neurological system must successfully collect, encode, translate, and integrate this information into a model that can be deployed by the motor system. This entire process must take place within a time course suitable for an effective movement response to the stimulus at hand. The result of the movement must be accurate enough to allow continued completion of activities of daily living. Given these constraints, it is unsurprising that a highly optimized sensory processing system has evolved to handle the translation of sensory input to motor output. In a fully intact system, visual and proprioceptive sensory signals are heavily relied upon to generate movement responses to environmental cues.

Visual information is taken in through the retina, travels through the optic nerve, and is projected across the brain for integration and interpretation. Continuous gathering of smooth visual information regarding self and the environment requires that our focal field is able to both change rapidly and fixate on targets. Saccadic eye movement allows for these actions and is essential to the visual control system (Goodale, 2011; Wurtz, 1996). Optic configuration also plays a role in successful movement control. As many elements of goal directed movement rely on cues of distance and location with respect to

self, binocular vision is important to movement control. The absence of binocular information results in slower movement times, longer movement decelerations, increased necessary online movement adjustments, and decreased movement accuracy than when binocular cues are available (Goodale, 2011). Together, saccadic eye movements and binocular visual cues enable the system to gather sufficient visual information for movement control.

Proprioceptive information is collected in the periphery by receptors in the skin, joints, tendons, and muscles (Enoka, 2002; Matthews, 1982; Proske and Gandevia, 2012; Riemann and Lephart, 2002a). This information is delivered to the spinal cord via afferent neurons, travels up the cord through the dorsal columns, and is projected on to the cortex and thalamus for further distribution and integration (Jankowska, 1992; Johansson and Silfvenius, 1977; Landgren and Silfvenius, 1971; Riemann and Lephart, 2002a; Wall and Noordenbos, 1977). Collectively, this information provides the central nervous system with insight about joint kinematics (Proske and Gandevia, 2012, 2009) and possible changes to the internal and external environment (Enoka, 2002), ultimately informing both feedforward and feedback control of motion (Riemann and Lephart, 2002b).

The combination of afferent information from multiple sensory inputs relies on multimodal sensory cells. These cells exhibit increased activity with a single input, and either amplified or decreased activity with the introduction of each subsequent input (Jiang et al., 2001; Meredith and Stein, 1986; Stein et al., 2009). The magnitude of this response is directly proportional to stimulus intensity in a unimodal stimulus and inversely proportional in a multimodal stimulus (Meredith and Stein, 1986; Stein et al.,

2009). Further, response frequency increases when multimodal inputs are in spatial agreement and decreases when they are in spatial disagreement (Jiang et al., 2001; Stein et al., 2009, 2002). Through these mechanisms, integration occurs in the brain through the tuning of response intensity and frequency of individual multisensory cells. This integrated information is then used to generate a response to the stimulus. Averaging and prior knowledge can be used to either select and update a movement plan or modify how the sensory information is interpreted to generate an appropriate response (Faisal et al., 2008; Van Der Kooij et al., 2013).

Frequently, averaging and prior knowledge are used in tandem to develop a weighted average wherein the weight attributed to each source of sensory information is dependent on its statistical variance (Block and Bastian, 2011, 2010; Faisal et al., 2008; van Beers et al., 1999). Reweighting can occur in response to a change in fidelity of the input, spatial disagreement between incoming information, or a conscious effort to increase reliance on a particular sensory cue (Block and Bastian, 2010; Van Der Kooij et al., 2013). This is modeled mathematically through the maximum likelihood principle, which states that the signal with the least statistical variability will be most heavily weighted (Ernst and Banks, 2002). An independent but highly related process of sensory realignment, in which the sensory system changes its mapping of one sensory input in relation to another, may occur after sensory reweighting (Block and Bastian, 2011). Generally, the lower weighted sensory input is realigned in this process, however this is not always the case, suggesting that input from prior experiences and contextual cues may be important in this process (Block and Bastian, 2011). The processes of reweighting and realignment each rely on inflow of sensory feedback into the system

(Harris and Wolpert, 1998). The differences between these processes are apparent when examining movement trajectories in sighted, blindfolded, and congenitally blind participants during targeted reaching movements. The reweighting of information in a blindfolded condition assists in but does not fully correct for, the sensory deficit, wherein a realignment in the congenitally blind population enables performance on par with a sighted population (Sergio and Scott, 1998). These mechanisms enable us to respond to sensory information, even if it is faulty, noisy, or inconsistent with prior experiences.

1.4 Summary

Virtual reality and other XR technologies have come a long way in their technical capabilities, price point, and usability in the past 55 years. A large rise has already begun, and will undoubtedly continue, in the use of these systems across multiple fields. The control that XR provides over a user's sensory experience is a valuable skill and resource to be harnessed for the scientific and clinical communities. Before bringing these systems in to settings with vulnerable populations, it is essential to understand if and how they affect the human sensorimotor system. This system is well tuned to perform many important activities of daily living and is at the same time adaptable and trainable under the right circumstances. Sensory cues are a very important component of the human ability to intake and respond to their surroundings, and the artificial presentation of those cues through screens and headphones may have unanticipated results. It is therefore essential to interrogate motor output in virtual environments. This dissertation is specifically interested in upper limb movement, as the upper limb is well within the field

of view of most modern headsets and is used as the primary point of contact between the user and virtual environment.

2. Aims and Overview

This dissertation is composed of seven (VII) chapters. Chapters II – VI discuss primary research studies and are written in journal format. Chapters I provides introductory material to the topics of virtual reality spaces and their interactions with the human sensory system, while chapter VII summarizes main findings from chapters II-VI. Bridge sections are included to link the content between chapters.

Chapters II and III aim to determine if commercially available virtual reality (VR) systems have the potential to be effective tools for simultaneous sensory manipulation and kinematic data collection. Both chapters were co-authored by Kate A. Spitzley and Andrew R. Karduna and are written in the style of a *Journal of Biomechanics* short communication. The study design, experimental work including data collection and analysis, and writing was performed by Kate A. Spitzley, Andrew R. Karduna provided research mentorship and editorial assistance. Chapter II was previously published in the *Journal of Biomechanics* under the title Feasibility of Using a Fully Immersive Virtual Reality System for Kinematic Data Collection.

Chapter IV aims to understand the importance of the weighted integration of visual and proprioceptive information in movement planning and execution using a VR environment. This chapter was co-authored by Kate A. Spitzley and Andrew R. Karduna and previously published in the *Journal of Motor Behavior* under the title Joint Position Accuracy is Influenced by Visuoproprioceptive Congruency in Virtual Reality. The study

design, experimental work including data collection and analysis, and writing was performed by Kate A. Spitzley, Andrew R. Karduna provided research mentorship and editorial assistance.

Chapters V and VI aim to elucidate the effect of VR environments on upper limb movements, and how those effects translate between real and virtual spaces. These chapters were co-authored by Kate A. Spitzley, Zachary A. Hoffman, Samuel E. Perlman, and Andrew R. Karduna. Kate A. Spitzley contributed to study design, experimental work including data collection and analysis, and writing. Zachary A. Hoffman and Samuel E. Perlman contributed to study design and data collection. Andrew R. Karduna contributed to study design, research mentorship, and editorial assistance.

CHAPTER II

FEASIBILITY OF USING A FULLY IMMERSIVE VIRTUAL REALITY SYSTEM FOR KINEMATIC DATA COLLECTION

This work was published in volume 87 of the *Journal of Biomechanics* in April 2019 as "Feasibility of Using a Fully Immersive Virtual Reality System for Kinematic Data Collection" and is co-authored by Kate A. Spitzley and Andrew R. Karduna. The study design, experimental work including data collection and analysis, and writing was performed by Kate A. Spitzley, Andrew R. Karduna provided research mentorship and editorial assistance.

1. Introduction

Recent advances in Virtual Reality (VR) technology have expanded our ability to integrate immersive 3D visual environments with optical motion capture. Platforms such as Vicon Reality and OptiTrack for VR have combined their marker-based systems with VR headsets and controllers to augment both the VR experience and research capabilities (Vicon.com, Optitrack.com, 2018). However, these systems still require the use of research-grade motion capture cameras to collect kinematic data. Although research-grade systems provide robust measures of position and orientation, there are limitations due to their high price and low portability. While these may not be barriers for more established institutions, those working in underfunded programs, teaching institutions, classroom settings, and clinics may find them restrictive. The use of a VR system for simultaneous immersion in 3D virtual environments and kinematic data collection could

provide the benefits of these integrated systems, the low price point of VR systems, and high portability that existing systems cannot offer.

The HTC VIVE Virtual Reality System (VIVE) and Oculus Rift systems are both prime candidates for this application as they are each available for under $1000 and extremely portable. However, the tracked area for the VIVE is about 5 m x 5 m while the tracked area for the Rift is about 1.5 m x 1.5 m, making the VIVE a more suitable option for kinematic data collection (Martindale, 2018). The VIVE system consists of two small light-emitting boxes (9 cm x 9 cm x 6 cm), two lightweight handheld controllers (0.31 kg), a round tracker (0.36 kg), and a lightweight fully immersive headset (0.47 kg). The shipping weight for this entire system is under 2 kg. The position and orientation of the tracker, headset, and controllers are tracked in real time, allowing for realistic motion feedback into the virtual visual environment.

The goal of this study was to determine the accuracy of the VIVE handheld controller and tracker, two different configurations of VIVE sensors, in comparison to an industry gold standard motion capture system, the Polhemus Liberty (Liberty) magnetic tracking system. This system has been used extensively in basic and clinical research settings (Amasay and Karduna, 2013; Kahol et al., 2009, 2008; Kwon et al., 2012). The manufacturer reported static accuracy of this system is 0.15° and 0.76 mm, and independent validation studies have corroborated these claims, showing root mean square (RMS) values as low as 0.2 mm (Nafis et al., 2006; Polhemus, 2012). This system was chosen for comparison due to its' high reported accuracy and frequent use for collecting kinematic data (Amasay and Karduna, 2013; Dadarlat et al., 2015; Kahol et al., 2009; Lin and Karduna, 2016; Nafis et al., 2006; Polhemus, 2012). Measures of static drift in

position and orientation, static translation, and static rotation were compared between the VIVE controller and the Liberty sensor and the VIVE tracker and the Liberty sensor. Feasibility of using the VIVE sensors for kinematic data collection was determined by their accuracy when compared to the Liberty sensor.

2. Methods

2.1 System Setup

The VIVE VR system was set up as detailed by the user's manual in order to establish proper tracking of the sensors. The lighthouses were set 6 m apart, mounted directly to the laboratory wall at a height of 2.1 m, angled downward at an angle of 30°, and connected by a synchronization cable ("htc VIVE User Guide," 2016). The VIVE headset was located on a stable, flat platform within the tracked space. The system's room setup protocol was run before each data collection session. This protocol establishes the location of the floor and the play area (the area in which the sensors will be tracked). The Liberty magnetic tracking system (Polheums, Colchester, VT) was set up according to the user's manual and best practices (Polhemus, 2012). The Liberty transmitter was placed approximately 0.5 m from the sensor and metal was cleared from the space to eliminate interference (**Fig. 2.1**).

2.2 Experimental Protocol

The VIVE sensor (tracker or controller) was mounted to a rigid segment opposite a sensor from the Liberty magnetic tracking system; the segment was then mounted to a ball-and-socket fixture, which was set on a linear gear track. This setup allowed for 360° of rotation about three axes and 61 cm of translation along three axes.

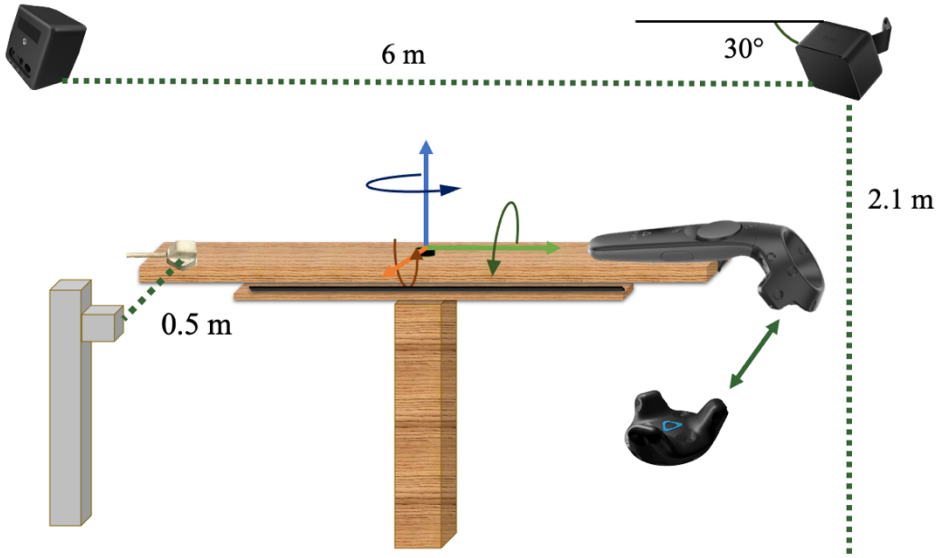

Fig. 2.1. HTC VIVE lighthouse boxes mounted 2.1 m high, 6 m apart, tilted downward by 30°, as suggested in the user guide. Polhemus Liberty base station positioned 0.5 m from the tracker. VIVE and Liberty sensors mounted to opposite ends of a rigid segment with six degrees of freedom. Graphics not to scale.

The segment holding both sensors was moved through fifty rotations about each axis and fifty translations along each axis of the respective sensor (**Fig. 2.2**). In total, 300 ten-second samples were collected while the segment was held static at each increment of motion. Increments ranged from 0 – 50° and 0 – 30 cm. All tests were completed first with the VIVE controller and Liberty sensor, then with the VIVE tracker and Liberty sensor. Testing order was chosen at random. The rig holding the sensors was stationed in the center of the VIVE system's tracked space. Both systems sampled at a rate of 120 Hz. Data were collected simultaneously from the sensors using a custom Unity program (Unity Technologies, San Francisco, CA, USA) and analyzed using a custom LabVIEW program (National Instruments, Austin, TX, USA).

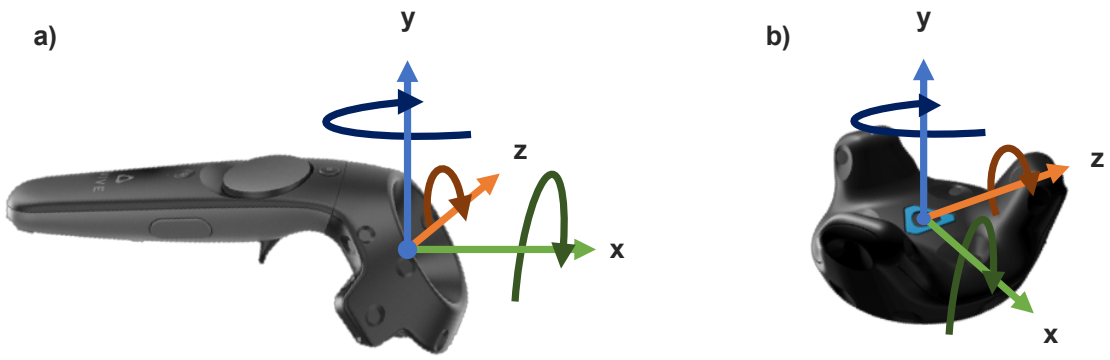

Fig. 2.2. Coordinate systems of the HTC VIVE controller (a) and tracker (b) overlaid on their respective models.

2.3 Data Reduction and Analysis

Translational error between the two systems was determined by taking the mean position over each ten-second period and using the distance formula to quantify the translation of each sensor from sample to sample. The distance measured by the VIVE was then subtracted from the distance measured by the Liberty. As neither system reported consistently higher or lower values than the other, indicating random error, the absolute value of the difference in measurement was used in order to avoid erroneously low error values.

Rotational error between the two systems was determined by comparing the change in helical angle measurement in each sensor from sample to sample. Helical angles were chosen because the global coordinate systems of the VIVE and Liberty systems were not aligned. The mean of each orientation component was taken over the ten-second collection period. The averaged Liberty components were decomposed from their Euler sequence using the system's reported attitude matrix (Polhemus, 2012). Helical angle change from sample to sample was calculated using these mean raw

rotational components from each system (Spoor and Veldpaus, 1980). The helical angle change was compared between the two systems by subtracting the change measured by the VIVE from the change measured by the Liberty. Again, random error was seen and as a result, the absolute value of these differences was used.

Drift in all six signal components was quantified using RMS of each ten second static collection period. The mean value of each signal component was first subtracted from each sample in that signal component; the remainders were used to determine RMS values for each signal component.

3. Results

The VIVE tracker and controller showed a mean rotational error of 0.13 ± 0.08° and 0.3 ± 0.07°, respectively (**Fig 2.3**a and b). Mean translational error for the tracker and controller was 1.7 ± 0.4 mm and 2.0 ± 0.8 mm, respectively (**Fig 2.3**c and d). When tested together, the tracker and Liberty sensor showed mean rotational drift of 0.06 ± 0.07° and 0.003 ± 0.000°, respectively (**Fig 2.4**a) and mean translational drift of 0.27 ± 0.13 mm and 0.02 ± 0.00 mm, respectively (**Fig 2.4**c). When tested alongside the controller, the controller and Liberty sensor showed mean rotational drift of 0.01 ± 0.00 ° and 0.0002 ± 0.0001°, respectively (**Fig 2.4**b) and mean translational drift of 0.28 ± 0.13 mm and 0.01 ± 0.00 mm, respectively (**Fig 2.4**d).

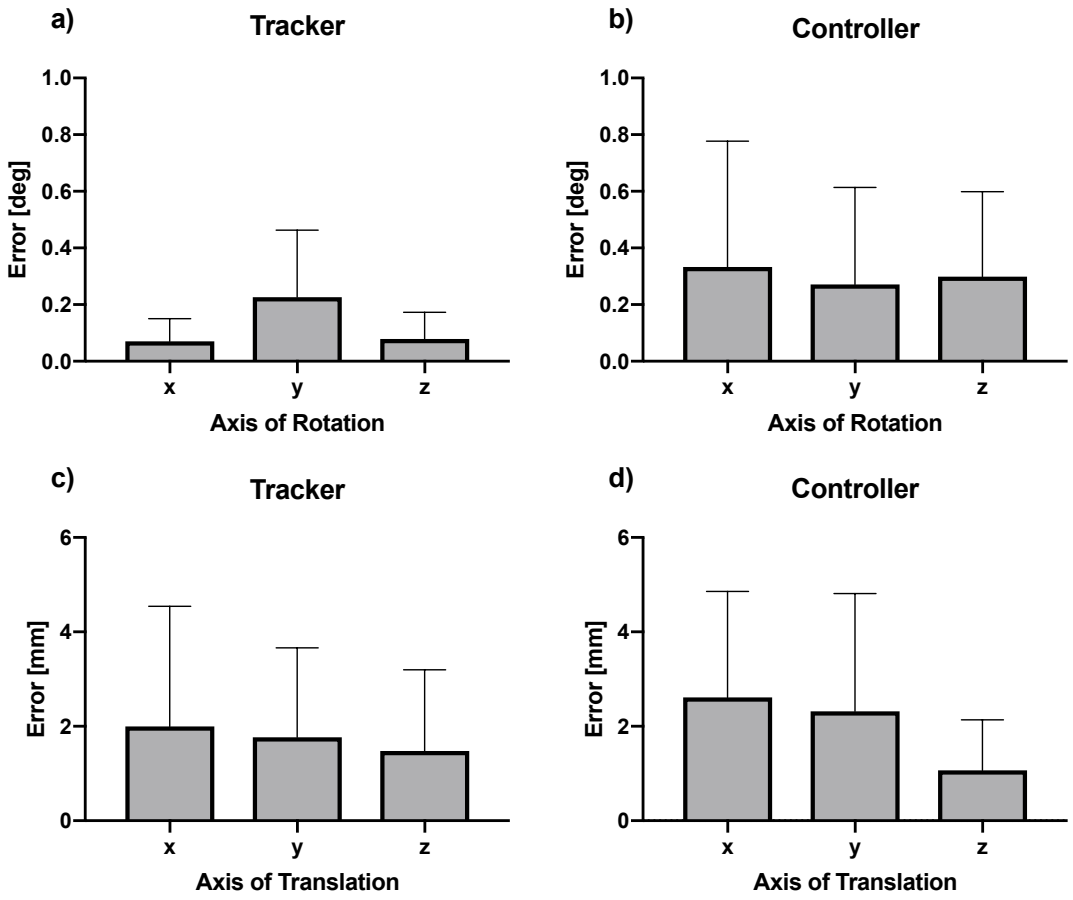

Fig. 2.3. Comparisons of rotational (a, b) and translational (c, d) measurement errors (mean ± SD) between the VIVE tracker and Liberty sensor (a, c) and the VIVE controller and Liberty sensor (b, d).

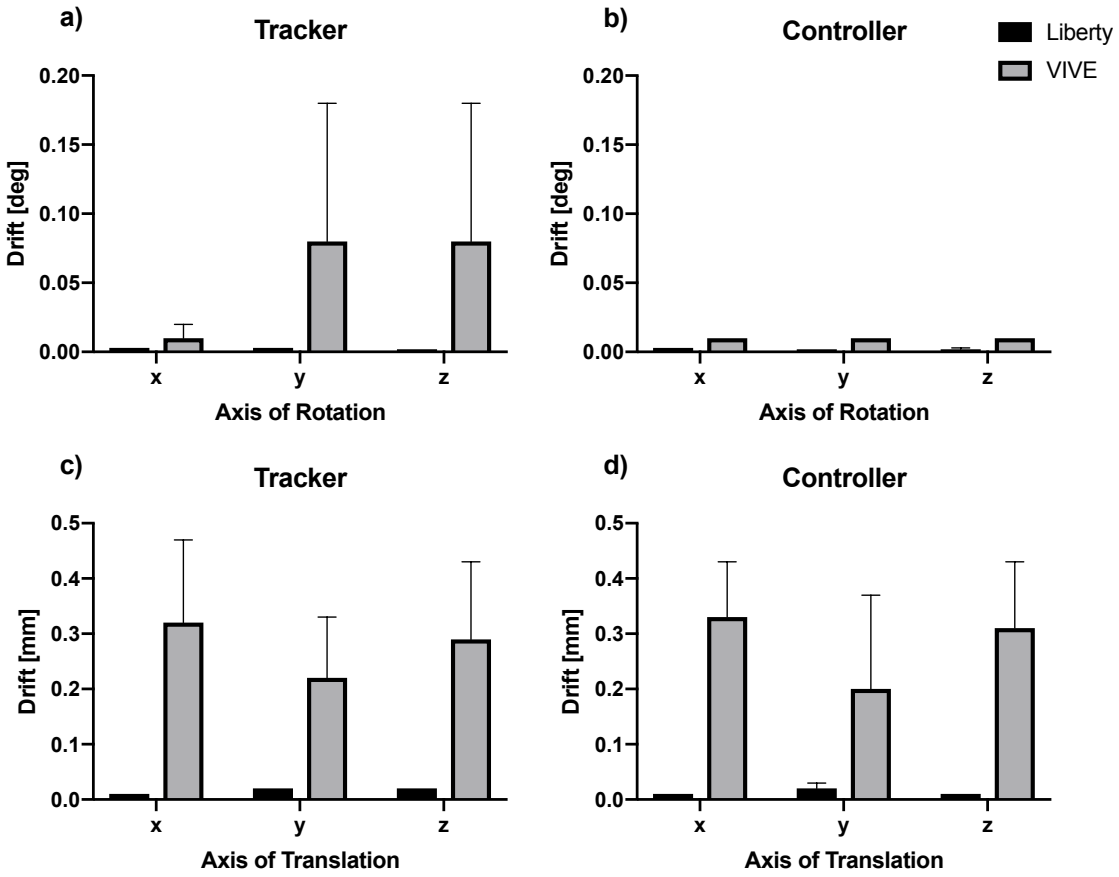

Fig. 2.4. Comparison of rotational (a, b) and translational (c, d) drift measurements (mean ± SD) between the VIVE tracker and the Liberty sensor (a, c) and the VIVE controller and Liberty sensor (b, d).

4. Discussion

This study aimed to compare measurements of static rotations and translations between the VIVE handheld controller and tracker to a Liberty sensor, and to quantify rotational and translational drift in all three sensors. These measurements were meant to inform whether the VIVE controller and tracker are accurate enough in measuring position and orientation to use for the collection of kinematic data.

The error measurements of both VIVE sensors were very low, with all mean rotational errors falling below 0.4° and mean translational errors below 3 mm. In all

instances when the rotation or translation increment was larger than zero, percent error was less than 0.1%. Rotational error across all three axes appeared to be consistent when using the controller. However, when using the tracker, error about the y-axis appeared to be higher than about the x and z-axes. Even with this inconsistency, mean error about the y-axis of the tracker was only 0.2°. Conversely, translational errors appeared consistent across all axes when using the tracker, and when using the controller error along the z-axis appeared to be lower than along the x and y-axes. Even with these slight variations between axes, all rotational and translational components of the controller and the tracker aligned very closely with the Liberty measurements. These errors fell well within the range of normalcy for research grade systems, which regularly report translational accuracy between 1.0 mm and 2.0 mm and rotational accuracy between 0.5 ° and 1.0 ° but often demonstrate much higher errors in practice (Frantz et al., 2003; Nafis et al., 2006).

Drift measurements throughout the 10 second capture periods from both VIVE sensors were consistently higher in all components than drift from the Liberty sensor. However, all mean rotational drift measures fell below 0.1° and all translational measures below 0.35 mm. The lowest measures of drift by the VIVE system were seen in the controller's rotational components, while the tracker displayed slightly higher measures of mean rotational drift. As these sensors use embedded IMUs, it is expected that drift would accumulate over time. However, the light-emitting boxes and optical sensors integrate with the output from the IMU to provide 60 drift corrections per second. This mechanism prevents accumulation of drift in the signal.

These slight differences between the VIVE tracker, VIVE controller, and Liberty sensor may be important to consider when making kinematic measurements over very small ranges of motion. Studies involving surgical tasks, for example, which require minimum system accuracy of 1.5 mm, may want to consider using other systems (Birkfellner et al., 1998). However, for larger movements we believe that all of these sensors are accurate enough for the collection of kinematic data. This study was performed using a single VR system, and therefore cannot be guaranteed to represent all systems of the same model. However, this practice is common in validation studies and the protocol is replicable a wider scale (Nafis et al., 2006). Additionally, these data are limited in that they are static measurements taken in the center of the calibrated space; further testing on temporal signal components and the entirety of the space would be necessary for studies with a strong timing requirement or those which plan to utilize all of the calibrated volume. Further, in comparison to a traditional motion capture system, the VIVE sensors are larger and more difficult to affix to segments. The main considerations when choosing between these sensors should therefore be study design, portability, and cost.

5. Bridge

This study assessed accuracy of the VIVE handheld controller and tracker in comparison to the Polhemus Liberty magnetic tracking system, an industry-standard motion capture system known for its high accuracy. Static drift in position and orientation, as well as translation and rotational error, were measured and compared between the VIVE sensors and the Liberty system. The VIVE tracker and controller demonstrated rotational and translational errors which fell within the range of research-

grade systems. The study also analyzed drift in all six signal components, finding that the VIVE sensors exhibited slightly higher drift compared to the Liberty sensor. However, the combination of embedded IMU and optical sensors prevent significant accumulation of drift over time, maintaining relatively low values.

Overall, this study highlights the potential of using VR systems like the HTC VIVE for simultaneous immersion in virtual environments and kinematic data collection. The next step in solidifying the utility of these systems is to examine the dynamic rotational accuracy of the VIVE sensors. The study outlined in Chapter III was designed to achieve this aim.

CHAPTER III

ACCURACY OF THE HTC VIVE TRACKER ROTATIONS UNDER CONTROLLED DYNAMIC CONDITIONS

This work is being prepared for submission to the *Journal of Biomechanics* as a short communication and is co-authored by Kate A. Spitzley and Andrew R. Karduna. The study design, experimental work including data collection and analysis, and writing was performed by Kate A. Spitzley, Andrew R. Karduna provided research mentorship and editorial assistance.

1. Introduction

Immersive virtual reality (VR) systems have recently undergone substantial technological updates and reductions in cost. This rise in accessibility has been paralleled by increased use of these systems in education, retail, sports, and healthcare settings (Wohlgenannt et al., 2020). In the healthcare domain, VR systems are being used to train surgeons (Egger et al., 2017), provide clinical and in-home health care (Ikbali Afsar et al., 2018; Janeh et al., 2019; Levin et al., 2015b; Waked and Eid, 2019), and teach sensorimotor skills (Wright, 2013). With the typical consumer VR product costing under $1,000, and the application market providing easy access to gamified rehabilitation tools, it is unsurprising that this technology has been readily adopted. The potential benefits from using a technology that easily provides 3D, fully controllable environments in-clinic or at-home certainly deserves the increased attention.

In addition to the benefits of a 3D environment, some of these systems have the potential to deliver simultaneous capture of six degree of freedom motion data. Position and orientation data from the HTC VIVE headset, controller, and tracker can easily be output. The HTC VIVE Tracker is an ideal candidate for capturing movement of body segments for kinematic study. It is small enough to mount on most segments, lightweight enough not to impede movement, and integrates optical and IMU sensor data for tracking. Platforms such as Vicon Reality and OptiTrack for VR have combined their marker-based systems with VR headsets and controllers to achieve segment tracking while using VR systems. However, these configurations still require a research-grade motion capture system to collect kinematic data. Although research-grade systems provide robust measures of position and orientation, their high price-points and low portability pose access limitations. Using the VIVE VR system for simultaneous immersion in 3D virtual environments and kinematic data collection could provide the same benefits of these integrated systems, the low price point of VR systems, and high portability that existing systems cannot offer.

Therefore, the goal of the study outlined in this chapter was to determine the rotational accuracy of the HTC VIVE tracker (version 3.0) under controlled dynamic conditions. To achieve this, the tracker and a potentiometer were rotated simultaneously. Their rotational measurements were compared over a range of speeds, at nine different positions throughout the room, and at different orientations with respect to the VIVE Lighthouse system. R-squared, root-mean-square-error (RMSE), and mean absolute error were used to determine the agreement between the two measurement sources. The study outlined in chapter 2 of this dissertation found no differences in static rotational or

translational error between three axes of movements in either the tracker or controller. This study therefore examined only rotations about the z-axis of the tracker.

2. Methods

2.1 Experimental device

A 1-degree of freedom rotational device was designed to synchronously rotate an HTC VIVE tracker 3.0 (HTC VIVE, Taoyuan City, Taiwan) and a potentiometer using a servomotor. The servomotor rotated a rigid arm to which the tracker was mounted in series and the potentiometer was mounted in parallel (**Fig. 3.1**). Analog voltage from the potentiometer was converted through a National Instruments A/D board (National Instruments Corporation, Austin, TX, USA) and the digital signal was recorded using a custom LabVIEW (National Instruments, Austin, TX, USA) program. Orientation from the tracker was recorded using a custom Unity (Unity, San Francisco, CA, USA) program. Samples were collected at a rate of 90 Hz from both the potentiometer and the tracker. The potentiometer voltages were calibrated to angles using 387 discrete points over a 180° range.

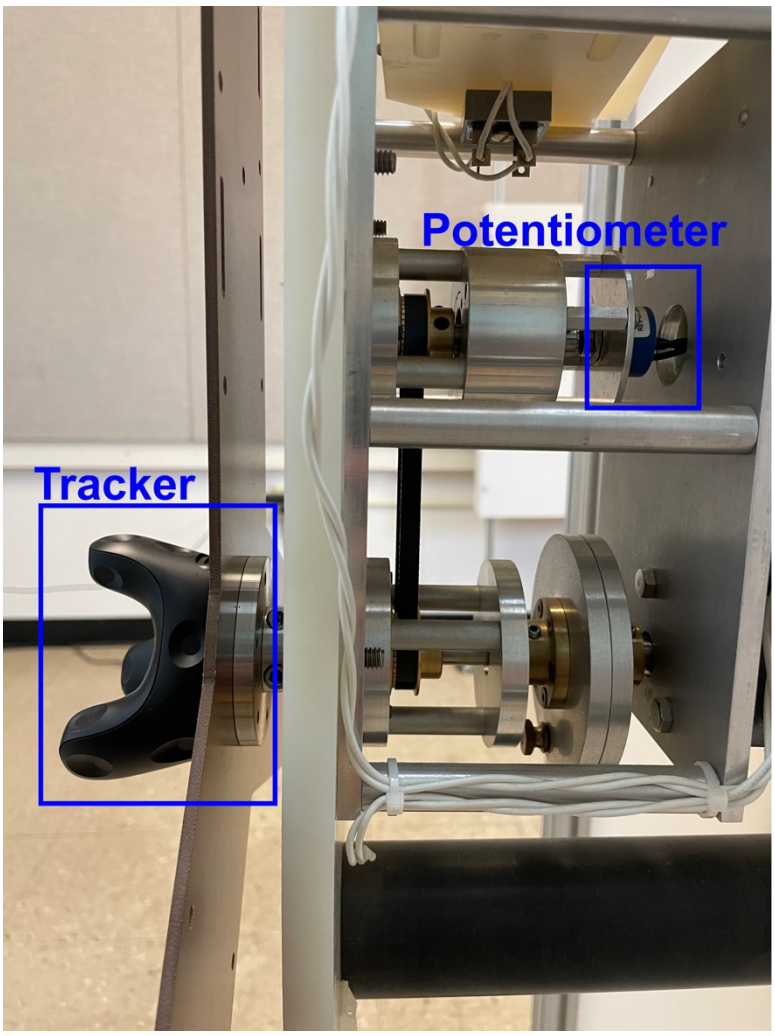

Fig. 3.1 The HTC VIVE tracker is mounted in series and the potentiometer is mounted in parallel with a rigid rod that is rotated by a servomotor.

2.2 Experimental conditions

Four VIVE system configurations were tested (**Fig. 3.2 a**). Configurations varied position of the lighthouse boxes and facing of the tracker. Configuration 1 tested the lighthouse boxes in adjacent corners, facing the center of the room with the tracker facing both boxes. Configurations 2-4 tested the lighthouse boxes in opposite corners, facing the center of the room with the tracker facing parallel to the line between the lighthouses (C3) and at a 45° angle to the line between the lighthouses (C2 & C4). In all

configurations, the lighthouse boxes were set up according to the manufacturer recommendations, mounted at a height of 3 m with an inclination of approximately 45 °.

In each configuration, the Steam VR Room Setup was completed to calibrate a 2.4 m square virtual space inside the 4.7 m square laboratory space. The virtual space was further subdivided into nine sections (**Fig. 3.2 b**). Once the setup was complete, all testing for the configuration was completed without turning off the system, moving the lighthouse boxes, or redoing the room setup process. Testing procedures were replicated in each configuration and each section.

Testing consisted of the servomotor being engaged to rotate the rigid arm. Rotations covered an approximately 180° range from 5±5° to 190±10°. Five rotations were completed at three speeds fast (15°/sec), medium (7°/sec), and slow (3°/sec). The speeds were selected to represent the full range of speed available from the testing device. This experimental design resulted in 135 tests per configuration: five tests at three speeds in each of the nine sections.

a) Configurations

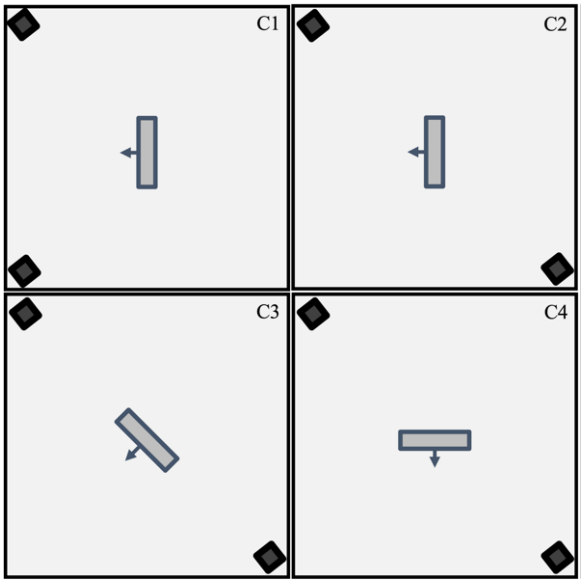

b) Sections

S7	S4	S1
S8	S5	S2
S9	S6	S3

Fig. 3.2 The VIVE system setup in four different configurations (a) which varied position of the lighthouse boxes (black squares) within the room and facing of the device holding the tracker and potentiometer (grey rectangle). The grey arrow indicates the direction in which the tracker was facing. The device was tested in nine different sections (b) of the calibrated space.

2.3 Data Reduction and Analysis

R-squared, root-mean-square error, and mean absolute error values were calculated to establish how closely the tracker angles matched the potentiometer angles throughout the full range of motion. Mean absolute error was calculated by determining the absolute difference between tracker and potentiometer readings at each 10° increment of movement, as determined by the potentiometer. Differences in each of these measures between speeds (fast, medium, and slow), sections of the calibrated space (S1 - S9), and configurations (C1 - C4) were determined using three-way repeated measures ANOVAs ($\alpha = 0.05$).

3. Results

No differences between speeds, sections, or configurations or interactions were observed in measures of r-squared, RMSE, and mean absolute error (**Fig. 3.3**). R-squared values ranged from 0.97 to 0.99, with an overall mean and standard deviation of 0.99±0.002. RMSE ranged from 0.90° to 1.1°, with an overall mean and standard deviation of 1.1±0.1°. Mean absolute errors ranged from 0.21° to 0.27°, with an overall mean and standard deviation of 0.23±0.01°.

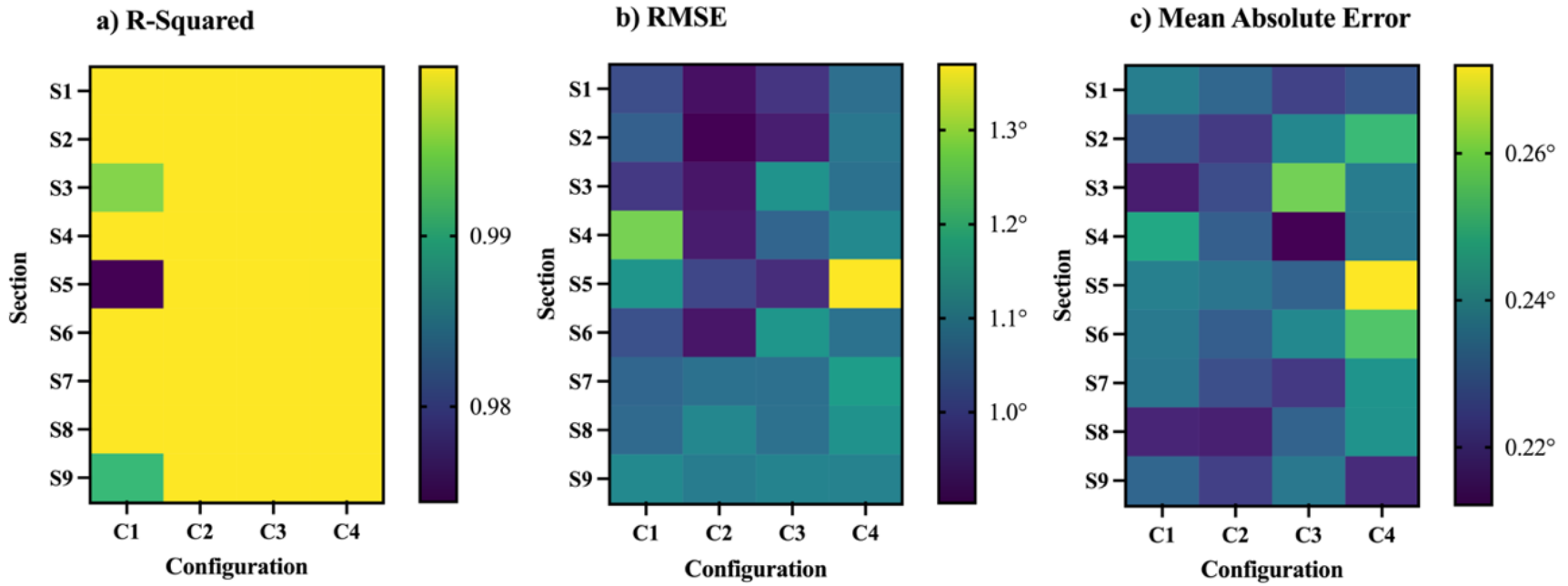

Fig. 3.3 Heatmaps showing results for r-squared (a), RMSE (b), and the mean absolute error between tracker and potentiometer readings in 10° increments (c). As no effect of speed was observed, all three speeds have been collapsed for these representations.

5. Discussion

The present study aimed to quantify rotational accuracy of the HTC VIVE tracker under dynamic conditions. A potentiometer was used as the source of gold standard data for comparison. The two measurement devices were rotated over an approximately 180° range of motion at three different speeds, fast (15°/sec), medium (7°/sec), and slow (3°/sec). The calibrated testing space was subdivided into nine sections and the tests were completed in each of these sections under four different room configurations (**Fig. 3.2**).

R-squared (**Fig. 3.3a**), RMSE (**Fig. 3.3b**), and the mean absolute error (**Fig. 3.3c**) showed no differences between speeds, sections of the room, configurations, or interactions. Additionally, the strong agreement between the tracker and our gold standard, the potentiometer, support the use of an HTC VIVE tracker for the collection of orientation data. Manufacturer reported RMS of rotational components for magnetic tracking systems range from 0.3° to 1.1° (Nafis et al., 2006). Dynamic testing of rotational components for two inertial based systems (Xsens MTx and APDM Opal) resulted in accuracy values of 2° and 2.8°, respectively (Lebel et al., 2013). Based on these values, the tracker's dynamic accuracy falls somewhere between that of a magnetic tracking system and inertial measurement system.

The results from this study join several others in finding low errors and strong agreement between the VIVE sensors and industry gold-standard systems (Jost et al., 2019; Sansone et al., 2022; Soares et al., 2021; Spitzley and Karduna, 2019). One main finding that differs between this study and others is the lack of differences that we observed around the edges of the room compared to the center. Others have seen a decline in accuracy, particularly in orientation measurements, at the edges of the room

(Niehorster et al., 2017; Sansone et al., 2022). In whole, these studies suggest that data collections in the center of the calibrated space should produce position and orientation outputs similar to those of other industry gold-standard systems.

One limitation to this study is that the tracker was only rotated about the z-axis. However, the study outlined in chapter 2 of this dissertation showed no differences in static rotational or translational error between three axes of movements in either the tracker or controller. We therefore felt comfortable using the z-axis of movement as a representative sample in the dynamic condition.

6. Bridge

This study focused on assessing the rotational accuracy of the HTC VIVE tracker under dynamic conditions. A rotational device was designed to synchronize the rotation of the tracker and a potentiometer using a servomotor. The tracker and potentiometer measurements were compared at different speeds, positions within the room, and orientations with respect to the VR system. No significant differences were found in rotational accuracy between speeds, positions, or configurations and no interactions were seen. Comparisons with other gold-standard systems showed that the HTC VIVE tracker's dynamic accuracy falls between that of magnetic tracking systems and inertial measurement systems.

The studies outlined in Chapters II and III conclude that the HTC VIVE tracker is a reliable tool for collecting accurate static and dynamic data in VR environments. The studies outlined in Chapters IV through VI capitalize on this functionality, using the HTC

VIVE headset to present a virtual environment and the tracker 3.0 to estimate position and orientation of body segments.

CHAPTER IV

JOINT POSITION ACCURACY IS INFLUENCED BY VISUOPROPRIOCEPTIVE CONGRUENCY IN VIRTUAL REALITY

This work is published in volume 54 of the *Journal of Motor Behavior* in June 2021 as "Joint Position Accuracy is Influenced by Visuoproprioceptive Congruency in Virtual Reality" and is co-authored by Kate A. Spitzley and Andrew R. Karduna. The study design, experimental work including data collection and analysis, and writing was performed by Kate A. Spitzley, Andrew R. Karduna provided research mentorship and editorial assistance.

1. Introduction

During movement planning, the brain combines sensory information from the current state of the body and the environment with sensory feedback. During movement execution, the brain continuously updates this plan with incoming sensory feedback regarding movement error. Vision and proprioception play important roles in these processes. Vision provides information about the state of the environment and the body within the environment and proprioception provides information about the internal state of the body (Riemann and Lephart, 2002b; Sarlegna and Sainburg, 2009). The integration of these two sensory signals helps to provide an accurate estimate of how the body is interacting with the environment. This step is essential in assessing movement goals and goal related movement errors to inform the feedback process (Wolpert et al., 1995).

Relative dependence on visual and proprioceptive sensory signals to inform movement is flexible depending on both the quality and quantity of sensory information available (Block and Bastian, 2011; Sober and Sabes, 2005, 2003; van Beers et al., 2002). This relationship can be described as an optimal integration problem wherein the goal is to reduce movement error by increasing reliance on signals with low statistical variability and decreasing reliance on signals with high statistical variability (Ernst and Banks, 2002). The mechanisms behind this have been explored in clinical populations (Blouin et al., 1993; Ghez et al., 1995; Guillaud et al., 2011; Rickards et al., 1997; Sarlegna et al., 2010; Seiss et al., 2003) and probed experimentally through induced distortions of either vision (Bagesteiro et al., 2006; Rossetti et al., 1995; Sober and Sabes, 2003; Welch and Warren, 1986) or proprioception (Ettinger et al., 2014; Goodman and Tremblay, 2018; Roll et al., 1989). These clinical and experimental paradigms show that mismatched sensory information in movement error feedback are treated as noise in the system and result in sensory signal reweighting. Reweighting is a temporary process by which the less variable signal is relied upon more heavily, prioritizing movement task success. Mismatches on a longer timescale may be accommodated for through a realignment of sensory mapping. Experiments dissociating signals for longer periods of time show that the system adapts on a more permanent level, as the brain accepts the new alignment as the updated normal state (Block and Bastian, 2011; Van Der Kooij et al., 2013). In both of these paradigms, sensory distortions are accommodated for by a change in the representation of sensory information in the brain, with the goal of preserving movement task performance. From a neurophysiological standpoint, these accommodations are likely facilitated through the gating of sensory information wherein the signal-to-noise

ratio and gain of sensory signals are adjusted before being stored in the CNS (Burgess et al., 2018; Ott and Nieder, 2019).

Previous studies have used a diverse set of paradigms to generate visuoproprioceptive offsets - spatial dissociations between visual and proprioceptive sensory information. The most commonly used are prism goggles (Goodman and Tremblay, 2018; van Beers et al., 1999) and mirror-screen couplings (Bagesteiro et al., 2006; Sarlegna and Sainburg, 2009; Sober and Sabes, 2003; Van Der Kooij et al., 2013). Fully immersive virtual reality (VR) systems provide an expanded opportunity for sensorimotor investigation by altering visuoproprioceptive congruency. These systems allow for full control over the visual environment, including the representation of the user's physical form. VR offers a unique paradigm in which each part of the environment can be controlled independently (as opposed to the universal shift with prisms) while preserving the three-dimensional world (as opposed to using a computer screen or projection table). Given the potential that VR provides for sensorimotor investigation, it is important to understand how movement consistency and accuracy of a shoulder flexion task are influenced by visuoproprioceptive offsets.

The aim of this study was to determine how movement consistency and accuracy are influenced by alterations in visuoproprioceptive congruency in a fully immersive VR environment. A simple one degree of freedom upper limb joint position matching task was performed while visual feedback of the upper limb was presented in one of three conditions; accurate visual feedback, no visual feedback, and offset visual feedback. Goals in the selection of the movement task were a) reduce potential sources of movement variability not linked to sensory feedback (such as joint coordination patterns)

and b) reduce task complexity to ensure that participants could easily follow the protocol even if they were new to the VR experience. Based on the above described principles of flexible sensory weighting and sensory statistical variability, with proprioception being more variable than vision, the following hypotheses were developed: a) Movements completed without vision of the upper limb will be less consistent, but no less accurate than movements completed with vision of the upper limb; b) Movements completed when vision and proprioception of the upper limb are spatially incongruent will be less consistent and less accurate than movements completed with vision of the upper limb; and c) Movements completed without vision of the upper limb will be more consistent and more accurate than movements completed when vision and proprioception of the upper limb are spatially incongruent. The offset used in the offset visual feedback condition was specifically selected to be below that which is noticeable to the participant. This experiment used the VR system to both apply visual perturbations and capture kinematics, exploring the use of integrated VR sensors to capture kinematic data.

2. Methods

2.1 Participants

Twenty participants, 10 females (age 24.4 ± 4.2 yrs, height 1.7 ± 0.1 m, weight 62.6 ± 6.2 kg) and 10 males (age 25.4 ± 4.5 yrs, height 1.8 ± 0.1 m, weight 88.7 ± 14.0 kg), were recruited from the general population. Participants were screened for limb dominance using a 10 question Edinburgh Handedness Inventory (Oldfield, 1971). Only individuals with a strong right upper-limb dominance (≥ 7/10) were included. Participants were excluded if they had experienced chronic upper body pain within the past three

weeks, upper limb injury within the past year, any neurological disorder, or impaired vision that could not be corrected using contact lenses. All participants read and signed an informed consent document as approved by the University of Oregon Institutional Review Board.

2.2 Instrumentation

Participants were outfitted with an HTC VIVE VR headset (2160x1200 resolution, PenTile OLED display) with over-ear headphones attached (**Fig. 4.1.,** HTC VIVE, Xindian District, New Taipei City, Taiwan). A wrist brace was fitted to their right arm, serving the dual function of stabilizing the wrist and securing an HTC VIVE tracker (0.36 kg). Auditory instructions and cueing were delivered through the over-ear headphones. A three-dimensional visual environment including a visual representation of upper limb position was displayed to the participant through the headset. Upper limb position was determined using output from the VIVE tracker, serving as the source of kinematic data for this study (Spitzley and Karduna, 2019).

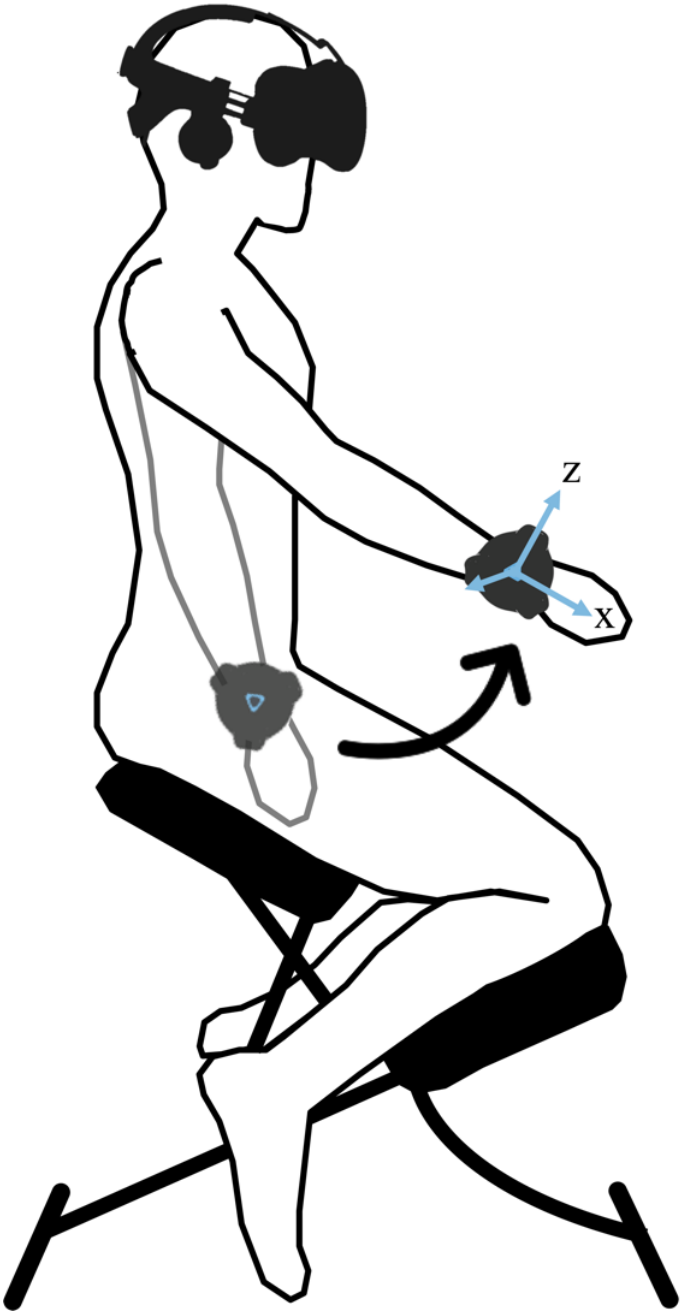

Figure 4.1. Participant seated in a kneeling chair, instrumented with HTC VIVE VR headset, and equipped with over-ear headphones. HTC VIVE tracker affixed to wrist with the x-axis of the tracker oriented along the long axis of the forearm and z-axis oriented along the anterior/posterior axis of the forearm. Visualization of the tracker was shifted 8° in the positive direction along the z-axis of the tracker in the OV testing condition. Curved arrow illustrates movement between initial resting position and a target flexion angle of 50°.

2.3 Experimental Overview

2.3.1 Matching Task

Participants were seated in a kneeling chair throughout the testing session, providing comfort for the individual and allowing for a full range of arm movement (**Fig. 4.1**). The chair was placed in a standardized position in both the real and virtual spaces to ensure that each participant received the same visual information of the virtual world and that kinematic data from the tracker were collected from the same location within the calibrated space. Participants were seated facing a white wall in the virtual world to eliminate environmental visual cues such as corners or wall intersections and were instructed to face forward and keep their head still throughout the experiment. Participants remained in the VR environment throughout the protocol without removing the headset, headphones, or tracker unless they experienced discomfort or requested a break. During tracker placement, the participant's right arm was positioned directly at their side, as close to perpendicular to the ground as possible. The tracker was then affixed to the wrist so that the z-axis read 0° of rotation, indicating 0° of shoulder flexion (**Fig. 4.1**). The tracker was not removed or repositioned during the protocol.

Trials began with participants seated in the kneeling chair with both arms straight and relaxed by their sides. Each trial consisted of two movement phases: a presentation phase and replication phase. In the presentation phase, participants were asked to raise their right arm to a target angle by flexing at the shoulder, as guided by auditory cues. The auditory cue 'find target' prompted participants to raise their arm in the sagittal plane. While the arm was below the target angle, a low tone was emitted from the headphones, indicating that participants should continue raising the arm. If the angular

target was passed, a high tone was emitted from the headphones indicating that participants should lower their arm. When the angular target was reached, the tone was silenced. Participants were required to stay within +/- 3 degrees of the angular target for 3 consecutive seconds, straying outside of this range would reengage the tonal cues to guide them back in. After holding the position for 3 seconds, an auditory cue to 'relax' was delivered, prompting the return of their arm to their side. Participants were instructed to keep their palm facing their side when relaxed, thumb pointed toward the ceiling during flexion tasks, and their elbow straight at all times. These instructions were followed without issue by each participant as confirmed by a supervisor. In the replication phase, participants were instructed to return to the angle that the auditory cues had guided them to in the presentation phase. During this phase, no auditory guidance was provided. Participants were instructed to find the angle that they believed was presented to them in the first phase and hold still until they heard the 'relax' cue. This phase was considered to be successful when the angular velocity of the tracker was stable under 5°/s for 3 consecutive seconds. Information regarding auditory cues and the phases of testing were given prior to beginning the session. During testing, the only guidance was given via automated auditory cuing delivered through the VR system.

This task was adapted for VR from previous studies probing proprioception at the shoulder. The auditory guidance provided during this experiment has been used extensively in position testing using motion analysis systems and mobile applications (Edwards et al., 2016; Erickson and Karduna, 2012). Tonal auditory cues were used for guidance during the presentation phase to ensure that visual information of target position would arise solely from the visual representation of the limb. In this configuration, visual

and proprioceptive information come from the same source, providing a body-centric target to match during the replication phase. Using this setup, visual and proprioceptive feedback during the replication phase could be directly compared to the visual and proprioceptive feedback from the presentation phase.

2.3.2 Testing Conditions

Trials were performed at three target angles under three visual conditions. Each testing session consisted of 36 trials broken down into three sets corresponding with the three visual conditions. Each set consisted of twelve trials: four trials at each of the three target angles. Target joint angles were randomized between each trial and the order of visual condition was randomized between sets of trials (**Fig. 4.2**). Target shoulder flexion angles of 50°, 70°, and 90° were used for continuity with previous joint angle replication studies (Edwards et al., 2016; King et al., 2013; Lin and Karduna, 2016).

Aside from a visual representation of the upper limb position, no external visual target was presented under any condition and visual information of the environment was uniform through all conditions. The tracker was modelled as a dark grey sphere to serve as a visual representation of upper limb position. During the presentation phase, the sphere was always in spatial alignment with the tracker, providing an accurate visual representation of limb position. During the replication phase, visual representation of the limb was varied in three conditions: accurate vision (AV), no vision (NV), and offset vision (OV). In the AV condition, the sphere was in spatial alignment with the tracker. In the NV condition, the sphere was not visible, therefore no visual representation of limb position was available. In the OV condition, the sphere was spatially misaligned with the

tracker by 8° in the positive direction along the z-axis of the tracker (**Fig. 4.1**), providing an inaccurate visual representation of limb position.

The z-axis of the tracker aligned with the anterior/posterior axis, or sagittal plane, of the participant (**Fig. 4.1**). With the participant's arm at their side (0° flexion), it appeared to be flexed 8° anteriorly when offset. During testing, the participant's arm was out of the field of view at 0° of flexion. The visual offset was induced at this angle so that the participant would be unaware of the shift.

Magnitude of the offset was calculated as a function of the participant's arm length to create an angular offset of positive 8° along the z-axis of the tracker. For example, if the participant's shoulder was flexed to 50°, the tracker would represent a flexion angle of 58°. The offset magnitude between an arc (i.e. angular offset) and a linear offset was determined to be negligible (≤ 0.5mm) for the current experimental paradigm. This offset magnitude was chosen as it was not noticeable to participants, as determined through pilot testing, but was outside of the range of normal positioning error. Participants were interviewed after the conclusion of testing to determine whether they had detected the offset during the protocol, none reported being aware of the visual offset before or during testing. As previous studies found that only 11% of participants noticed a 15° offset (Bourdin et al., 2019) and that embodiment of a virtual representation in VR is very strong regardless of visual dissociations (Caola et al., 2018), it is unsurprising that an 8° offset was not noticed.

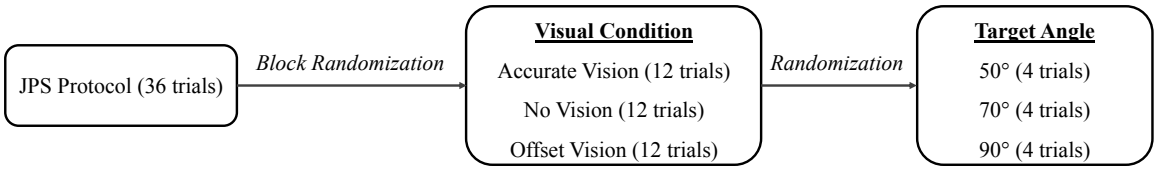

Figure 4.2. Testing sessions consisted of 36 trials of the joint position matching protocol, these were block randomized by visual condition and then further randomized by target angle.

2.4 Data Collection and Reduction

Data were sampled from the VIVE tracker at 50 Hz and collected using a customized Unity (Unity Technologies, San Francisco, CA) program. Shoulder joint angles were estimated with respect to vertical (the 0° starting position of the tracker). Mean shoulder joint angles in the presentation and replication phases were calculated by averaging 100 data points (2 seconds) prior to each 'relax' cue. The relax cue occurred after the three second hold time both in the presentation and replication phases of the trials (**Fig. 4.3**).

Mean presentation and replication angles were used to calculate variable error (VE) and constant error (CE). Variable error, a measure of consistency, was calculated as

$$VE = \sqrt{\frac{\sum(x_i - M)^2}{n}}$$

where x is the replicated angle, M the mean replication difference, and n the number of trials. Constant error (CE), a measure of accuracy which takes direction into account, was calculated as

$$CE = \frac{\sum(x_i - P)}{n}$$

where x is the replicated angle, P the presented angle, and n the number of trials.

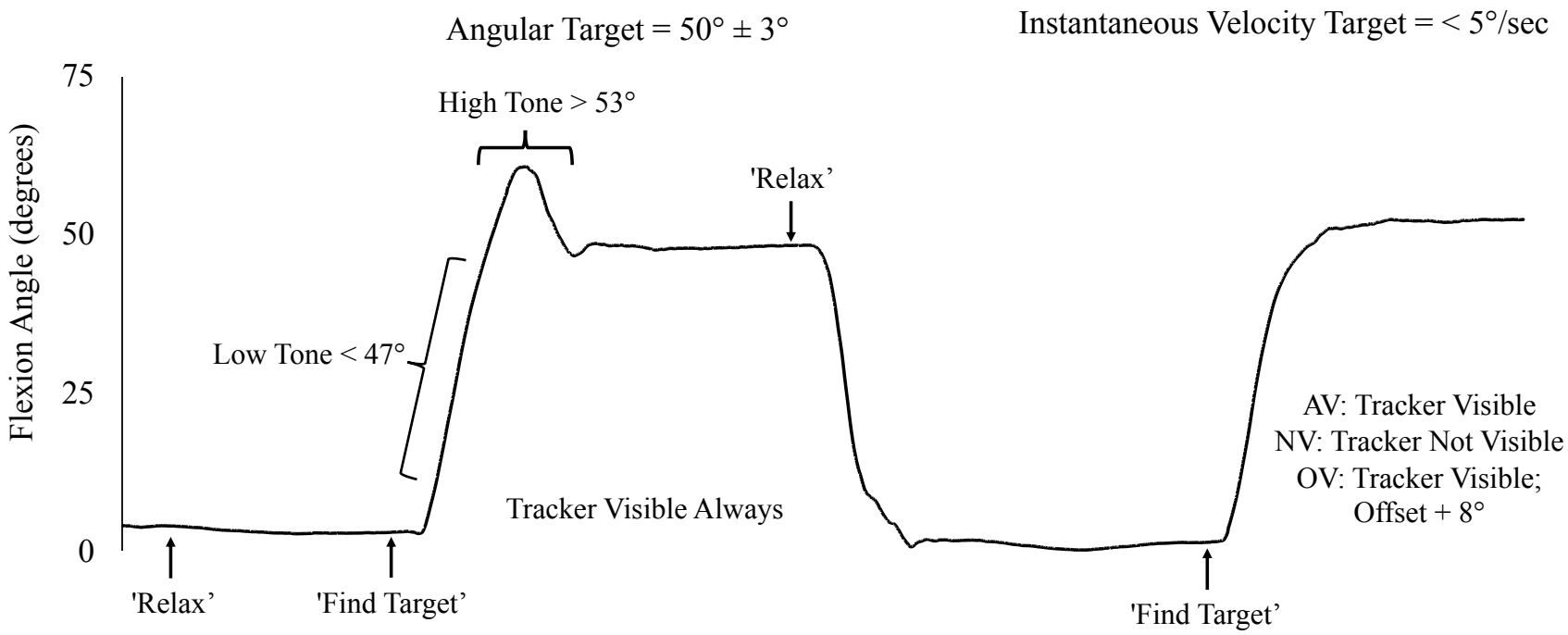

Figure 4.3. Sample trace of shoulder flexion angle data from a single trail at the 50° target angle. Visual cues, auditory cues, and movement targets for each phase of movement are labeled.

2.5 Statistical Analysis

The effect of visual condition (AV, NV, and OV) and angle (50°, 70°, and 90°) on VE and CE were examined within participants using two-way repeated measures ANOVAs. The alpha level was set at 0.05. If a significant interaction was seen, main effects in the two-way ANOVA were not examined. Instead, post hoc one-way within-subjects repeated measures ANOVAs were performed at each angle to examine the effect of visual condition. If no significant interaction was seen, main effects in the two-way ANOVA were examined. A Sidak correction was used to control for familywise error. Statistical analyses were performed using SPSS, version 25 (SPSS, Chicago, IL).

3. Results

All participants were able to follow the protocol after a single explanation. No participant required more than one period of auditory guidance to successfully complete the presentation or replication phases of the test. No data point was identified as a major outlier, defined as a point that falls more than 3 times the interquartile range above the third quartile or below the first quartile. As a result, all subjects and data points were included in the analyses.

3.1 Variable Error

No main effect of visual condition ($F(2,19) = 1.27$, $p = 0.29$, or angle $F(2,19) = 1.70$, $p = 0.20$), and no interaction between angle and visual condition ($F(4,19) = 0.38$, $p = 0.83$) were found (**Fig. 4.4a**).

3.2 Constant Error

Significant main effects of visual condition ($F(2,19) = 43.30$, $p < 0.001$), angle ($F(2,19) = 9.63$, $p < 0.001$), and an interaction effect ($F(4,19) = 4.80$, $p < 0.05$) were found. Outcomes of the post hoc one-way repeated measures ANOVAs at each target angle are summarized in **Table 4.1** and displayed in **Figure 4.4b**. At all target angles, error was greater in the offset vision condition than in the accurate vision condition and in the no vision condition. No difference was seen between accurate vision and no vision at any target angle.

Table 4.1 Summary of post hoc 1-way repeated measures ANOVA for Constant Error

	AV	NV	OV	$F(2,19)$	p
50°	-0.2° (4.1)	-0.02° (4.4)	-3.0° (5.0)	7.8	< 0.01
70°	-2.1° (3.0)	-1.7° (3.1)	-6.6° (3.3)	14.4	< 0.001
90°	-1.6° (2.7)	-2.1° (2.7)	-9.0° (3.2)	55.0	< 0.001

Mean and (standard deviation) CE values for each testing condition. Resulting F and p values from post hoc 1-way repeated measures ANOVA are presented in the corresponding rows. At all angles, significant differences were seen between AV and OV and NV and OV. At no angle was a difference seen between AV and NV.

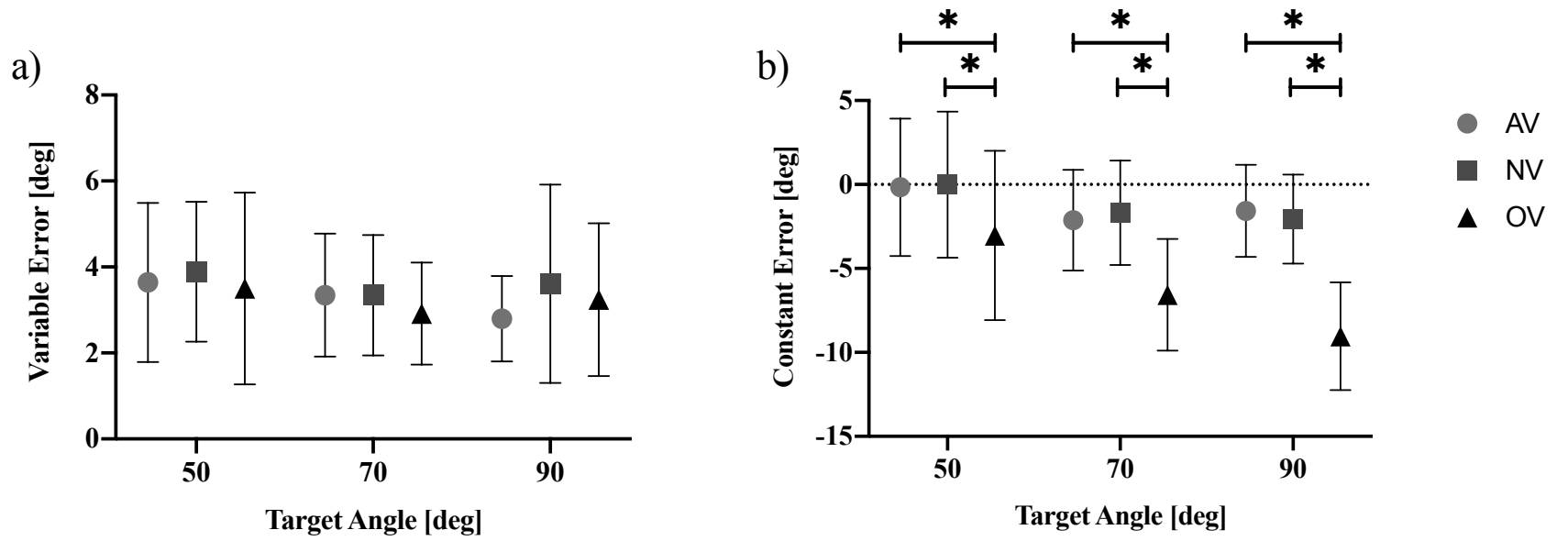

Figure 4.4. Variable and constant error in degrees between accurate, no, and offset visual conditions over each target angle. Data represent means and standard deviations (n ¼ 20, $p < 0.001$). (a) No differences in VE were seen based upon either target angle or visual condition, nor was an interaction between target angle and visual condition seen. (b) At all angles, CE was greater (further from zero) in the OV condition than in both the AV and NV conditions and no difference was seen between AV and NV conditio

3.3 Sensory Reliance

The reliance on visual and proprioceptive information during the offset vision condition was estimated using the equation

$$\left(\left(\frac{CE_{Offset\ Vision} - CE_{Accurate\ Vision}}{8}\right) \times -1\right)$$

wherein the difference in CE between accurate and offset visual conditions and the induced offset of 8° are compared (**Fig. 4.5**). A score of 1 indicated that participants positioned their arm 8° higher in the OV condition than in the AV condition. This suggests that they were not using the accurate proprioceptive information available to guide replication, instead using the inaccurate visual information and matching the location where they saw the arm instead. A score of 0 indicated that participants positioned their arm in the same place during the OV and AV conditions. This suggests that they were relying on accurate proprioceptive information and/or offline control mechanisms while disregarding the inaccurate visual information. CE from the AV condition was used in this comparison because it represents the participants ability to accurately replicate the target when both accurate visual and accurate proprioceptive information is available. Position during the presentation phase was also considered for use in this comparison but was ultimately not chosen because the guidance provided during this phase means that it is not representative of participant ability. For the OV condition at the 50° (M = 0.4, SD = 0.5) and 70° (M = 0.6, SD = 0.7) target angles, scores indicated that participants matched to a representation between the visual and proprioceptive arm locations, with ranges spanning exact visual and exact proprioceptive matches. At the 90° (M = 0.9, SD = 0.5) target angle, scores indicated that participants tended to match the visual arm location more closely but did not rely exclusively on

visual location. When interpreting this metric, it is important to note the high variance across all target angles.

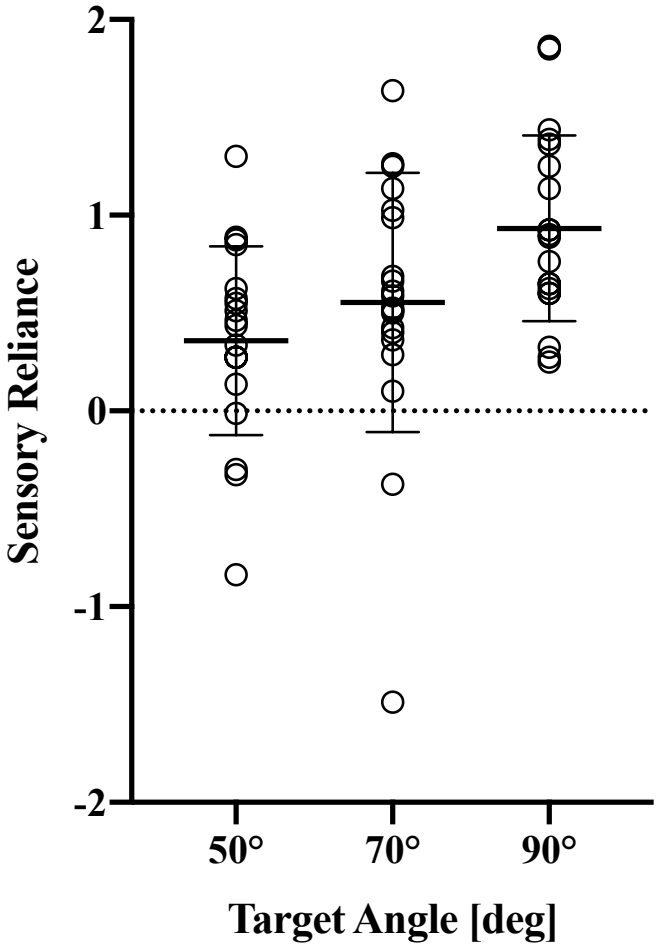

Figure 4.5. Sensory reliance as the difference between offset and accurate vision, as a ratio of total visual offset. A score of 1 indicates that the arm was repositioned to the location where the arm was seen (visual location), a score of 0 indicates that the arm was repositioned to the location where the arm was in space (proprioceptive location). Data represented are individual subjects (open circles) as well as group mean and standard deviation (horizontal lines).

4. Discussion

The integration of vision and proprioception in movement planning and execution can be flexibly weighted in order to achieve task success (Rossetti et al., 1995; Sober and Sabes, 2005, 2003). There is evidence that visual alteration of the body or environment in movement tasks can be compensated for by increasing reliance on proprioception (Block and Bastian, 2011; Rossetti et al., 1995; van Beers et al., 2002). The goal of this study was to determine how accuracy and consistency of a joint position matching task are influenced by alterations in visuoproprioceptive congruency in a VR environment. This study tested the hypotheses that a) Movements completed without vision of the upper limb will be less consistent, but no less accurate than movements completed with vision of the upper limb; b) Movements completed when vision and proprioception of the upper limb are spatially incongruent will be less consistent and less accurate than movements completed with vision of the upper limb; and c) Movements completed without vision of the upper limb will be more consistent and more accurate than movements completed when vision and proprioception of the upper limb are spatially incongruent. These hypotheses were based upon previous evidence of sensory weighting strategies and their relationship to the statistical variability of sensory signals (Block and Bastian, 2011; Ernst and Banks, 2002; Sober and Sabes, 2005, 2003; van Beers et al., 2002).

The VR environment provided the experimenter full control over the visual and auditory spaces while allowing participant movement in three dimensions. Variable and constant error were examined under three visual conditions (AV, NV, OV) at three target angles (50°, 70°, 90°). The visual offset of 8° was selected as it is below the threshold for a detectible visual offset as determined by pilot work and is outside the range of typical

joint position error for this testing paradigm (Edwards et al., 2016; King et al., 2013; Suprak et al., 2006).

No differences were seen between the AV and NV conditions at any target shoulder angle, supporting the prediction that removal of visual information would not alter movement accuracy. The values of CE in both the accurate vision and no vision conditions were well within the range of those seen in previous studies (Erickson and Karduna, 2012; Goble, 2010; Zuckerman et al., 1999). Over all angles, an average CE of -1.3 ± 3.4° was found in the accurate vision condition, where participants had both visual and proprioceptive information available, and -1.3 ± 3.5° in the no visual feedback condition, where only proprioceptive feedback information was available. Previous studies using active position matching tasks on the ipsilateral limb in similar populations have also shown error values between 1.5° and 3° in the absence of vision (Erickson and Karduna, 2012; Goble, 2010; Zuckerman et al., 1999). However, error increases in both younger (< 16 y) and older (> 35 y), topping out at approximately 6° in children (8 – 10 y) and 5° in elderly (70+ y) populations (Goble, 2010). Much of this error can likely be attributed to an underdeveloped central model of movement in younger populations and a degrading proprioceptive feedback system in older populations (Goble, 2010; Lei and Wang, 2018; Seidler et al., 2010). As proprioceptive feedback relies heavily on muscle spindles and cutaneous receptors in active joint positioning tasks (Hillier et al., 2015; Nyland et al., 1998), the degeneration of these systems leads to a stronger reliance on memory and centrally stored models of movement, which can also be compromised as a factor of age. While children generally have a healthy and intact sensory system, they lack the prior experience to develop reliable motor programs. The population represented

in this study (healthy, 25 ± 4 yrs) likely has an intact peripheral nervous system with well-functioning memory and CNS processing, enabling them to utilize proprioceptive feedback information effectively even in the absence of vision.

Lack of difference between AV and NV conditions could also be explained by the presentation modality. Results from the NV condition may be attributed to the fact that the presentation phase for all conditions provided accurate visual and proprioceptive information regarding the target, regardless of the replication condition. Therefore, the argument could be made that during the replication phase, participants utilized offline control systems, or an efference copy model, to successfully complete the movement (Barden et al., 2005; Cheng et al., 2008). Cheng et al. (2008) tested aiming movements with alternating presentations of either accurate vision or no vision and found that visual conditions from the previous trial influenced performance on the subsequent trial. These findings provide both an alternate explanation for the lack of difference between AV and NV conditions and support the methodology of providing the same sensory information during each presentation phase regardless of replication condition. The presentation phase between each replication phase provides a chance to update the stored model with accurate information, decreasing the chances that our results are merely an accumulation of error.

Note that with only four trials per condition, the interpretation of VE results should be taken with caution. No differences in VE were seen between target angles or visual conditions (**Fig. 4.4a**). The consistency between conditions in combination with the low averages across conditions indicates high task reliability among participants. Had participants been guessing at the target angles, much higher variable error would be

expected. This is in agreement with previous repositioning studies investigating vision and proprioception (van Beers et al., 1996) and further supports the choice of 8° as an unnoticeable offset, assuming that a noticeable perturbation would decrease participant reliability. However, some increase in VE in the OV condition was expected as visuoproprioceptive mismatches introduce noise into the system. Previous studies have seen that both alterations in a sensory signal and issues during integration of sensory signals can lead to large changes in movement outcomes (Berkinblit et al., 1995; Cruse et al., 1990; Darling and Miller, 1993; Soechting and Flanders, 1989). This being the case, one of the following likely occurred in the present study: participants a) completed the task by relying on feedforward information from motor planning and efference copy mechanisms, b) did not interpret the visual offset as an error, or c) interpreted the visual offset as an error and changed how they relied on sensory information to accommodate.

Support for a sensory reweighting strategy being employed in the OV condition is provided by the observed increase in CE at all angles. Specifically, the presentation of an 8° visual offset resulted in an undershoot of 6.6° at the 70° target and 9.0° at the 90° target. These error values closely match the magnitude of the induced visual offset, indicating that participants matched the visual representation of the arm as opposed to the proprioceptive representation. This holds true in light of the fact that the presentation phase of the task was completed with accurate visual and proprioceptive information, meaning that the most recent update to an efference copy being used in the replication phase should also have this accurate information (Cheng et al., 2008). Results are in close agreement with reaching studies which visually distort hand location using mirrors or prism goggles and demonstrate consistent errors in favor of visual information

(Bagesteiro et al., 2006; Holmes and Spence, 2005; Rossetti et al., 1995; Sainburg et al., 2003; Sarlegna and Sainburg, 2007; Sober and Sabes, 2003). This is particularly true in end point reaching studies which also use a distortion that is not noticeable to the participant (Bagesteiro et al., 2006; Goodale et al., 1986). An estimation of this sensory reliance is provided in **Figure 4.5**, in which the difference between AV and OV conditions are compared to the total induced visual offset.

Sensory reliance scores at 50° (M = 0.4) and 70° (M = 0.5) indicate that visual and proprioceptive sensory feedback are both being relied upon to inform movement. Sensory reliance scores at 90° (M = 0.9) indicate that offset visual feedback is being relied upon more heavily than the accurate proprioceptive feedback. Given these results, it is unlikely that participants completed the task by relying on feedforward information from motor planning and efference copy mechanisms. The results support the idea that participants relied on sensory feedback when determining the repositioning angle. As accurate visual and proprioceptive information from the presentation phase were available for use during feedforward control, a heavy reliance on this control strategy would have resulted in a closer match to the proprioceptive target during the OV condition. In terms of the variables measured in this study, a feedforward control dominant strategy would have resulted in values of CE and reliance scores close to 0 during all conditions. Similar values of VE across conditions, increases in CE in the OV condition, and the estimated reliance on visual information support the idea that vision was the more dominant mode of sensory feedback for control of joint position matching in a VR environment. This held true even when vision of the limb was offset and proprioception of the limb was accurate.

One limitation to the present study was that while participants were instructed to follow the auditory cues as guidance during the presentation phase of the task, they were not given instruction on what inputs to use in the replication phase. Due to this design, we cannot account for varying movement strategies employed by participants during the replication phase. However, this was done intentionally to avoid the introduction of a conscious bias to the visual or proprioceptive cues. Further, we cannot rule out a reduction in movement accuracy due to boredom. Participants performed 36 trials in this study, equating to 72 shoulder flexion movements and some participants did report becoming bored. Any potential effect of boredom should be attenuated in the randomization process of our study design. Additionally, there was no effect of sequence (order of visual conditions) on either accuracy ($p = 0.75$) or consistency ($p = 0.94$). In combination with the lack of difference in VE between conditions indicates that variability did not increase over time due to boredom or fatigue.

Another possible limitation to our analysis could be low trial numbers, 4 trials were collected at each combination of visual and angular condition. However, this is a standard in the field of active joint position matching study (Han et al., 2016) and therefore makes this study comparable to many others in the field. Finally, some participants reported their vision of the tracker being occluded at 50° due to a limited field of view in the VR goggles. This could explain the increase in variability at this target angle, as seen in the higher standard deviations across the 50° target angle. In future studies it will be prudent to either select a goggle with a wider field of view or eliminate flexion angles in the low and high visual range.

In summary, neither accuracy (CE) nor consistency (VE) was altered with the removal of visual information. A coordinated effort between online proprioceptive sensory information and offline feedforward control systems and efference copy mechanisms provided sufficient information to successfully complete the movement task. Consistency remained unchanged with the introduction of a visual offset, which induced a visuoproprioceptive mismatch, indicating that this mismatch was accommodated for by the sensorimotor system. Accuracy does decrease with the introduction of an unnoticeable visual offset, with resultant movement patterns showing a close match between repositioning angle and visual target angle. Sensory reliance estimates suggest that at the higher target angle, vision is being relied on much more than proprioception and at lower target angles, vision and proprioception are being relied on equally.

5. Bridge

The study outlined in this chapter investigated how alterations in visuoproprioceptive congruency affects the accuracy and consistency of a joint position matching task in a VR environment. No differences were found in accuracy between movements completed with or without vision of the upper limb and CE values in both conditions were within the range observed in previous studies. The introduction of a visual offset resulted in an increase in CE values, indicating that participants matched the visual representation of the arm rather than the proprioceptive representation. Sensory reliance scores were estimated, indicating that visual feedback was relied upon more heavily than proprioceptive feedback.

These findings contribute to the extensive body of knowledge emphasizing the significance of vision in movement planning and execution within an intact system. Virtual reality systems inherently disrupt vision by occupying the visual field with a screen. Chapters V and VI of this dissertation aim to explore the impact of such alterations in the presentation of visual information on the generation of subsequent movements.

CHAPTER V

REACHING TO A VISUAL TARGET IN THE VIRTUAL AND REAL-WORLDS

This work is currently in preparation for submission to the *Journal of Virtual Reality* and is co-authored by Kate A. Spitzley, Zachary A. Hoffman, Samuel E. Perlman, and Andrew R. Karduna. Kate A. Spitzley contributed to study design, experimental work including data collection and analysis, and writing. Zachary A. Hoffman and Samuel E. Perlman contributed to study design and data collection. Andrew R. Karduna contributed to study design, research mentorship, and editorial assistance.

1. Introduction

Immersive virtual reality (VR) systems have recently undergone substantial technological updates and reductions in cost. This rise in accessibility has been paralleled by increased use of these systems in gaming, education, retail, sports, and healthcare settings (Wohlgenannt et al., 2020). In the healthcare domain, VR systems are being used to train surgeons (Egger et al., 2017), provide clinical and in-home health care (Ikbali Afsar et al., 2018; Janeh et al., 2019; Levin et al., 2015b; Waked and Eid, 2019), and teach sensorimotor skills (Wright, 2013). With the average consumer VR product costing under $1,000, and the application market providing easy access to gamified rehabilitation tools, it is unsurprising that this technology has been readily adopted. The potential benefits from using a technology that easily provides 3D, fully controllable environments in-clinic or at-home certainly deserve the increased attention. The potential clinical benefits are evident in research showing VR interventions to be effective in reducing pain

during physical therapy treatment (Waked and Eid, 2019), aiding in stroke rehabilitation (Ikbali Afsar et al., 2018; Mekbib et al., 2020), and providing gait training in populations with Parkinson's disease (Janeh et al., 2019). With the adoption of tools made accessible by the use of VR systems, each of these clinical populations stand to benefit from a less expensive and more portable therapeutic option.

However, increasing evidence of altered movement patterns (Bourdin et al., 2019; Gonzalez-Franco et al., 2019; Harris et al., 2019) and unintended aftereffects of sensorimotor training (Drew et al., 2020; Wright, 2014) in virtual environments highlight the shortcomings of deploying VR applications in clinical settings without first fully testing the effects (Keshner et al., 2019). For example, individuals routinely underestimate distances by 10% during walking in VR (Gonzalez-Franco et al., 2019) and a VR-based sensorimotor training routine reduced accuracy in a throwing task (Drew et al., 2020). These results suggest that ecological validity and transferability of training received in a VR environment should be assessed before deployment. It is particularly important that interventions for clinical populations be designed to minimize unexpected and detrimental outcomes.

Imaging studies have provided some insight into the behavioral differences seen between real and virtual environments, demonstrating that the brain processes depth cues differently in VR compared to real-world (RW) (Beck et al., 2010). Limitations to depth perception could explain disturbances in gait and throwing tasks, as depth estimations are essential for both. Additionally, properties that differ between the presentation of a visual field on a screen and in the RW such as refresh rate, field of view, and resolution can contribute to differences in central processing. Uncertainty or reduced fidelity introduced

to the visual system may cause a change in sensory integration strategy or alter movement response to stimuli (Faisal et al., 2008; Körding and Wolpert, 2006). It is difficult to balance the potential benefits of providing healthcare options that are accessible and increase compliance to rehabilitation protocols, with the potential risks of the unknown aftereffects from their use. An important step in this decision-making process is gaining an understanding of task-specific differences in outcomes between virtual and real settings. With greater knowledge of the potential differences, clinicians can be empowered to make well informed decisions for their patients.

Upper limb movements are particularly interesting in the context of VR because the upper limbs are generally well within the field of view of current headsets and are the main point of contact between the user and the virtual environment. Due to this, developers are continually working to release improved tracking of hands, including gesture-based controls. Virtual reality applications for stroke recovery and injury rehabilitation which involve the upper limb are of interest to both the scientific and clinical communities and are gaining popularity in both (Juan et al., 2022; Keshner et al., 2019; Mekbib et al., 2020). One analysis demonstrated that in a patient population recovering from stroke, VR training produced significantly greater improvements in upper limb function when compared to conventional training (Mekbib et al., 2020). As the upper limb appears to be an emerging area of expansion for VR-based clinical tools, it is important to identify differences between movements in real and virtual environments.

Reaching movements toward a visual target are popular goal-oriented tasks for both scientific testing and functional rehabilitation protocols. This task paradigm requires that a visual goal for movement be identified, a plan of action for reaching the goal be

formed, and that the plan be executed as intended (Goodale, 2011). These tasks therefore require multi-step processing and transformation of sensory information into motor output, each of which can be disrupted by injury or unexpected noise within the nervous system (Faisal et al., 2008; Körding and Wolpert, 2006). It has been specifically proposed that presenting sensory information using artificial inputs such as screens, headphones, and vibratory haptic cues leads to a shift in the neural pathways used to process sensory information for the production of movement (Harris et al., 2019). If this is the case, differences in activation could be seen in brain areas associated with sensory processing, motor planning, and movement execution as well as functional outcome measures.

Indications that artificially presented visual information may alter both central processing and movement output, paired with the widespread and rapidly expanding use of VR systems across a variety of fields, highlight the importance of understanding interactions between VR and the user. As the main point of contact between user and environment, the upper limb is an essential component of this interaction. Understanding how movement of the upper limb changes in response to cues in the virtual visual environment can provide insight into the appropriateness of these systems for applications in healthcare and other domains. The present study aims to determine if there are differences in upper limb kinematics and kinetics between VR and RW environments during a visually cued, reaching to target movement. It was hypothesized that movement in VR would be a) slower and b) less smooth than movement in RW, as reflected by both kinematic and kinetic measures.

2. Methods

2.1 Participants

Fifty-one right-upper limb dominant participants were recruited to perform a reaching task to visual targets in RW and VR environments. Eligibility criteria included healthy individuals ages 18 to 45, free of upper body pain within the two weeks prior, upper limb injury within the past year, neurological disorder, and uncorrected impaired vision. All participants completed the informed consent and study protocols as approved by the Internal Review Board at the University of Oregon before undergoing any research activities.

Participants were randomly assigned to one of two groups. Group 1 (RWG, n = 25, 20.5±2.7 yrs., 14 F 11 M) performed three blocks of the reaching task in the RW. Group 2 (VRG, n = 26, 22.7±5.1 yrs., 18 F 8 M) performed three blocks of the reaching task in VR. Each block consisted of 27 reaches in total, three reaches to each of nine visual targets [**Fig. 5.1**]. The order of target presentation was randomized within each block.

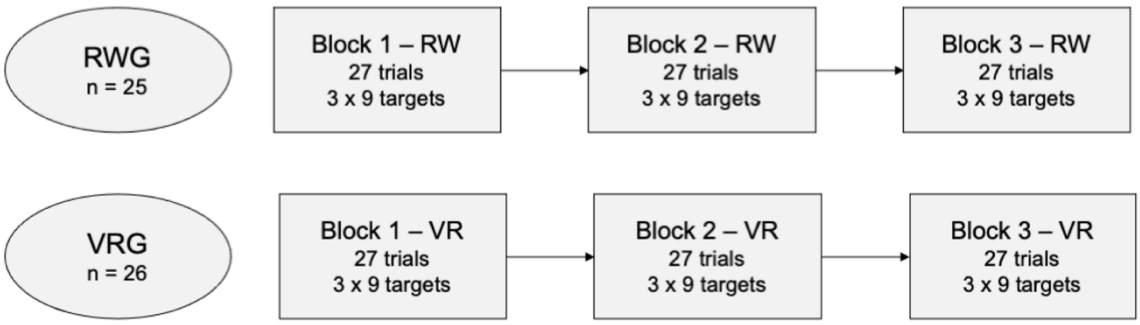

Fig. 5.1 Study design schematic demonstrating the breakdown of 51 participants into two groups, RWG and VRG. Each group performed three blocks of the task consisting of 27 trials each, 3 reaches to each of the 9 visual targets.

2.2 Setup

2.2.1 Environments

In the RW, visual reaching targets were presented using a custom-made LED board. The board was designed using a three-foot square opaque white plastic sheet behind which LEDs were mounted within 3D printed, cone shaped mounting brackets. The effect of this was to diffuse the light from each LED through the plastic, creating 5 cm visual targets on the front of the board. Targets were 23 cm apart at their center and arranged in a three-by-three grid evenly across the board. Individual targets will be referred to with reference to their position on the board. Targets in the top row are represented with a 'T', the middle row represented with a 'M', and the bottom row represented with a 'B'. Targets in the right column are represented with a 'R', the middle column represented with a 'M', and the left column represented with a 'L' [**Fig. 5.2**]. As participants performed reaching movements with their right upper limb, and were positioned facing the board, right column targets elicited ipsilateral reaches and left column targets elicited contralateral reaches. Participants were positioned so that the middle of their body was in alignment with the middle column of targets.

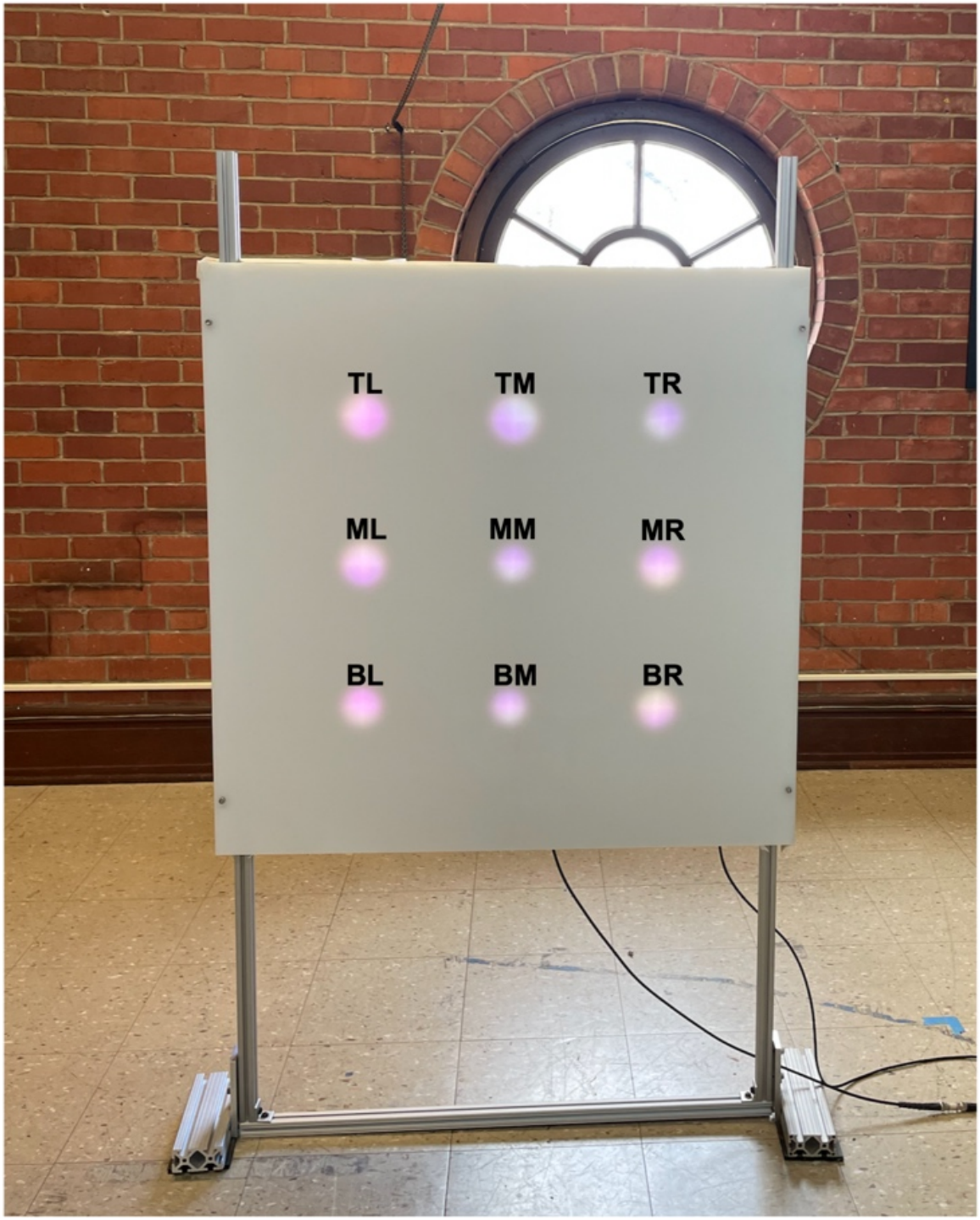

Fig. 5.2 Visual target board with all targets activated. Targets are denoted with respect to their row then column position on the board. TL: top left, TM: top middle, TR: top right, ML: middle left, MM: middle middle, MR: middle right, BL: bottom left, BM: bottom middle, BR: bottom right.

In VR, a digital recreation of the laboratory environment, including the LED board, was generated using Blender (Blender, Amsterdam, Netherlands) [**Fig. 4.3**]. Reference measurements and photographs were obtained to minimize discrepancies in scale between the real and virtual spaces. Image textures were applied to the models, providing color, roughness, and normal (simulated depth) data. Careful consideration was taken when determining polygon/texture resolution to balance physical accuracy and computational workload, ensuring stable framerates. The completed 3D models were imported into Unity in FBX format. In Unity, the High-Definition Render Pipeline and realistic global illumination light system were used. Calibration of the VR and Unity camera rig positions and the position of the target board within the virtual and real spaces ensured that the participants found themselves in the same position and orientation in the real and virtual environments.

Fig. 5.3 The real-world (a) virtual (b) environments. Target board in positioned in the bottom left corner of both images.

2.2.2 Equipment

An HTV VIVE Pro Eye headset (2880 x 1600 combined resolution, Dual OLED 3.5” diagonal display, 110° field of view) and VIVE version 3.0 Trackers (HTC VIVE, Taoyuan City, Taiwan) displayed the virtual environment and captured position and orientation of the trunk, right arm, and right wrist segments, respectively (Spitzley and Karduna, 2019). A rigid wrist brace was used to reduce the hand and forearm into a single distal segment. In VR, a hand-model was fixed to the wrist tracker and placed in alignment with the participants own hand using visual landmarks in the virtual space. A static reference pose was captured prior to movement trials.

Electrical activity of the right biceps brachii, triceps brachii, anterior deltoid, middle deltoid, and upper trapezius muscles was captured using a Delsys Trigno wireless EMG system (Delsys Inc., Boston, MA, USA). These muscles were selected to represent activity related to movement at the elbow, glenohumeral, and scapulothoracic joints, respectively. Skin sites were cleaned and lightly abraded using 70% isopropyl alcohol wipes. Surface sensor placement followed standards developed by Hermens et al. (2000).

2.2.3 Data Output and Synchronization

Customized Arduino (Arduino, New York, New York, USA), Unity (Unity, San Francisco, CA, USA), and LabVIEW (National Instruments, Austin, TX, USA) programs in concert with an Arduino Mega 2560 REV3 microcontroller board facilitated communication between and data output from the light board, VR, and EMG systems. To turn an LED on or off, a Unity script sent information containing the desired target name to an Arduino script. This information was used to turn on or off specified channels on

the microcontroller board to which the LEDs were connected. To select targets on the virtual LED board, Unity used the target name to select an emission texture on the virtual target board, reflecting the corresponding target location and luminance.

Kinematics and EMG were synchronized using a 5V square wave, communicated to both an A/D board (National Instruments Corporation, Austin, TX, USA) and Unity. The A/D board also received data from the surface EMG sensors, which was captured wirelessly by the base station and ported to the board for synchronization. A customized LabVIEW program captured the EMG and synchronization channels. Unity recorded the 5V wave within the kinematics file and a custom Unity script output synchronization data, along with position and orientation from the trackers. EMG was captured at 1925 Hz and kinematics at 90 Hz, reflecting the maximum sample rate of each system.

2.3 Task Protocol

Following sensor placement and static reference pose capture, participants were seated with their arm flexed to 90° directly in front of their shoulder and positioned one inch more than arm's distance from the LED board, facing the board. A research team member talked through the experimental protocol with the participant and confirmed that they understood the task and were prepared to continue. If a participant was completing the task in VR, a team member assisted in placement and fitting of the headset, confirming comfort, field of view, and clarity of visual signal with the participant. If a participant was completing the task in RW, a team member placed the headset in a standardized position within the room and confirmed that the participant was comfortable and ready to proceed. Once the participant confirmed that they were prepared to begin, all

trials within each block were completed without a break. Breaks between blocks were provided, and participants were informed that they could request added breaks at any point. No extra breaks were requested nor was removal of the headset needed for any reason prior to task completion.

Participants were instructed to wait with their arms relaxed by their side until a target light came on, to reach to the target using their right arm until the it turned off, then to return to the relaxed waiting position [**Fig. 5.4**]. Task completion was indicated by the light turning off and a simultaneous sound from the system confirming success. Target lights were triggered to turn on when the wrist tracker was at the participant's side and moving less than 0.2 m/s and was triggered to turn off when the wrist tracker was within 0.2 m of the target. These thresholds were determined during pilot testing and allowed for normal ambient movement and for the hand to come close to touching the board without making contact.

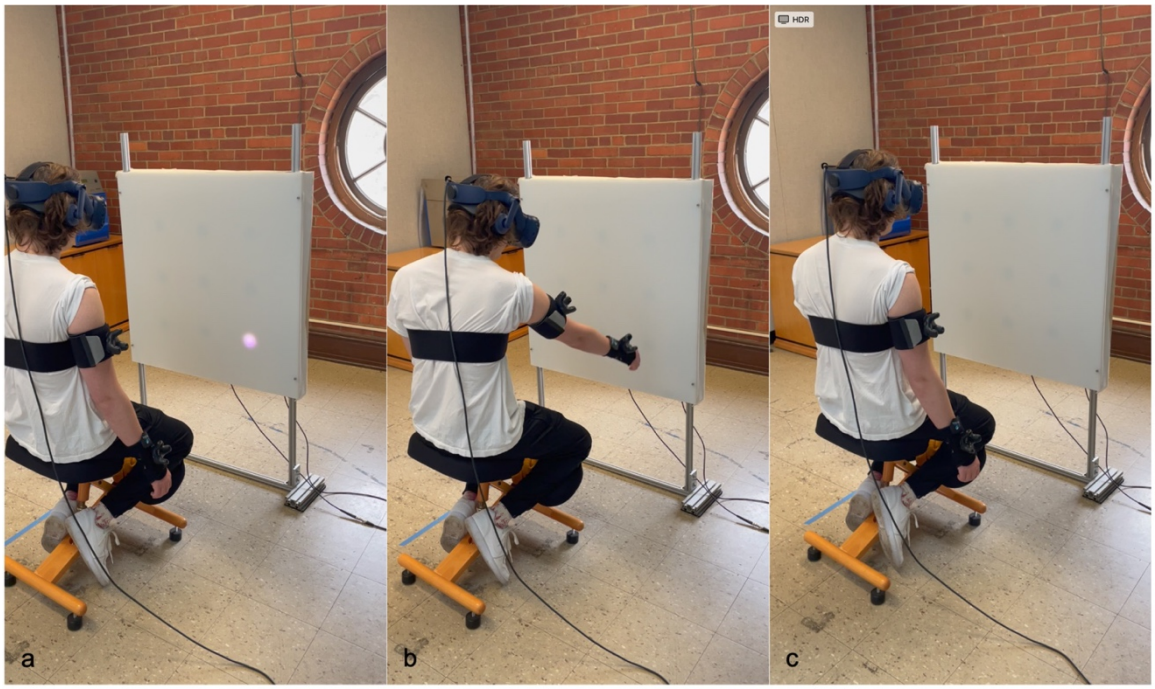

Fig. 5.4 Participant performing a reaching trial in a virtual environment. During each trial, participants waited until the target lit up (a), reached toward the target until the light turned off (b), and returned to the starting position (c). In this example, the BR target is activated.

2.4 Data Reduction and Statistical Analysis

Orientation of the VIVE trackers was output in quaternion format to avoid computational issues related to Unity's use of multiple left-handed coordinate systems. Relative orientations between trunk and arm and arm and wrist represented shoulder angle and elbow angle, respectively. These were solved for by converting quaternions to direction cosign matrices and then to Euler angles using rotation sequences outlined in Wu et al. (2005) during the static pose and dynamic trials. Peak shoulder elevation was calculated as the maximum shoulder elevation angle during the reaching phase of movement. Functional range of motion (fROM) was calculated as the maximum flexion or elevation angle minus the minimum flexion or elevation angle during the reaching phase of movement.

The tracker mounted on the forearm/wrist segment approximated endpoint position for all measures related to movement timing. Response time was measured as the time between when the target light came on to the time when the participant began moving toward the target. Time to target was measured as the time between when the participant began moving toward the target and the time when they reached the target. Time at target was measured as the time between when the participant reached the target and when they began moving away from the target. Outcomes related to endpoint speed were calculated during the reaching phase of movement only.

Delsys hardware filtered all EMG channels using a band-pass of 20-450 Hz. The Common Mode Rejection Ratio of this system is greater than 80 dB. Digital signals were

collected as a single file for each block, the trigger signal was used to separate individual trials in post-processing. Signals were mean centered, rectified, and smoothed using an RMS sliding window of 50 milliseconds. For all muscles number of EMG amplitude peaks and location of EMG amplitude peaks were identified during the reaching phase of movement using the *findpeaks* function in MATLAB.

Trials were cropped to begin when the target was lit and end when the endpoint reached the target and was at its lowest speed. Cropped trials were normalized to 101 data points, representing a complete reaching cycle. For analysis of EMG signals, one participant was removed from RWG and two were removed from VRG due to equipment malfunction. To examine the differences in kinematics and kinetics in RW and VR, block 3 was compared between RWG and VRG. By this block, participants had already performed 54 trials during blocks 1 and 2 to familiarize themselves both with the task and the environment.

Block 3 of RWG and VRG was compared at each target using either a two-sample *t*-test ($\alpha = 0.05$) or Welch's *t*-test ($\alpha = 0.05$), as determined by a two-sample *F*-test for equal variances. For measures in which either no differences were found, or differences were found across all targets, data from targets were combined and are reported as a single comparison between RWG and VRG. For measures in which differences were found in some, but not all the targets, data from each target was analyzed separately and comparisons between RWG and VRG are reported for each target individually. Additionally, two-sample *t*-tests using One-Dimensional Statistical Parametric Mapping (SPM1d, Pataky 2012) analysis were used to compare shoulder angles and elbow angles between RWG and VRG from 0 –100% of the reaching to target phase.

3. Results

3.1 Kinematic Measures

Three kinematic measures were significantly different between RWG and VRG across all targets. Response time was lower in RWG as compared to VRG (0.28±0.008 sec, 0.35±0.01 sec; $p < 0.0001$, $t_{49} = 1.86$). Mean endpoint speed was faster in RWG as compared to VRG (0.65±0.02 m/s, 0.57±0.02 m/s; $p < 0.01$, $t_{49} = 3.07$). Peak endpoint speed was higher in RWG as compared to VRG (1.7±0.06 m/s, 1.5±0.04 m/s; $p = 0.04$, $t_{41.18} = 2.1$). Peak endpoint speed was also calculated during the reaching phase of the task and used the wrist tracker as an endpoint. [**Fig. 5.5**].

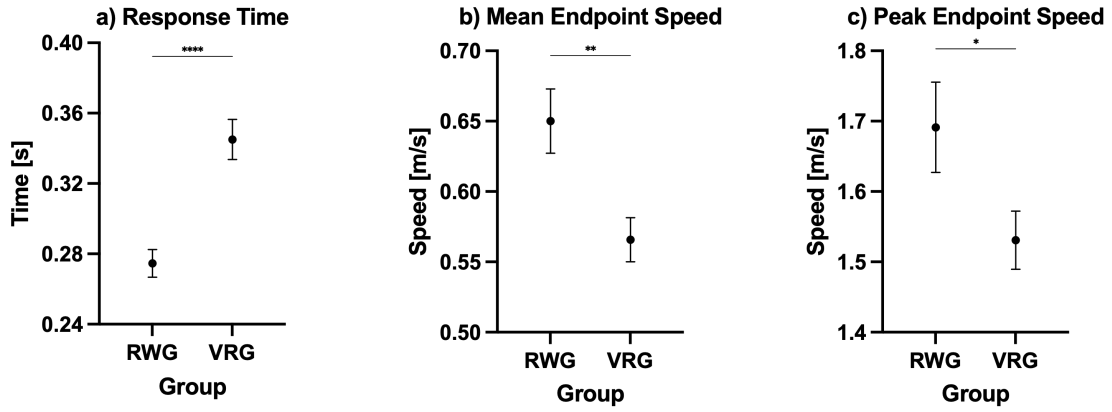

Fig. 5.5 Significant differences were found between RWG and VRG across all targets in the kinematic measures of response time (a), mean endpoint speed (b), and peak endpoint speed (c). Mean ± SEM is represented for each group. * = $p < 0.05$, ** = $p < 0.01$, **** = $p < 0.0001$

Time to target and elbow functional range of motion (fROM) were significantly different between RWG and VRG across some targets, but not all. Time to target was lower in RWG as compared to VRG at the TR (0.47±0.03 sec, 0.56±0.03 sec; $p = 0.03$, $t_{49} = 2.24$), MR (0.42±0.03 sec, 0.50±0.02 sec; $p = 0.04$, $t_{49} = 2.12$), BM (0.48±0.04 sec, 0.58±0.03 sec; $p = 0.04$, $t_{49} = 2.14$), and BR (0.45±0.04 sec, 0.62±0.05 sec; $p < 0.01$, t_{49}

= 2.80) targets [**Fig. 5.6**]. Time to target was measured as the time between when the participant began moving toward the target and the time when they reached the target. Elbow fROM was lower in RWG as compared to VRG at the TL (19±2 °, 26±3 °, p = 0.03; t_{49} = 2.27), TR (19±3 °, 28±3 °; p = 0.03, t_{49} = 2.21), ML (15±2 °, 22±2 °; p = 0.04, t_{49} = 2.15), and MR (15±2 °, 21±2 °; p = 0.02, t_{49} = 2.44) targets [**Fig. 5.7**].

No differences between RWG and VRG were seen in measures of peak shoulder elevation (71±2 deg, 73±2 deg; p = 0.54, t_{49} = 0.62), shoulder fROM (60±2 deg, 61±2 deg; p = 0.61, t_{49} = 0.52), and time at target (0.55±0.02 sec, 0.43±0.02 sec; p = 0.66, t_{49} = 0.45) at any of the targets.

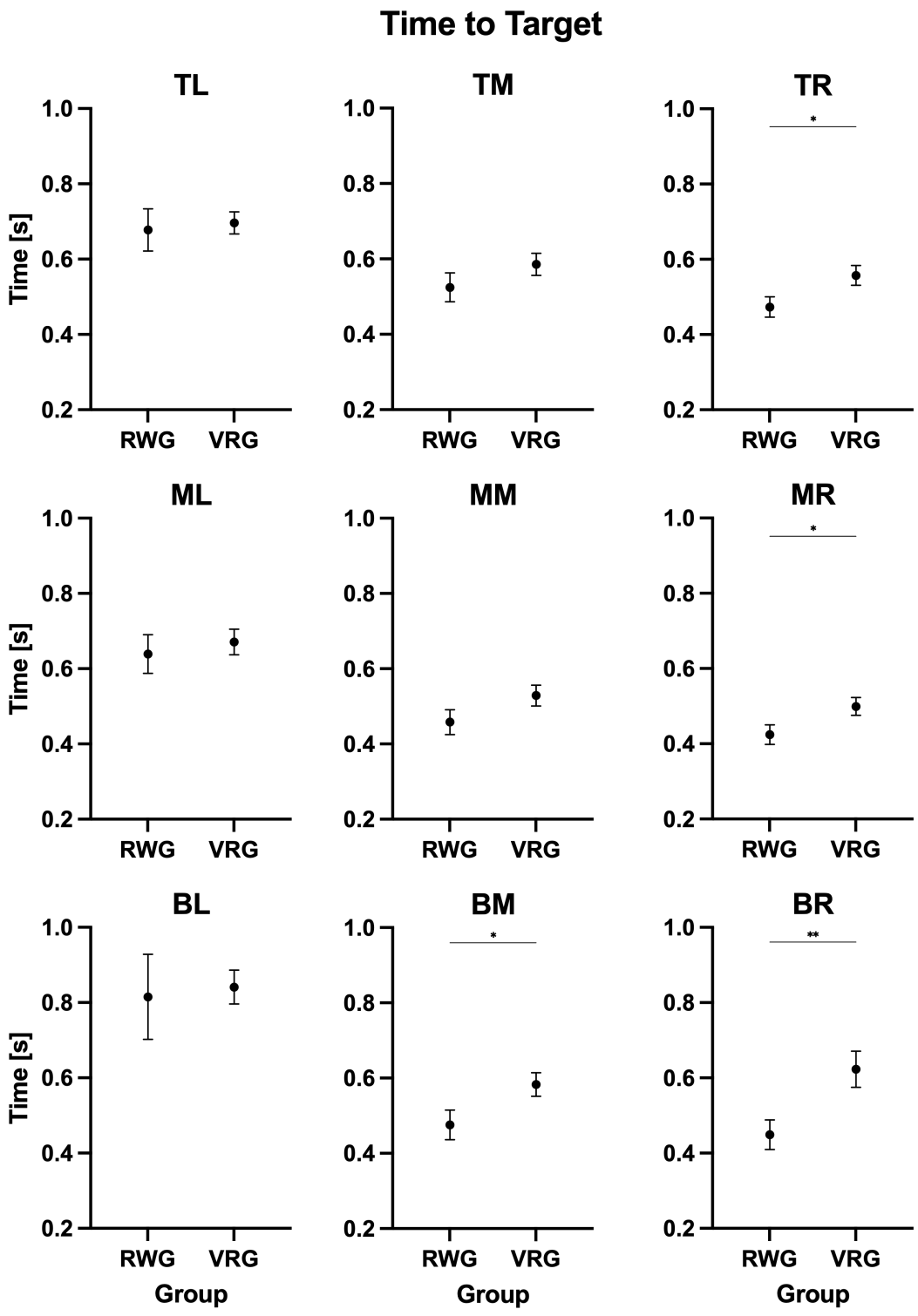

Fig. 5.6 Time to target was significantly lower in RWG as compared to VRG at the TR, MR, BM, and BR targets. Mean ± SEM is represented for each group at each target. * = $p < 0.05$, ** = $p < 0.01$

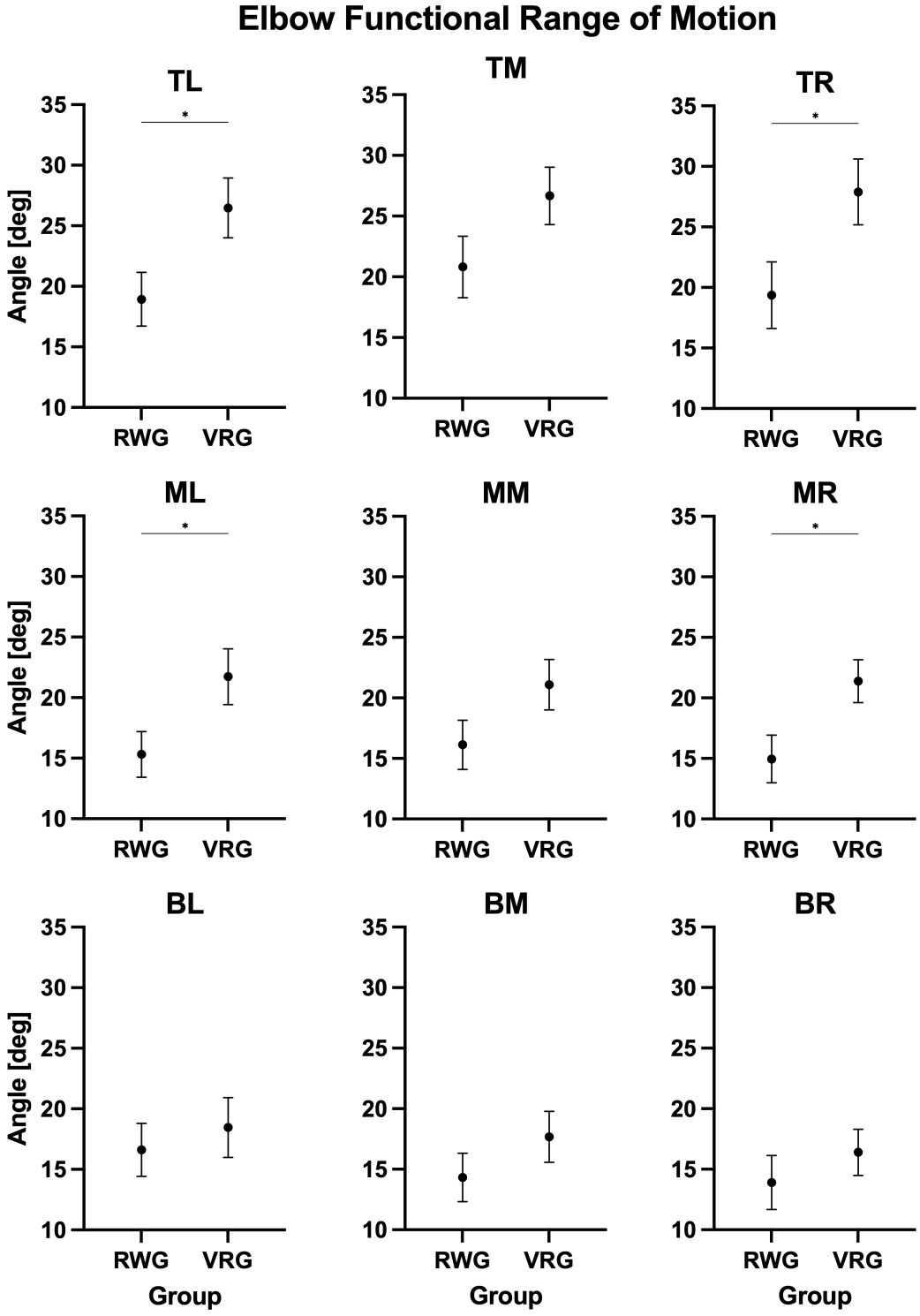

Fig. 5.7 Elbow fROM was significantly lower in RWG as compared to VRG at the TL, TR, ML, and MR targets. Mean ± SEM is represented for each group at each target. * = $p < 0.05$

SPM1d analysis of shoulder angle over the reaching movement showed that from 13 to 60% of movement, shoulder angle was higher in RWG than VRG ($p = 0.05$, $t = 2.563$, **Fig. 5.8**). The same analysis of elbow angle showed that from 0 and 23% of movement ($p = 0.032$, $t = 2.529$), elbow angle was higher in RWG than VRG and from 40 and 80% of movement, elbow angle was lower in RWG than VRG ($p = 0.05$, $t = 2.529$, **Fig. 5.9**).

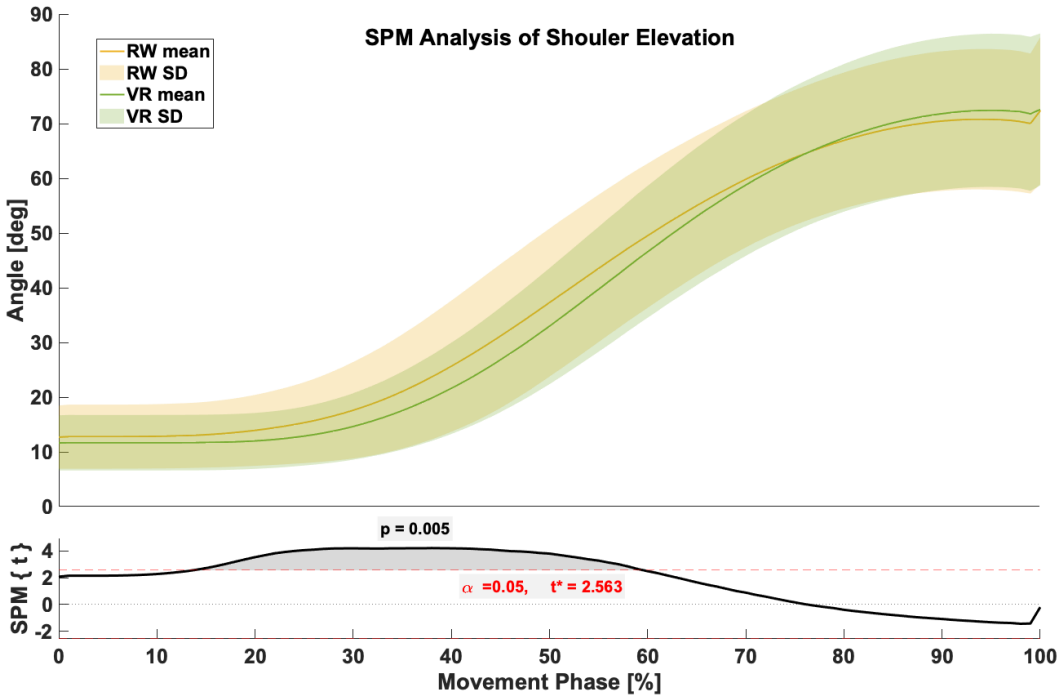

Fig. 5.8 Shoulder elevation angles from 0 – 100% of the movement phase are represented on the primary y-axis. Mean ± SD of RWG in yellow and VRG in green. SPM1d results are displayed on secondary y-axis. Between 13 and 60% of movement, shoulder elevation angle was higher in RWG than VRG.

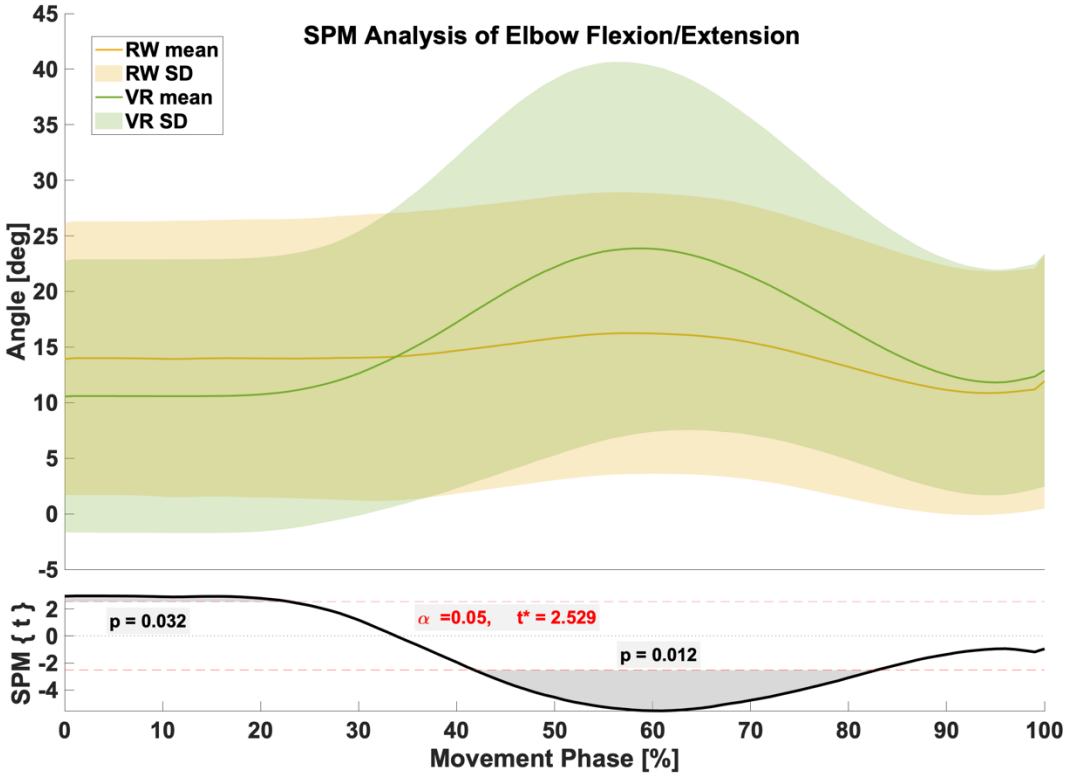

Fig. 5.9 Elbow angles from 0 – 100% of the movement phase are represented on the primary y-axis. Mean ± SD of RWG in yellow and VRG in green. Positive numbers represent flexion, negative numbers represent extension. SPM1d results are displayed on secondary y-axis. Between 0 and 23% of movement, elbow angle was higher in RWG than VRG. Between 40 and 80% of movement, elbow angle was lower in RWG than VRG.

3.2 Kinetic Measures

Three kinetic measures were significantly different between RWG and VRG across all targets [**Fig. 5.10**]. There were fewer amplitude peaks in the Bicep EMG in RWG as compared to VRG (3.0±0.1, 3.4±0.1; $p = 0.03$, $t_{46} = 2.27$). The highest peak in the biceps brachii EMG signal was earlier in the reaching phase in RWG as compared to VRG (39±3 %, 55±3 %, $p < 0.001$, $t_{46} = 3.56$). The highest peak in the anterior deltoid

EMG signal was earlier within the reaching phase in as compared to VRG (65±2 %, 73±1 %%, $p < 0.01$, $t_{35.52} = 3.07$).

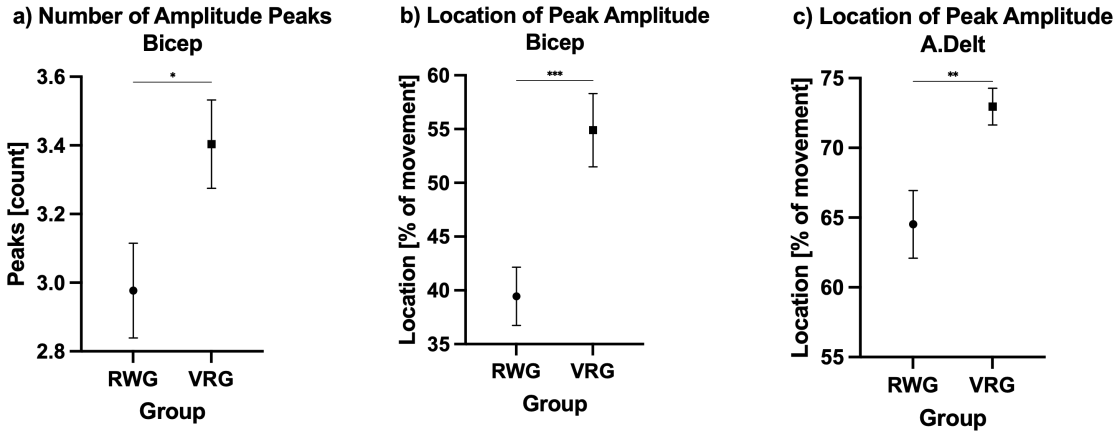

Fig. 5.10 Significant differences were found between RWG and VRG across all targets in the kinetic measures of number of amplitude peaks in the bicep brachii (a), location of peak amplitude in the bicep brachii (b), and location of peak amplitude in the anterior deltoid (c). Mean ± SEM is represented for each group. * = $p < 0.05$, ** = $p < 0.01$, *** = $p < 0.001$

Number of amplitude peaks in the anterior deltoid and upper trapezius EMG signals and the location of the highest peak in the upper trapezius EMG signal were different between RWG and VRG across some targets, but not all. There were fewer amplitude peaks in the anterior deltoid EMG signal in RWG as compared to VRG at the BM (2.7±0.1, 3.1±0.1; $p = 0.02$, $t_{46} = 2.53$) and BR (2.9±0.2, 3.6±0.3; $p = 0.03$, $t_{38.7} = 2.24$) targets [**Fig. 5.11**]. There were fewer amplitude peaks in the upper trapezius EMG signal in RWG as compared to VRG at the TR (2.7±0.1, 3.3±0.1; $p = 0.001$, $t_{46} = 3.53$) target [**Fig. 5.12**]. The highest peak in the upper trapezius EMG signal was earlier in the reaching phase in RWG as compared to VRG at the TM (45±3 %, 59±4 %; $p < 0.01$, $t_{46} = 2.72$), TR (45±3 %, 56±4 %; $p = 0.02$, $t_{46} = 2.32$), and MR (46±4 %, 56±3 %; $p = 0.04$, $t_{46} = 2.05$) targets [**Fig. 5.13**].

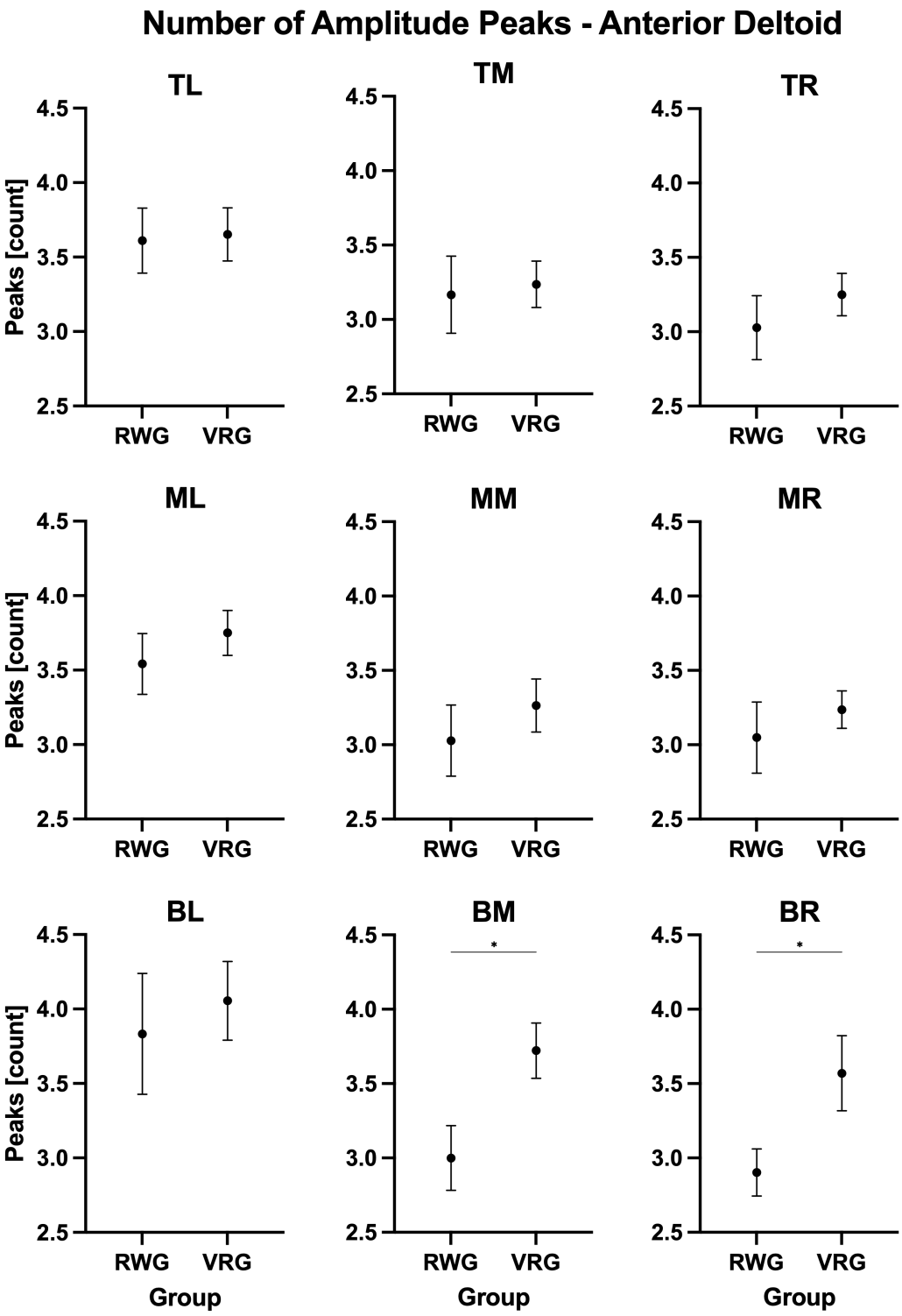

Fig. 5.11 There were significantly fewer amplitude peaks for the anterior deltoid EMG signal in RWG as compared to VRG at the BM and BR targets. Mean ± SEM is represented for each group at each target. * = $p < 0.05$

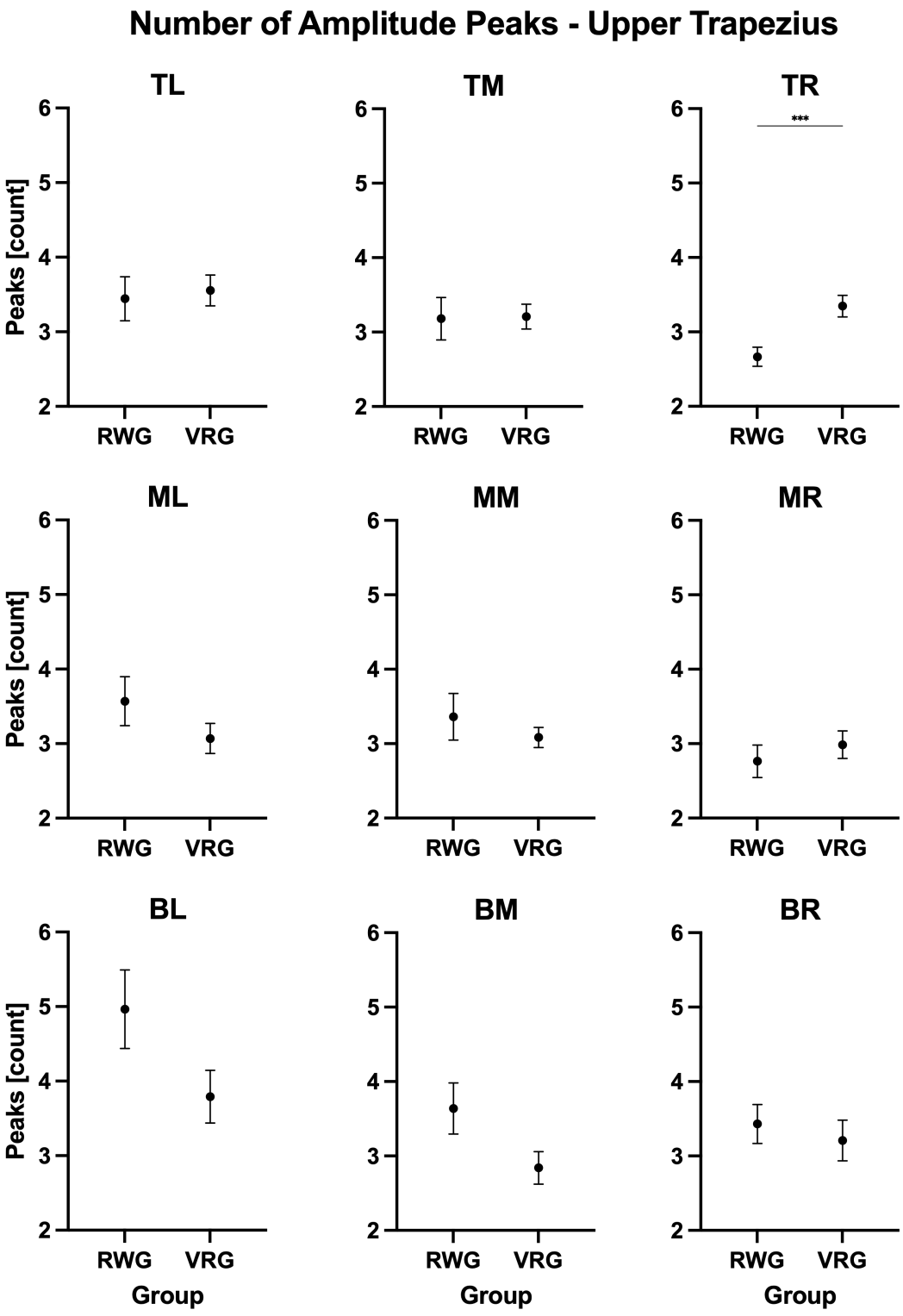

Fig. 5.12 There were significantly fewer amplitude peaks the upper trapezius EMG signal in RWG as compared to VRG at TR target. Mean ± SEM is represented for each group at each target. *** = $p < 0.001$

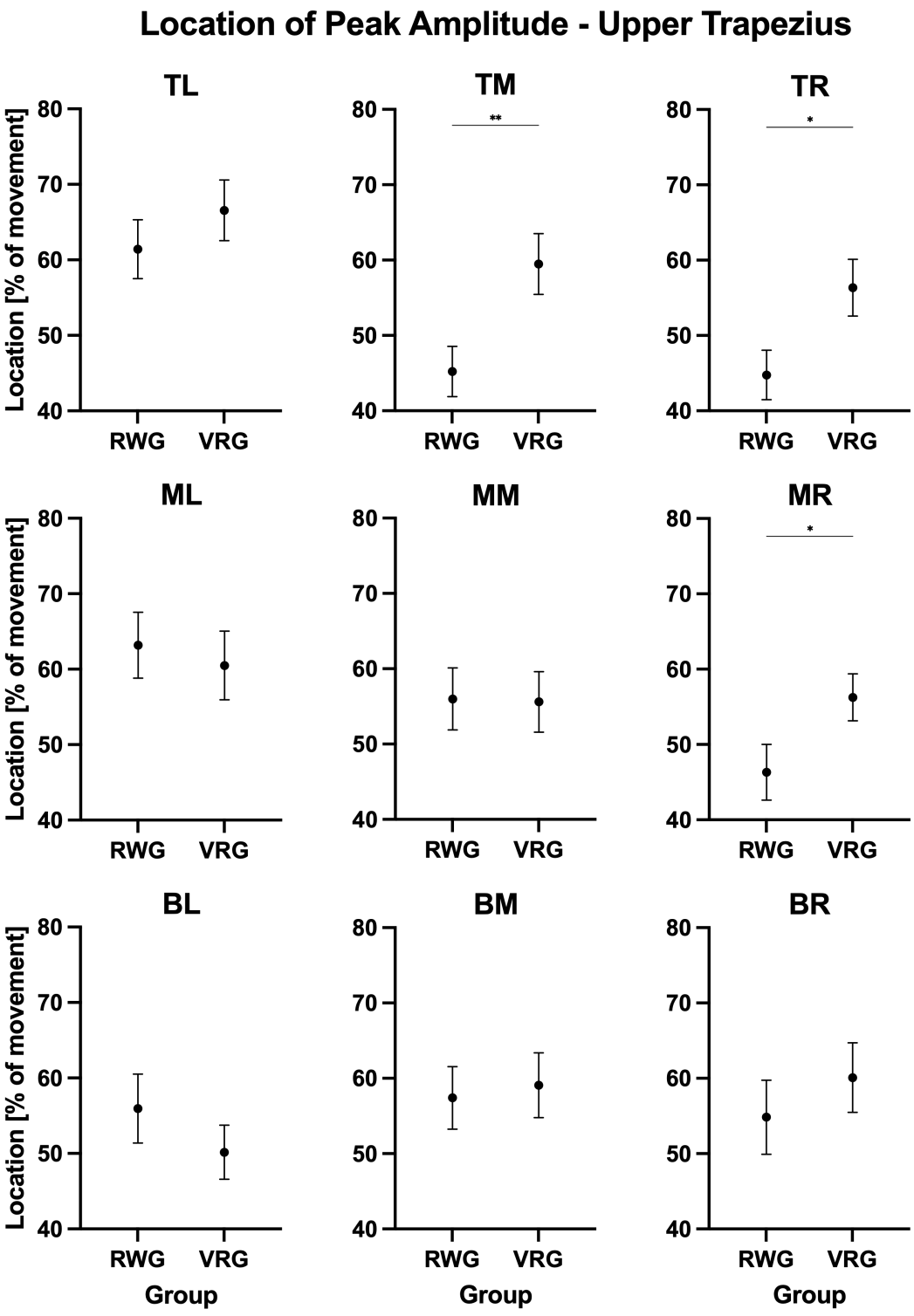

Fig 5.13. The highest peak in the upper trapezius EMG amplitude was significantly earlier in RWG as compared to VRG at the TM, TR, and MR targets. Mean ± SEM is represented for each group at each target. * = $p < 0.05$

4. Discussion

4.1 Study Design

Fifty-one participants were randomly assigned to perform a reaching to visual target task in either a RW or VR environment. Every participant performed a total of 81 reaching trials split into three blocks of 27 trials each. Each block consisted of three reaches to each of nine visual targets. The first two blocks were considered task familiarization and practice blocks. Kinematic and kinetic measures from the third block were compared between groups to identify differences between upper limb movements in real and virtual environments. To isolate the effect of visual presentation from a virtual or real visual source, other causes of variation were minimized to the best of our ability. The virtual room was modeled as a replication of the real room, auditory stimuli were the same in both environments, and apart from the headset worn in VR, haptic cues were equal between environments.

The virtual hand is a key area of difference between the VR and RW settings, the virtual hand was not modified for participant hand size or skin color. This choice was made in consideration of the uncanny valley principle (Mori and Macdorman, 2017) and the importance of embodiment to natural movements in virtual spaces (Pritchard et al., 2016). Additionally, an arm was not modeled in VR. When designing this study, we were not able to identify an arm model, or method of modelling an arm, to track accurately and reliably with the physical arm. There is sufficient evidence to show that humans are able to move accurately in the absence of visual cues about their body but are not able to fully ignore inaccurate visual information (Bourdin et al., 2019; Spitzley and Karduna, 2022).

Therefore, we decided that representing the hand without an arm was less likely to skew results than visualizing a likely inaccurate arm position.

4.2 Kinematics

Across all nine visual targets, participants moved more slowly on average and at peak during the reaching phase of movement in VR than in the RW [**Fig. 5.5 b, c**]. At four targets (TR, MR, BM, and BR) participants took longer to reach the target in VR than in RW [**Fig. 5.6**]. These results agree with other studies investigating movement times in VR and RW environments under several task paradigms. Slower movements in VR as compared to RW have been demonstrated during a dart-throwing training program (Drew et al., 2020), a reach-to-grasp and transport task (Arlati et al., 2022), and a full-body standing and reaching task (Thomas et al., 2016). This discrepancy in movement quality could be an important consideration when designing and deploying VR applications for clinical use. Upper-limb and full-body reaching movements are important re-training elements in neurorehabilitation such as recovery from stroke. As it has been demonstrated that individuals experiencing impairment from stroke are already prone to slower and less smooth movements, both at mean and peak (Hussain et al., 2018), the potential of augmenting this pre-existing difference should be considered. A recent study added to these findings by testing upper limb kinematics in VR and RW in partnership with a population undergoing recovery from stroke. In a reaching and grasping task in a stroke recovery population, reaches in VR were slower and less smooth compared to a RW environment (Levin et al., 2015a).

While it is not entirely clear why the time to target was different for only four targets, this may be explained in part by the position of those targets in reference to the working limb and the center line of the body. Three of the targets (TR, MR, and BR) were on the ipsilateral side and two of the targets (BM and BR) were below the horizontal center field of vision. Differences in movement quality between reaches to ipsilateral and contralateral visual targets have been long observed. Reaching to ipsilateral targets in a real environment produces faster and more accurate movement than to contralateral targets (Fisk and Goodale, 1985). Additionally, Mineiro and Buckingham 2023 showed a distinct preference for hand movements within the lower visual field in a real environment. Our time to target results show that it took more time to reach the target in VR for all targets on the ipsilateral side and two targets in the bottom row, but no differences were seen for contralateral targets or targets in the TM or MM positions. Given these findings, it is possible that previously observed patterns related to contralateral vs ipsilateral and field of view reaching characteristics are either different or experienced to different degrees in RW and VR environments. As this was not a main purpose of the current study, it is suggested that further investigation is needed to draw additional conclusions.

Response time across all targets also showed that participants took longer to begin moving toward the target after it was activated in VR than in RW [**Fig. 5.5 a**]. A delayed response to the visual target in VR supports the idea of different central processing for visual and real sources of sensory information. Harris et al. 2019 suggested that the processing limitations stemming from stereoscopically presented depth information may lead VR users to experience a broad redirection between neural pathways of visual

processing. The idea of semi-distinct, context dependent neural pathways involved in processing visual information has been long studied. Vision-for-action (or dorsal pathway) is more dependent on binocular visual information while vision-for-perception (or ventral pathway) is more dependent on monocular visual information (Goodale and Westwood, 2004; Harris et al., 2019). It is possible that the virtual depth information is being processed similarly to a monocular cue, due to its mode of presentation. This idea is supported by fMRI data during spatial processing of visual signals in real and virtual spaces. fMRI studies of visual processing in the RW show areas along the dorsal pathway being activated more strongly in response to objects in near space, while areas along the ventral pathway were activated more strongly in response to objects in far space (Weiss et al., 2000). In direct opposition to this, fMRI studies of visual processing in VR show the reverse activation patterns for objects in near and far space (Beck et al., 2010). The slower response time and slower overall movements found in VR within this study are consistent with other movement studies and the current ideas behind discrepancies in visual processing within a virtual as compared to real space. As a whole, these results suggest that a cautious approach should be taken when deciding to use virtual environments, particularly in the context of clinical populations.

Functional range of motion in the elbow joint was significantly lower in RW as compared to VR at the TL, TR, ML, and MR targets [**Fig. 5.7**]. Although statistical differences were not seen across all targets, the same trend can be observed. SPM analyses also showed that at various points during the reaching movement, differences in shoulder [**Fig. 5.8**] and elbow [**Fig. 5.9**] angle were observed between RW and VR. From 13 – 60% of movement, shoulder angle was higher in RW than VR. From 0 – 23% of

movement elbow angle was higher in RW than VR, then from 40 – 80% elbow angle was lower in RW than VR. Though shoulder angles were different during the movement, peak shoulder angle was not different between groups. In this case, peak shoulder angle is seen when the hand reaches the target, at the end of the reaching phase of movement. These results indicate that participants used a more shoulder-focused movement strategy in RW and a more elbow-focused movement strategy in VR to reach the same endpoint at the shoulder. Other studies of upper limb kinematics in real and virtual settings do not show consistent results. Some studies have shown no differences (Arlati et al., 2022; Levin et al., 2015a) while others also see a shift to the elbow-focused movements strategy (Drew et al., 2020) or greater joint excursions overall (Thomas et al., 2016) in VR. These results contribute to the body of work indicating that altered movement strategies are being employed to complete upper limb movements in virtual settings. The lack of agreement between studies on this point supports the idea that task-specific testing is needed when designing VR-based protocols.

4.3 Kinetics

Across all targets, location of peak amplitude of the EMG signal from the biceps brachii and anterior deltoid [**Fig. 5.10 b, c**] muscles was earlier in RW as compared to VR. Location of peak amplitude of the upper trapezius muscle was earlier in RW as compared to VR at the TM, TR, and MR targets [**Fig. 5.13**]. These activation patterns agree with the kinematic measures discussed previously [**Fig. 5.8, 5.9**]. In the RW, a shoulder-focused movement strategy is employed with little contribution from the elbow joint. The biceps brachii, anterior deltoid, and upper trapezius muscles all activate early

to lift the entire arm from the resting position and begin moving it toward the target, peaking around 39%, 65%, and 45% of movement respectively. In VR, elbow flexion beginning around 25% of movement brings the load of the forearm closer to the arm, reducing the moment on the shoulder. Around 80% of movement, when the shoulder is flexed to approximately 65°, the elbow is nearly fully extended again, increasing the moment on the shoulder. Peak amplitude of all three muscles occurs during this period of simultaneous shoulder elevation and elbow extension with the biceps brachii peaking around 55%, anterior delt around 73%, and upper trapezius around 57% of movement.

There were fewer EMG amplitude peaks in the RW as compared to VR at the biceps brachii across all targets [**Fig. 5.10 a**], in the anterior deltoid at BM and BR targets [**Fig. 5.11**], and in the upper trapezius at the TR target [**Fig. 5.12**]. The number of amplitude peaks is an indirect measure of movement smoothness, as a peak in the EMG signal is indicative of a burst of electrical activity in the muscle that subsides quickly.

5. Conclusions

This study examined upper limb kinematics and kinetics during a visually cued, reaching to target movement and came to the following conclusions. In VR as compared to RW: a) movement is slower when reaching to a visual target; b) possible differences exist in patterns related to ipsilateral vs contralateral movement and field of view movement characteristics; c) it takes longer to respond to a visual cue, d) an elbow-focused as opposed to shoulder-focused movement strategy is employed; and d) muscle activation is less smooth. The hypotheses that movement in VR would be a) slower and b) less smooth than in the RW were supported.

While immersive VR systems show great promise in terms of accessibility and customization for applications in many fields including healthcare, there is reason to carefully consider the appropriateness of 3D virtual environments depending on use case. Along with previous fMRI and movement research (Beck et al., 2010; Bourdin et al., 2019; Drew et al., 2020; Gonzalez-Franco et al., 2019; Harris et al., 2019; Wright, 2014), the current study calls in to question the parallels between visually guided movements in virtual and real environments. This study supports the ideas that visually cued upper limb movements in VR may correspond with different neural pathways than similar movements in RW. In some settings, such as gaming, this is unlikely to be substantially impactful to the user. However, when considering their use with clinical or other vulnerable populations, extensive task-specific testing may be very important to complete before deploying VR-based applications.

6. Bridge

The study outlined in this chapter investigated differences in upper limb movements during visually guided reaching tasks in VR and the RW, revealing several significant differences between environments. In VR as compared to RW, participants moved more slowly, took longer to initiate movement, employed a more elbow-focused movement strategy, exhibited a greater number of EMG amplitude peaks, and later EMG amplitude peaks. These results call to question the parallels between visually guided movements performed in real and virtual environments.

While the present study successfully identified differences in upper limb movements between VR and RW environments, it did not investigate the impact of task

familiarization in one environment on task performance in the other environment. Considering that transitioning between environments is common in various use cases, and VR training is often intended to enhance performance in the RW, it is crucial to explore this aspect. Chapter VI of this dissertation addresses this gap by examining whether there are immediate, short-term variations in upper limb kinematics and kinetics when individuals switch from a VR environment to the RW after being familiarized with the task in VR, and vice versa. This study aims to provide insight into the transferability of skills acquired in VR to the RW, as well as the potential effects of RW experience on VR performance. By exploring these aspects, a more comprehensive understanding of the relationship between VR and RW environments can be achieved.

CHAPTER VI

SHORT-TERM TRANSLATION OF UPPER LIMB MECHANICS BETWEEN VIRTUAL AND REAL-WORLD ENVIRONMENTS

This work is currently in preparation for submission to the *Journal of Virtual Reality* and is co-authored by Kate A. Spitzley, Zachary A. Hoffman, Samuel E. Perlman, and Andrew R. Karduna. Kate A. Spitzley contributed to study design, experimental work including data collection and analysis, and writing. Zachary A. Hoffman and Samuel E. Perlman contributed to study design and data collection. Andrew R. Karduna contributed to study design, research mentorship, and editorial assistance.

1. Introduction

Technological advances and increases in affordability of immersive virtual reality (VR) systems have preceded their rise in popularity within many fields including, but not limited to, education, retail, sports, and healthcare (Wohlgenannt et al., 2020). In most of these settings, the purpose of employing a VR system is to provide low cost, accessible training environments. For example, offering physical and other therapies at-home is a popular goal being pursued by researchers and clinicians alike. The ability to send a patient home with technology that allows for a fully controllable 3D environment in any setting is certainly appealing and deserving of investigation. Current research on clinically applied VR applications have shown interventions to be effective in reducing pain during physical therapy treatment (Waked and Eid, 2019), aiding in stroke rehabilitation (Ikbali Afsar et al., 2018; Mekbib et al., 2020), and providing gait training

in populations with Parkinson's disease (Janeh et al., 2019). Patients, and other target populations, stand to benefit from a less expensive and more portable training environment.

Before deploying these systems within training environments, it is important to ensure that the effects, both during and after use, are fully understood. While the previously mentioned studies highlight potential benefits of VR systems in clinical settings, others have found evidence of altered movement patterns (Bourdin et al., 2019; Gonzalez-Franco et al., 2019; Harris et al., 2019) and unintended aftereffects of sensorimotor training (Drew et al., 2020; Wright, 2014) in virtual environments. This conflicting evidence suggests that ecological validity and transferability of training received in a VR environment should be assessed before deployment. Some insight into behavioral differences between VR and the real-world (RW) can be found in imaging studies, which have demonstrated that the brain processes depth cues differently between environments (Beck et al., 2010). The naturalistic vs virtual presentation of visual properties such as refresh rate, field of view, and resolution could contribute to differences in central processing. Uncertainty or reduced fidelity introduced to the visual system may cause a change in sensory integration strategy and alter movement response to stimuli (Faisal et al., 2008; Körding and Wolpert, 2006). While it is difficult to balance the potential benefits with unknown risks associated with the use of VR systems for training purposes, understanding how task-specific mechanics transfer between VR and RW settings is an important step in this decision-making process. Knowledge about the effect of switching between settings on outcomes of interest will help clinicians make well informed decisions for their patients.

Of all the task-specific mechanics to investigate, upper limb reaching movements are particularly interesting in the context of VR. The upper limbs are well within the field-of-view of modern headsets and are the main point of interaction between the user and virtual environment. This level of interaction only stands to increase as developers continually work to release improved tracking of the hands, including gesture-based controls. Reaching toward a visual target requires multi-step processing of sensory information for motor output (Goodale, 2011), each step of which can be disrupted by injury or unexpected noise within the nervous system (Faisal et al., 2008; Körding and Wolpert, 2006). Upper-limb movements are also important targets for clinical rehabilitation and training programs. Deployment of these programs in stroke and injury recovery populations are gaining popularity in the scientific and clinical communities (Juan et al., 2022; Keshner et al., 2019; Mekbib et al., 2020). As the upper limb appears to be an emerging area of expansion for VR-based clinical tools, it is important to understand how movements change when switching between real and virtual environments.

The study outlined in Chapter 5 of this dissertation found differences in upper limb kinematics and kinetics between two groups, one who performed an upper limb reaching task in VR and another who performed the same task in the RW. That study concluded that in VR, as compared to RW, participants were slower to initiate movement in response to visual cues, were slower throughout their movement once initiated, employed different joint movement patterns to reach the same target, and demonstrated less smooth muscle activation. This called to question the parallels between visually guided movements performed in virtual and real environments but did not examine the effect of

becoming familiarized with the task in one environment on the performance of the task in the other environment. Because switching between environments is inevitable in most use cases, and training in VR is currently meant to augment performance in the RW, this is an important distinction to make. Therefore, the present study aims to determine if there are immediate, short-term, differences in upper limb kinematics and kinetics when entering a RW environment after being familiarized with the task in VR, and vice versa. It was hypothesized that the patterns observed in the previous study would be maintained in this testing paradigm, regardless of which environment was used for familiarization.

2. Methods

2.1 Participants

Fifty-one participants were recruited to perform a reaching task to visual targets in RW and VR environments. Eligibility criteria included healthy individuals ages 18 to 45, free of upper body pain within the two weeks prior, upper limb injury within the past year, neurological disorder, and uncorrected impaired vision. All participants completed the informed consent and study protocols as approved by the Internal Review Board at the University of Oregon before undergoing any research activities.

Participants were randomly assigned to one of two groups. Group 1 (G1, n = 25, 20.5±2.7 yrs., 14 F 11 M) performed three blocks of the reaching task in the RW followed by one block of the task in VR. Group 2 (G2, n = 26, 22.7±5.1 yrs., 18 F 8 M) performed three blocks of the reaching task in VR followed by one block of the task in RW. Each block consisted of 27 reaches in total, three reaches to each of nine visual targets [**Fig. 6.1**]. The order of target presentation was randomized within each block.

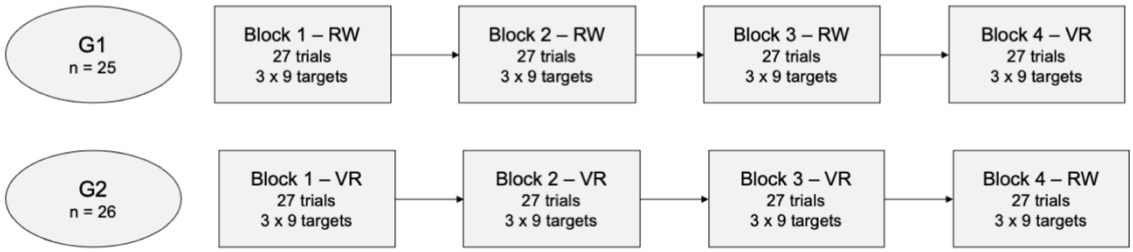

Fig. 6.1 Study design schematic demonstrating the breakdown of 51 participants into two groups, G1 and G2. Each group performed three blocks of the task consisting of 27 trials each, 3 reaches to each of the 9 visual targets.

2.2 Setup

2.2.1 Environments

In the RW, visual reaching targets were presented using a custom-made LED board. The board was designed using a three-foot square opaque white plastic sheet behind which LEDs were mounted within 3D printed, cone shaped mounting brackets. The effect of this was to diffuse the light from each LED through the plastic, creating 5 cm visual targets on the front of the board. Targets were 23 cm apart at their center and arranged in a three-by-three grid evenly across the board. Individual targets will be referred to with reference to their position on the board. Targets in the top row are represented with a 'T', the middle row represented with a 'M', and the bottom row represented with a 'B'. Targets in the right column are represented with a 'R', the middle column represented with a 'M', and the left column represented with a 'L' [**Fig. 6.2**]. As participants performed reaching movements with their right upper limb, and were positioned facing the board, right column targets elicited ipsilateral reaches and left column targets elicited contralateral reaches. Participants were positioned so that the middle of their body was in alignment with the middle column of targets.

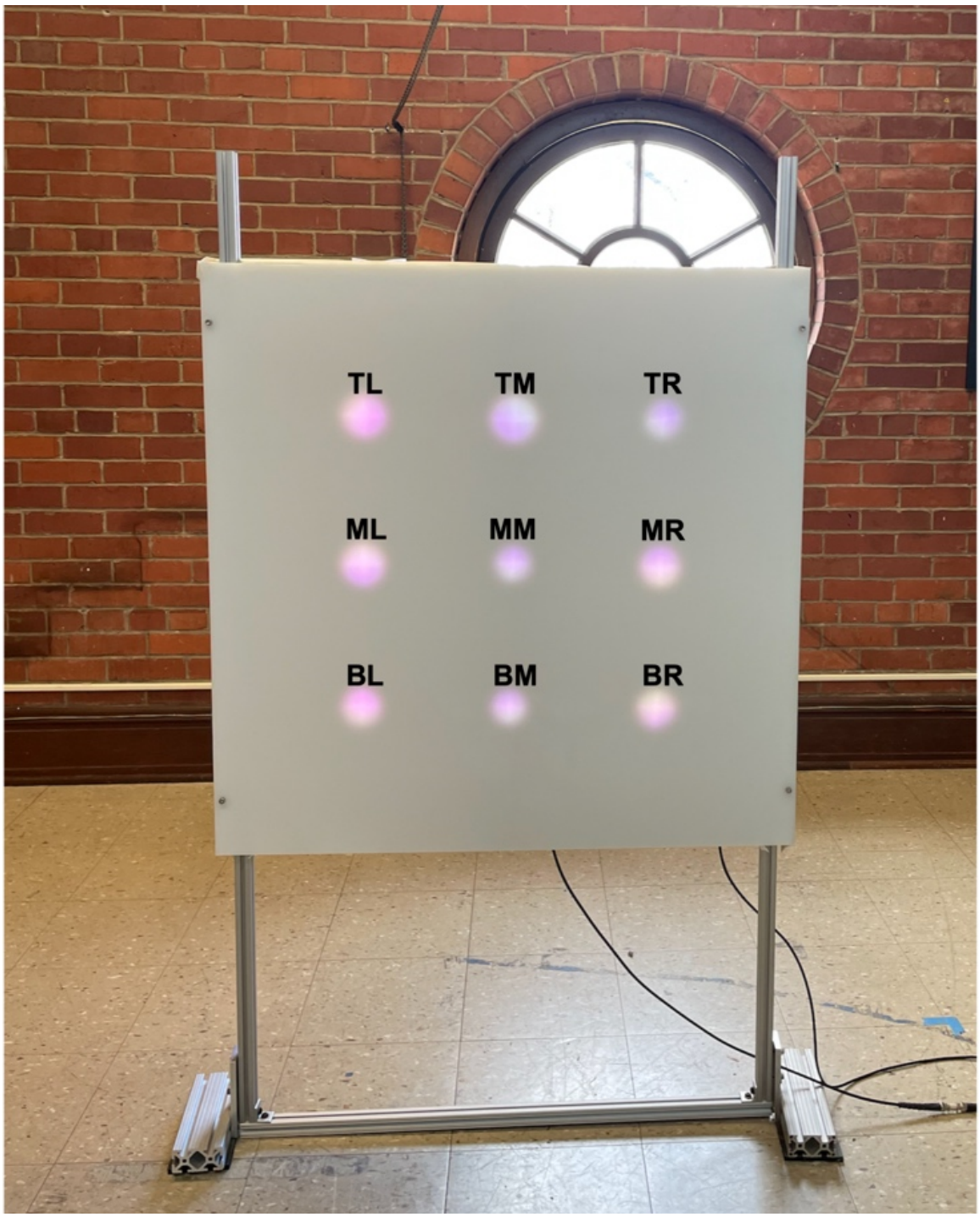

Fig. 6.2 Visual target board with all targets activated. Targets are denoted with respect to their row then column position on the board. TL: top left, TM: top middle, TR: top right, ML: middle left, MM: middle middle, MR: middle right, BL: bottom left, BM: bottom middle, BR: bottom right.

In VR, a digital recreation of the laboratory environment, including the LED board, was generated using Blender (Blender, Amsterdam, Netherlands) [**Fig. 6.3**]. Reference measurements and photographs were obtained to minimize discrepancies in scale between the real and virtual spaces. Image textures were applied to the models, providing color, roughness, and normal (simulated depth) data. Careful consideration was taken when determining polygon/texture resolution to balance physical accuracy and computational workload, ensuring stable framerates. The completed 3D models were imported into Unity in FBX format. In Unity, the High-Definition Render Pipeline and realistic global illumination light system were used. Calibration of the VR and Unity camera rig positions and the position of the target board within the virtual and real spaces ensured that the participant found themselves in the same position and orientation in the real and virtual environments.

Fig. 6.3 The real-world (a) virtual (b) environments. Target board in positioned in the bottom left corner of both images.

2.2.2 Equipment

An HTV VIVE Pro Eye headset (2880 x 1600 combined resolution, Dual OLED 3.5” diagonal display, 110° field of view) and VIVE version 3.0 Trackers (HTC VIVE, Taoyuan City, Taiwan) displayed the virtual environment and captured position and orientation of the trunk, right arm, and right wrist segments, respectively (Spitzley and Karduna, 2019). A rigid wrist brace was used to reduce the hand and forearm into a single distal segment. In VR, a hand-model was fixed to the wrist tracker and placed in alignment with the participants own hand using visual landmarks in the virtual space. A static reference pose was captured prior to movement trials.

Electrical activity of the right biceps brachii, triceps brachii, anterior deltoid, middle deltoid, and upper trapezius muscles was captured using a Delsys Trigno wireless EMG system (Delsys Inc., Boston, MA, USA). These muscles were selected to represent activity related to movement at the elbow, glenohumeral, and scapulothoracic joints, respectively. Skin sites were cleaned and lightly abraded using 70% isopropyl alcohol wipes. Surface sensor placement followed standards developed by Hermens et al. (2000).

2.2.3 Data Output and Synchronization

Customized Arduino (Arduino, New York, New York, USA), Unity (Unity, San Francisco, CA, USA), and LabVIEW (National Instruments, Austin, TX, USA) programs in concert with an Arduino Mega 2560 REV3 microcontroller board facilitated communication between and data output from the light board, VR, and EMG systems. To turn an LED on or off, a Unity script sent information containing the desired target name to an Arduino script, this information was used to turn on or off specified channels on the

microcontroller board to which the LEDs were connected. To select targets on the virtual LED board, Unity used the target name to select an emission texture on the virtual target board, reflecting the corresponding target location and luminance.

Kinematics and EMG were synchronized using a 5V square wave, communicated to both an A/D board (National Instruments Corporation, Austin, TX, USA) and Unity. The A/D board also received data from the surface EMG sensors, which was captured wirelessly by the base station and ported to the board for synchronization. A customized LabVIEW program captured the EMG and synchronization channels. Unity recorded the 5V wave within the kinematics file and a custom Unity script outputted synchronization data, along with position and orientation from the trackers. EMG was captured at 1925 Hz and kinematics at 90 Hz.

2.3 Task Protocol

Following sensor placement and static reference pose capture, participants were seated with their arm flexed to 90° directly in front of their shoulder and positioned one inch more than arm's distance from the LED board, facing the board. A research team member talked through the experimental protocol with the participant and confirmed that they understood the task and were prepared to continue. If a participant was completing the task in VR, a team member assisted in placement and fitting of the headset, confirming comfort, field of view, and clarity of visual signal with the participant. If a participant was completing the task in RW, a team member placed the headset in a standardized position within the room and confirmed that the participant was comfortable and ready to proceed. Once the participant confirmed that they were prepared to begin, all

trials within each block were completed without a break. Breaks between blocks were provided, and participants were informed that they could request added breaks at any point. No extra breaks were requested nor was removal of the headset for any reason prior to task completion.

Participants were instructed to wait with their arms relaxed by their side until a target light came on, to reach to the target using their right arm until the it turned off, then to return to the relaxed waiting position [**Fig. 6.4**]. Task completion was indicated by the light turning off and a simultaneous sound from the system confirming success. Target lights were triggered to turn on when the wrist tracker was at the participant's side and moving less than 0.2 m/s and was triggered to turn off when the wrist tracker was within 0.2 m of the target. These thresholds were determined during pilot testing and allowed for normal ambient movement and for the hand to come close to touching the board without making contact.

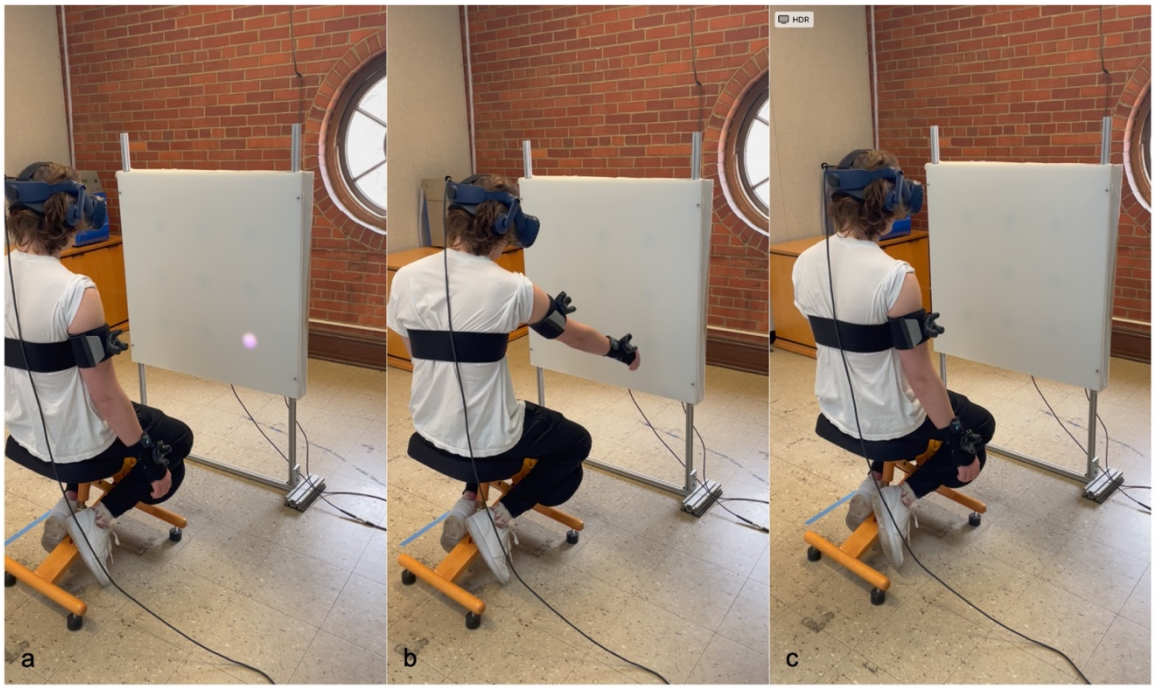

Fig. 6.4 Participant performing a reaching trial in a virtual environment. During each trial, participants waited until the target lit up (a), reached toward the target until the light turned off (b), and returned to the starting position (c). In this example, the BR target is activated.

2.4 Data Reduction and Statistical Analysis

Orientation of the VIVE trackers was outputted in quaternion format to avoid computational issues related to Unity's use of multiple left-handed coordinate systems. Relative orientations between trunk and arm and arm and wrist represented shoulder angle and elbow angle, respectively. These were solved for by converting quaternions to direction cosign matrices and then to Euler angles using rotation sequences outlined in Wu et al. (2005) during the static pose and dynamic trials. Peak shoulder elevation was calculated as the maximum of shoulder elevation angle during the reaching phase of movement. Functional range of motion (fROM) was calculated as the maximum flexion or elevation angle minus the minimum flexion or elevation angle during the reaching phase of movement.

The tracker mounted on the forearm/wrist segment approximated endpoint position for all measures related to movement timing. Response time was measured as the time between when the target light came on to the time when the participant began moving toward the target. Time to target was measured as the time between when the participant began moving toward the target and the time when they reached the target. Time at target was measured as the time between when the participant reached the target and when they began moving away from the target. Outcomes related to endpoint velocity were calculated during the reaching phase of movement only.

Delsys hardware filtered all analog EMG channels using a band-pass of 20-450 Hz. The Common Mode Rejection Ratio of this system is greater than 80 dB. Digital

signals were collected as a single file for each block, the trigger signal was used to separate individual trials in post-processing. Signals were mean centered, rectified, and smoothed using an RMS sliding window of 50 milliseconds. For all muscles, peak EMG amplitude, number of EMG amplitude peaks, and location of EMG amplitude peaks were identified during the reaching phase of movement using the *findpeaks* function in MATLAB.

Trials were cropped to begin when the target was lit and end when the endpoint reached the target and was at its lowest speed. These cropped trials were normalized to 101 data points, representing a complete reaching cycle. For analysis of EMG signals, one participant was removed from G1 and two were removed from G2 due to equipment malfunction.

Two-way repeated-measures ANOVA's ($\alpha = 0.05$) determined within-subject's differences between testing blocks, reaching targets, and interactions between blocks and targets. If Mauchly's test of sphericity was violated, a Greenhouse-Geisser corrected *p* value was used to determine significance. If no interaction was found, multiple comparisons to determine relationships between adjacent blocks were performed with all targets combined. If an interaction was found, the effect was examined, and targets were regrouped to determine the relationships between blocks with respect to target. Groups 1 and 2 were analyzed separately. Additionally, two-sample *t*-tests ($\alpha = 0.05$) using One-Dimensional Statistical Parametric Mapping (SPM1d, Pataky 2012) analyses were used to compare shoulder angles and elbow angles from 0 –100% of the reaching phase between testing blocks 3 and 4 within each group. All comparisons were constrained

within groups. As comparisons were made within-subjects, EMG amplitudes are reported in millivolts (mV) and not normalized to maximum voluntary contractions.

3. Results

Means and standard error of the means (SEM) for all kinematic and kinetic measures are displayed in **Table 6.1**, results from multiple comparisons are displayed on the graphs within this section.

3.1 Kinematic Measures

Differences between testing blocks were seen within both groups for measures of response time, time to target, and time at target. Response time was different between blocks 1 and 2 and blocks 3 and 4 for both groups [**Fig. 6.5 a**]. In Group 1, response time was slower in block 1 as compared to block 2 and was faster in block 3 as compared to block 4. In Group 2, response time was slower in block 1 as compared to block 2 and in block 3 as compared to block 4. Time to target was different between blocks 1 and 2 and 3 and 4 for Group 1, and different between all adjacent blocks for Group 2 [**Fig. 6.5 b**]. In Group 1, time to target was slower in block 1 as compared to block 2 and was faster in block 3 as compared to block 4. In Group 2, time to target was faster in each progressive block. Time at target was different between blocks 1 and 2 and blocks 2 and 3 for Group 1, and different between all adjacent blocks for Group 2 [**Fig. 6.5 c**]. In Group 1, time at target was greater in block 1 as compared to block 2 and in block 2 as compared to block 3. In Group 2, time at target was greater in block 1 as compared to block 2 in block 2 as compared to block 3 but was less in block 3 as compared to block 4.

Table 6.1. Mean ± SEM for all kinematic and kinetic measures displayed within groups for each block of testing.

	Group 1				Group 2			
	B1 – RW	**B2 – RW**	**B3 – RW**	**B4 – VR**	**B1 – VR**	**B2 – VR**	**B3 – VR**	**B4 – RW**
				Kinematic Measures				
Response Time [s]	0.30±0.01	0.28±0.00	0.27±0.00	0.35±0.01	0.40±0.01	0.35±0.01	0.35±0.01	0.30±0.00
Time to Target [s]	0.67±0.03	0.56±0.02	0.55±0.02	0.66±0.02	0.80±0.03	0.65±0.02	0.62±0.01	0.51±0.01
Time at Target [s]	0.57±0.01	0.48±0.01	0.45±0.01	0.46±0.01	0.52±0.01	0.45±0.01	0.43±0.01	0.46±0.01
Mean Endpoint Speed [m/s]	0.61±0.01	0.66±0.01	0.65±0.01	0.55±0.01	0.50±0.01	0.56±0.01	0.57±0.01	0.63±0.01
Peak Endpoint Speed [m/s]	1.6±0.03	1.7±0.03	1.7±0.03	1.6+0.03	1.4±0.02	1.5±0.02	1.5±0.02	1.6±0.02
Endpoint Speed Peaks [count]	1.3±0.04	1.3±0.03	1.3±0.04	1.4±0.04	1.6±0.05	1.3±0.03	1.3±0.03	1.2±0.02
Peak Shoulder Elevation [deg]	71±0.8	71±0.9	71±0.9	69±1.0	71±0.9	71±0.9	73±0.9	74±0.9
Shoulder fROM [deg]	62±0.8	61±0.9	60±0.8	58±0.9	62±0.8	61±0.8	61±0.8	63±0.8
Elbow fROM [deg]	15±0.7	16±0.7	17±0.7	20±0.9	25±1.0	22±0.9	22±0.8	19±0.7
				Kinetic Measures				
Bicep EMG Peak [mV]	31±1.2	34±1.3	36±1.6	38±2.6	33±1.9	35±2.2	37±2.8	56±7.5
Bicep EMG Peaks [count]	3.5±0.10	3.0±0.06	3.0±0.07	3.4±0.07	3.9±0.09	3.4±0.06	3.4±0.07	3.0±0.06
Bicep EMG Peak Location [%]	43±1.2	40±1.1	39±1.1	44±1.1	55±1.4	56±1.4	55±1.3	50±1.3
ADelt EMG Peak [mV]	78±3.8	106±14	113±13	92±8.5	76±2.7	75±2.7	81±3.1	95±5.8
ADelt EMG Peaks [count]	3.6±0.08	3.4±0.08	3.2±0.09	3.9±0.10	4.4±0.09	3.7±0.07	3.5±0.06	3.2±0.06
ADelt EMG Peak Location [%]	67±1.0	66±0.9	65±1.0	72±1.0	72±0.8	74±0.8	73±0.7	68±0.9
UTrap EMG Peak [mV]	30±1.7	29±1.7	27±1.6	28±1.6	33±1.9	35±2.0	34±2.0	35±2.3
UTrap EMG peaks [count]	3.8±0.14	3.4±0.10	3.4±0.11	3.6±0.13	3.8±0.09	3.3±0.07	3.2±0.07	2.9±0.07
UTrap EMG Peak Location [%]	53±1.3	54±1.3	54±1.4	56±1.2	59±1.4	59±1.3	58±1.3	55±1.4

Differences between testing blocks were seen within both groups for measures of mean endpoint velocity, peak endpoint velocity, and number of endpoint velocity peaks. Mean endpoint velocity was different between blocks 1 and 2 and blocks 3 and 4 for group 1 and different between all adjacent blocks for Group 2 [**Fig. 6.6 a**]. In Group 1, the endpoint moved slower in block 1 as compared to block 2 and moved faster in block 3 as compared to block 4. In Group 2, the endpoint moved faster in each progressive block. endpoint velocity was different between blocks 1 and 2 and blocks 3 and 4 for group 1 and different between all adjacent blocks for Group 2 [**Fig. 6.6 b**]. In Group 1, the endpoint speed peaked lower in block 1 as compared to block 2 and peaked higher in block 3 as compared to block 4. In Group 2, the endpoint speed peaked higher in each progressive block. Number of endpoint velocity peaks was different between blocks 1 and 2 and blocks 3 and 4 for both groups [**Fig. 6.6 c**]. In Group 1, the endpoint peaked more times in block 1 as compared to block 2 and peaked fewer times in block 3 as compared to block 4. In Group 2, the endpoint peaked more times in block 1 as compared to block 2 and more times in block 3 as compared to block 4.

Differences between testing blocks were seen within both groups for measures of peak shoulder elevation, shoulder fROM, and elbow fROM. Peak shoulder elevation was different between blocks 3 and 4 of Group 1 and different between all adjacent blocks for Group 2 [**Fig. 6.7 a**]. In Group 1, peak shoulder elevation was higher in block 3 than in block 4. In Group 2, peak shoulder elevation was higher in each progressive block. Shoulder fROM was different between blocks 3 and 4 of Groups 1 and 2 [**Fig. 6.7 b**]. In Group 1, shoulder fROM was larger in block 3 as compared to block 4. In Group 2, shoulder fROM was smaller in block 3 as opposed to block 4. Elbow fROM was different

between blocks 1 and 2 and blocks 3 and 4 of Groups 1 and 2 [**Fig. 6.7 c**]. In Group 1, elbow fROM was smaller in block 1 as compared to block 2 and in block 3 as compared to block 4. In Group 2, elbow fROM was larger in block 1 as compared to block 2 and in block 3 as compared to block 4.

Between zero and 100 % of the reaching movement, differences in elbow angles were seen for both groups. In Group 1, elbow angles were lower in block 3 as compared to block 4 from 21 -73% of movement [**Fig. 6.8 a**]. In Group 2, elbow angles were lower in block 3 as compared to block 4 from 0 – 20% of movement [**Fig. 6.8 b**]. SPM analysis revealed no difference in shoulder angle at any phase of movement.

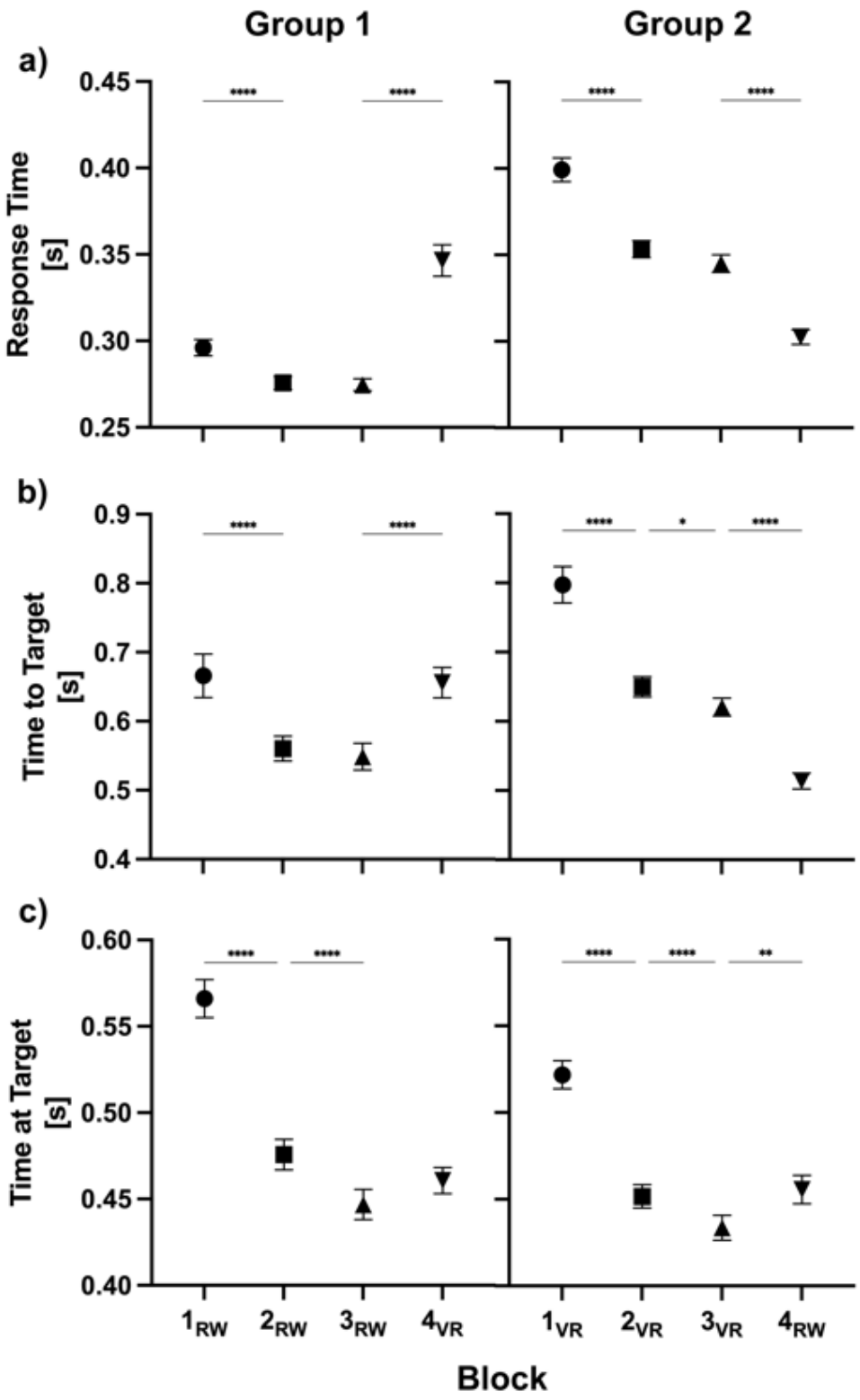

Fig. 6.5 Within-subjects differences between blocks are shown both Group 1 and 2 for measures of response time (a), time to target (b), and time at target (c). Mean ± SEM is represented for each block. * = $p < 0.05$, ** = $p < 0.01$, **** = $p < 0.0001$

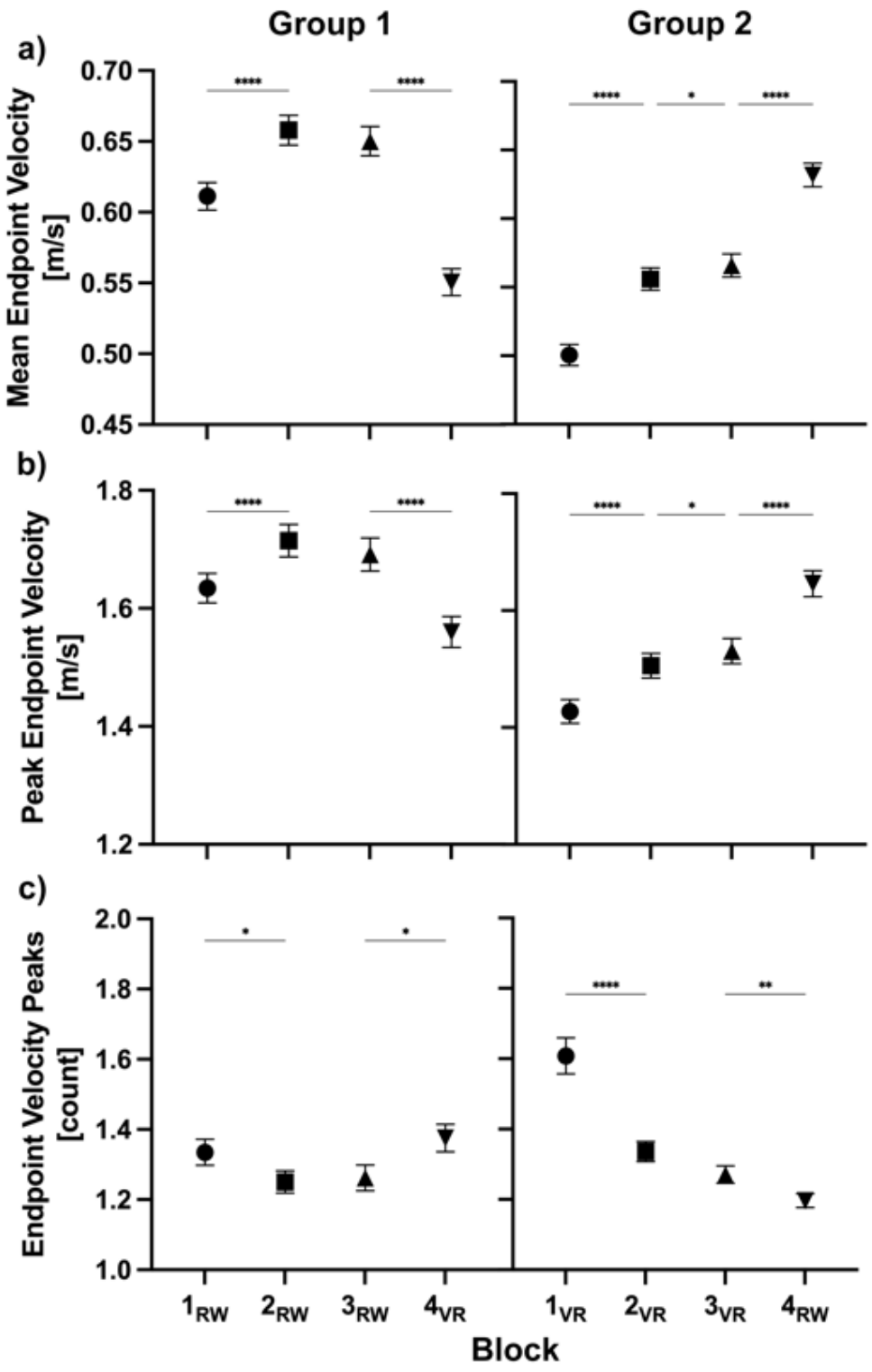

Fig. 6.6 Within-subjects differences between blocks are shown both Group 1 and 2 for measures of mean endpoint velocity (a), peak endpoint velocity (b), and number of endpoint velocity peaks (c). Mean ± SEM is represented for each block. * = $p < 0.05$, ** = $p < 0.01$, **** = $p < 0.0001$

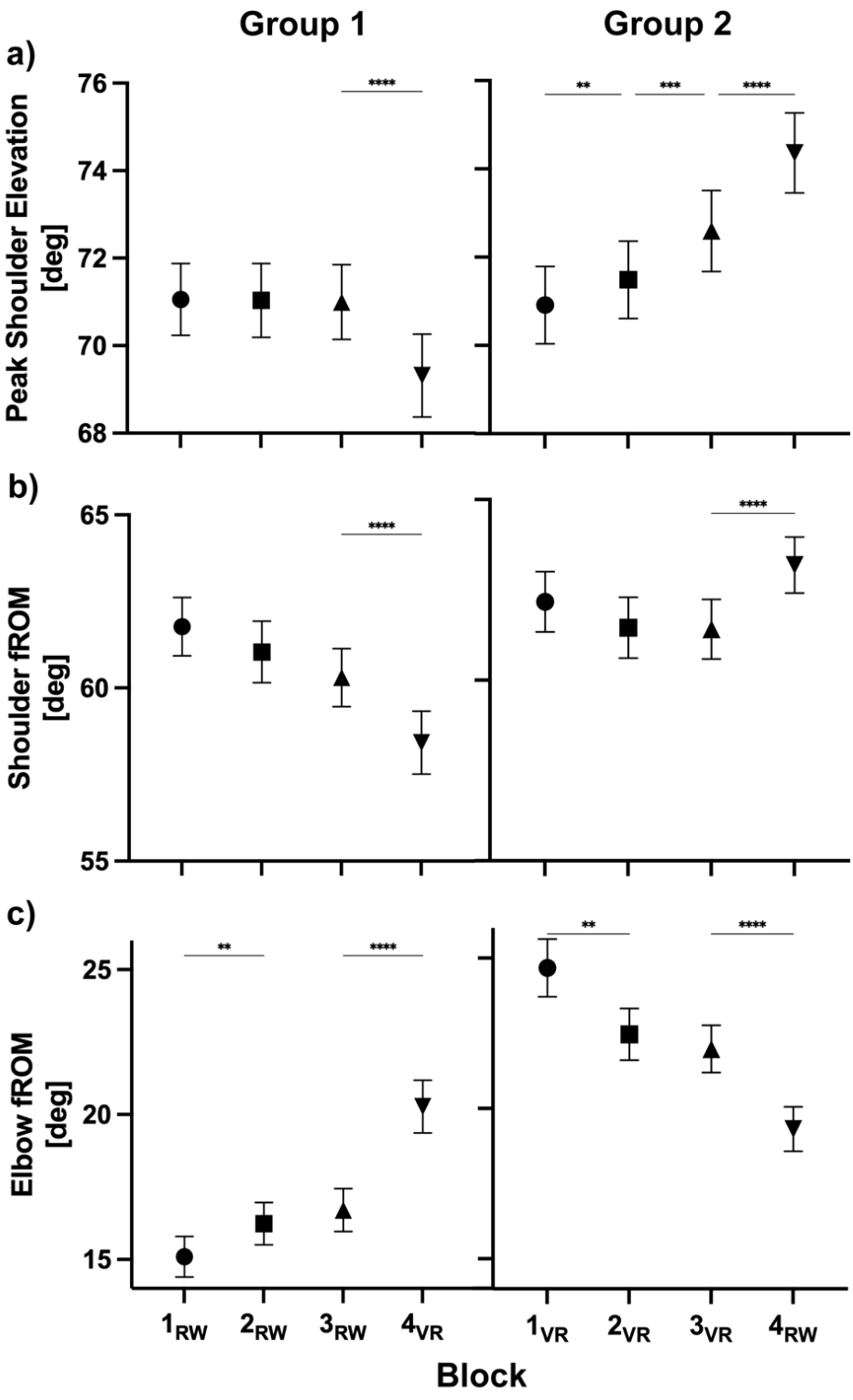

Fig. 6.7 Within-subjects differences between blocks are shown for both Group 1 and 2 for measures of peak shoulder elevation (a), shoulder fROM (b), and elbow fROM (c). Mean ± SEM is represented for each block. * = $p < 0.05$, ** = $p < 0.01$, *** = $p < 0.001$, **** = $p < 0.0001$

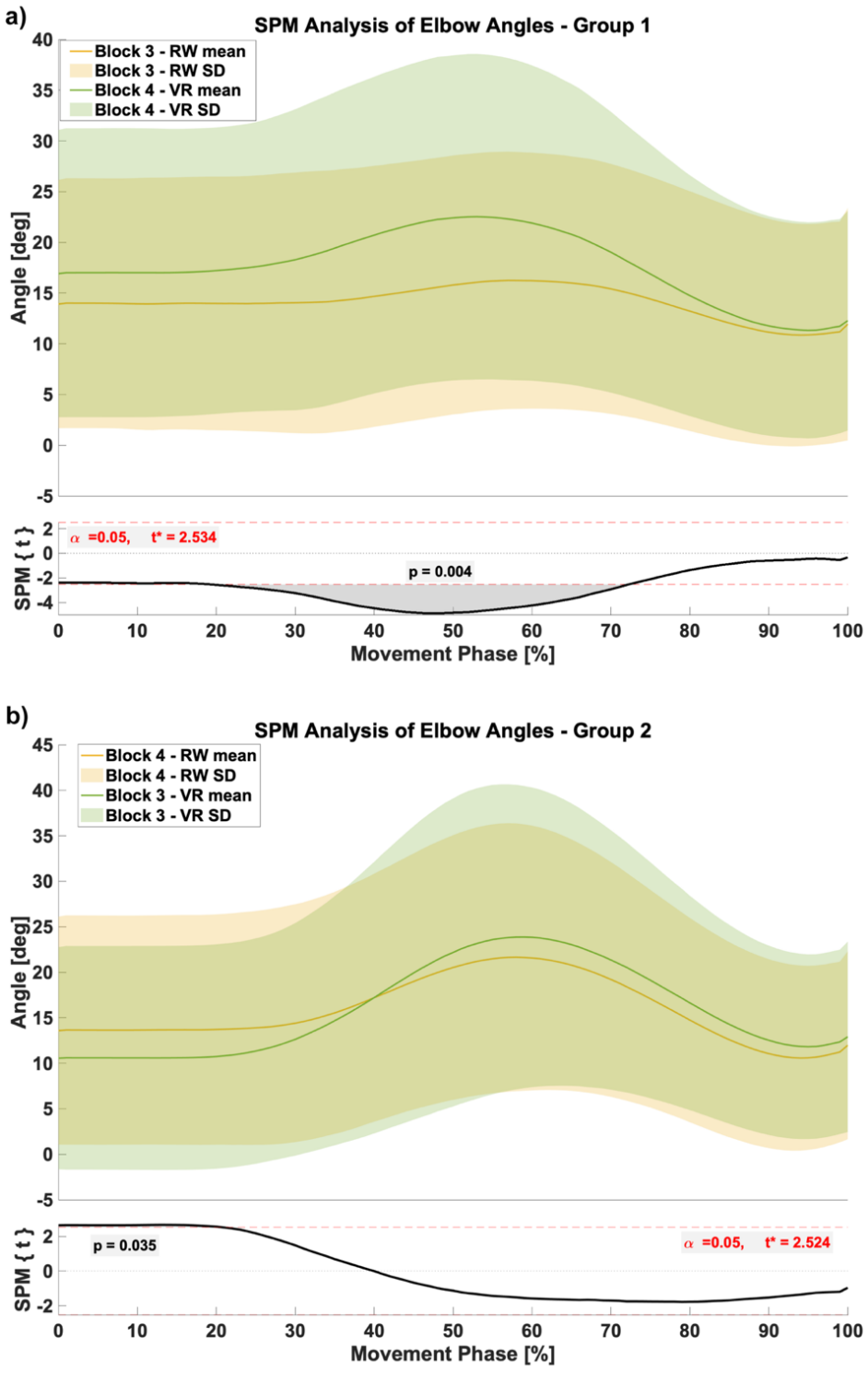

Fig. 6.8 In Group 1, differences in elbow angles were found between blocks 3 and 4 from 21-73% of movement (a). In Group 2, differences in elbow angles were found between blocks 3 and 4 from 0-20% of movement (b). Green lines and fields represent VR mean ± SD, yellow lines and fields represent RW mean ± SD.

3.2 Kinetic Measures

At the bicep brachii muscle, differences between testing blocks were seen within both groups for measures of peak EMG amplitude, number of EMG peaks, and EMG peak location. Peak EMG amplitude was different between blocks 1 and 2 of Group 1 and between blocks 3 and 4 of Group 2 [**Fig. 6.9 a**]. In Group 1, peak amplitude was lower in block 1 as compared to block 2. In Group 2, peak amplitude was lower in block 3 as compared to block 4. Number of EMG peaks was different between blocks 1 and 2 and blocks 3 and 4 of both groups [**Fig. 6.9 b**]. In Group 1, the number of peaks was higher in block 1 as compared to block 2 but was lower in block 3 as compared to block 4. In Group 2, the number of peaks was also higher in block 1 as compared to block 2 and was also higher in block 3 as compared to block 4. EMG peak location was different between blocks 3 and 4 of both groups [**Fig. 6.9 c**]. In Group 1, the EMG peaked earlier in block 3 as compared to block 4. Conversely, in Group 2, the EMG peaked later in block 3 as compared to block 4.

At the anterior deltoid muscle, differences between testing blocks were seen within both groups for measures of number of EMG peaks and EMG peak location, and within Group 2 for the measure of peak EMG amplitude. Peak EMG amplitude was different between blocks 2 and 3 and blocks 3 and 4 of Group 2, no differences between blocks were seen in Group 1 [**Fig. 6.10 a**]. In Group 2, peak amplitude grew progressively higher between blocks 2 and 4. Number of EMG peaks was different between blocks 3 and 4 of Group 1, and different between all adjacent blocks for Group 2 [**Fig. 6.10 b**]. In Group 1, the number of peaks was lower in block 3 as compared to block 4. In Group 2, the number of peaks grew lower with each progressive block. EMG peak

location was different between blocks 3 and 4 of both groups [**Fig. 6.10 c**]. In Group 1, the EMG peaked earlier in block 3 as compared to block 4. Conversely, in Group 2, the EMG peaked later in block 3 as compared to block 4.

At the upper trapezius muscle, differences between testing blocks were seen within both groups for measures of number of EMG peaks, and within Group 2 for the measure of peak EMG amplitude and EMG peak location. No differences in EMG peak location were seen in either group. Peak EMG amplitude was different between blocks 1 and 2 of Group 2, no differences between blocks were seen in Group 1 [**Fig. 6.11 a**]. In Group 2, peak amplitude was lower in block 1 as compared to block 2. Number of EMG peaks was different between blocks 1 and 2 of Group 1, and different between blocks 1 and 2 and blocks 3 and 4 for Group 2 [**Fig. 6.10 b**]. In Group 1, the number of peaks was higher in block 1 as compared to block 2. In Group 2, the number of peaks was higher in block 1 as compared to block 2 and higher in block 3 as compared to block 4.

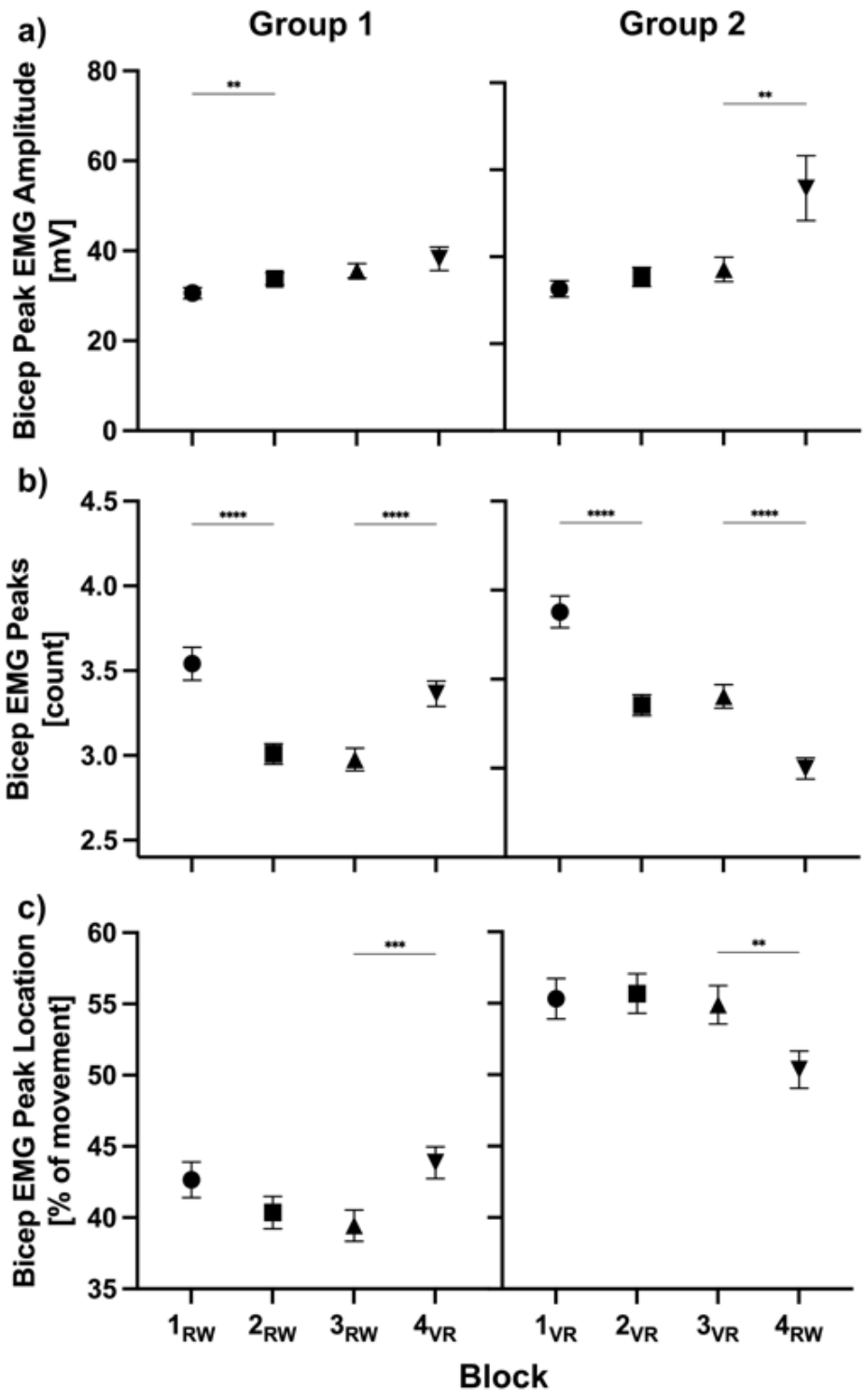

Fig 6.9. Within-subjects differences between blocks are shown both Group 1 and 2 for measures of bicep brachii (bicep) peak EMG amplitude (a), bicep EMG peaks (b), and bicep EMG peak location (c). Mean ± SEM is represented for each block. ** = $p < 0.01$, *** = $p < 0.001$, **** = $p < 0.0001$

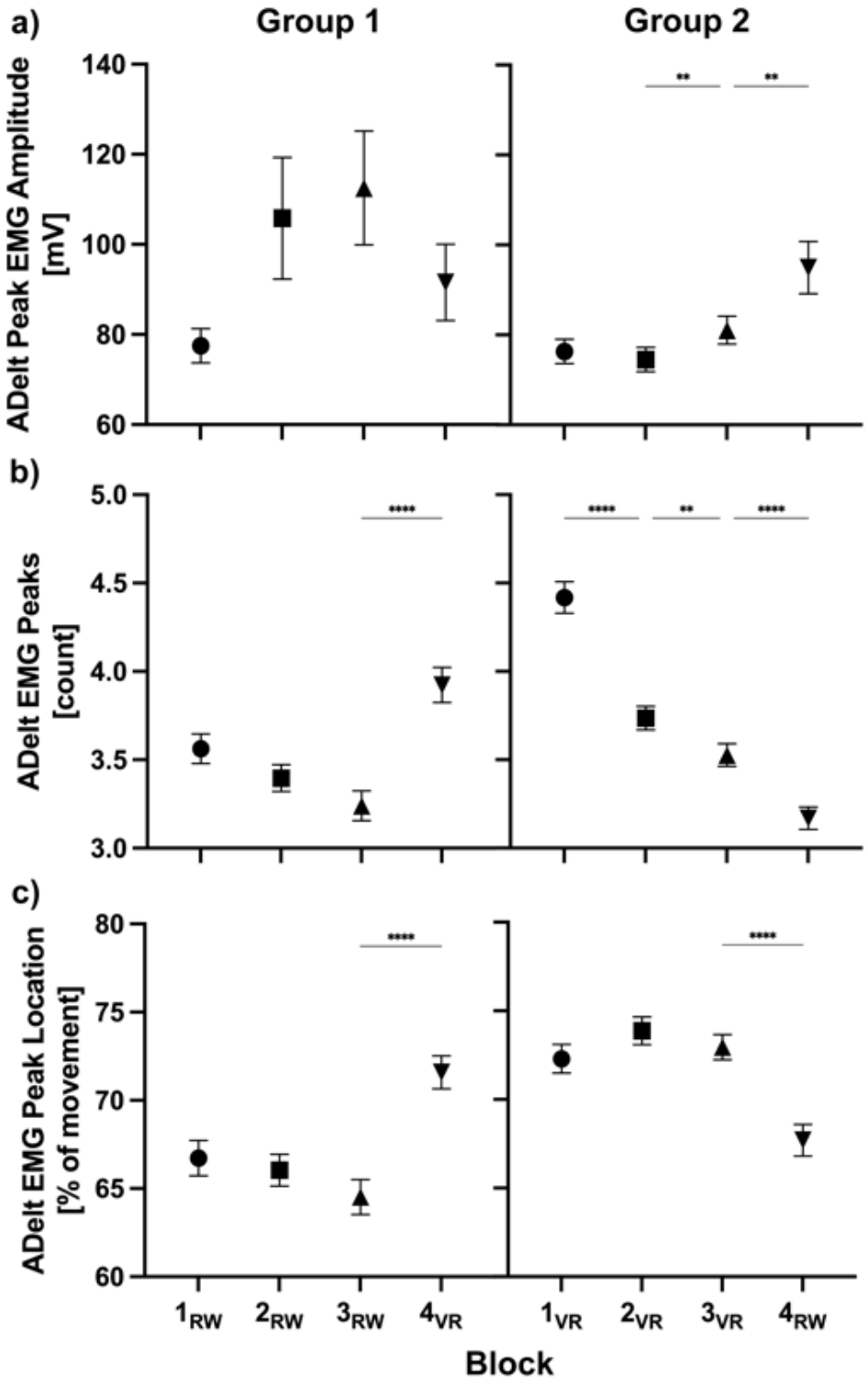

Fig 6.10. Within-subjects differences between blocks are shown both Group 1 and 2 for measures of anterior deltoid (ADelt) peak EMG amplitude (a), ADelt EMG peaks (b), and ADelt EMG peak location (c). Mean ± SEM is represented for each block. ** = $p < 0.01$, **** = $p < 0.0001$

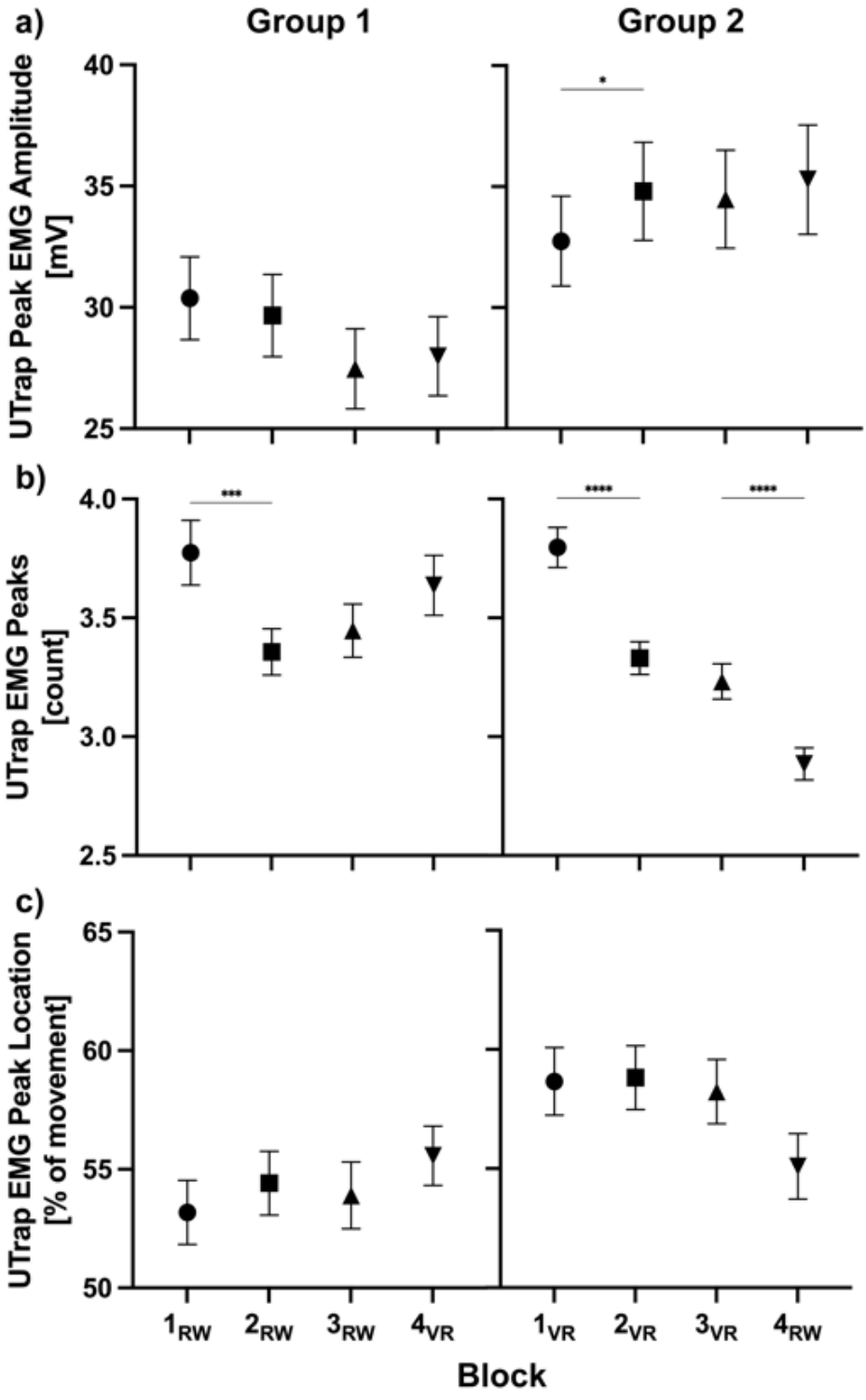

Fig 6.11. Within-subjects differences between blocks are shown both Group 1 and 2 for measures of upper trapezius (UTrap) peak EMG amplitude (a), UTrap EMG peaks (b), and UTrap EMG peak location (c). Mean ± SEM is represented for each block. * = $p < 0.05$, *** = $p < 0.001$, **** = $p < 0.0001$

4. Discussion

4.1 Study Design

Fifty-one participants performed a reaching to visual target task in both RW and VR environments. Every participant performed a total of 108 reaching trials split into four blocks of 27 trials each. Each block consisted of three reaches to each of nine visual targets. Participants were randomly assigned to either perform three blocks in RW, followed by one block in VR (Group 1) or three blocks in VR, followed by one block in RW (Group 2). This design allowed for task familiarization and practice to occur in one environment, then a change of environment for the testing of short-term task translation. Upper limb kinematic and kinetic measures were compared between all adjacent blocks, and shoulder and elbow angles were compared between blocks 3 and 4 from 0-100% of the reaching phase.

To isolate the effect of visual presentation from a virtual or real visual source, other causes of variation were minimized to the best of our ability. The virtual room was modelled as a replication of the real room, auditory stimuli were the same in both environments, and apart from the headset worn in VR, haptic cues were equal between environments. The virtual hand is a key area of difference between the VR and RW settings, the virtual hand was not modified for participant hand size or skin color. This choice was made in consideration of the uncanny valley principle (Mori and Macdorman, 2017) and the importance of embodiment to natural movements in virtual spaces (Pritchard et al., 2016). Additionally, an arm was not modelled in VR. When designing this study, we were not able to identify an arm model, or method of modelling an arm, to track accurately and reliably with the physical arm. There is sufficient evidence to show

that humans are able to move accurately in the absence of visual cues about their body but are not able to fully ignore inaccurate visual information (Bourdin et al., 2019; Spitzley and Karduna, 2022). Therefore, we decided that representing the hand without an arm was less likely to skew results than visualizing a likely inaccurate arm position.

4.2 Kinematics

Participants took more time to respond to the visual stimulus, moved more slowly, and moved less smoothly when in VR as compared to RW. This was demonstrated through measures of response time **[Fig. 6.5 a],** time to target **[Fig. 6.5 b],** mean endpoint velocity **[Fig. 6.6 a],** peak endpoint velocity **[Fig. 6.6 b],** and number of endpoint velocity peaks **[Fig. 6.6 c]** and was consistent regardless of order of environments or number of trials performed in either environment. Overall, the following trends were observed. Participants who familiarized themselves with the task over three blocks performed in RW (Group 1) became faster between blocks 1 and 2, stabilized between blocks 2 and 3, and then slowed significantly when changing from RW to VR between blocks 3 and 4. Participants who familiarized themselves with the task over three blocks performed in VR (Group 2) also became faster between blocks 1 and 2, and stabilized between blocks 2 and 3, then conversely sped up significantly when changing from VR to RW between blocks 3 and 4. Even after being familiarized with the task over 81 trials (blocks 1-3), timing related performance measures were effected by a transition between environments. These results agree with other studies investigating movement times in VR and RW environments under several task paradigms. Slower movements in VR as compared to RW have been demonstrated during a dart-throwing training program (Drew

et al., 2020), a reach-to-grasp and transport task (Arlati et al., 2022), and a full-body standing and reaching task (Thomas et al., 2016). This discrepancy in movement quality could be an important consideration when designing and deploying VR applications for clinical use. Upper-limb and full-body reaching movements are important re-training elements in neurorehabilitation such as recovery from stroke. As it has been demonstrated that individuals experiencing impairment from stroke are already prone to slower and less smooth movements, both at mean and peak (Hussain et al., 2018), the potential of augmenting this pre-existing difference should be considered. A recent study added to these findings by testing upper limb kinematics in VR and RW in partnership with a population undergoing recovery from stroke. In a reaching and grasping task in a stroke recovery population, reaches in VR were slower and less smooth compared to a RW environment (Levin et al., 2015a). While the general trend shown in this study indicates that there are differences in movement performance between RW and VR environments, one important note is that change in environment does not always lead to detrimental outcomes. While timing related performance improvements made in RW did not transfer to VR, improvements in those same metrics did appear in RW when familiarization occurred in VR. This may lend support to the idea that training in VR could benefit timing-related performance in RW.

Participants performed reaching movements using more motion at the elbow and less motion at the shoulder when in VR as compared to RW. This was demonstrated through measures of peak shoulder elevation **[Fig. 6.7 a],** shoulder fROM **[Fig. 6.7 b],** elbow fROM **[Fig. 6.7 c],** and elbow angles over the movement phase **[Fig. 6.8].** Group 1 showed no change in peak shoulder elevation or shoulder fROM over the first three

blocks. When switching from RW to VR between blocks 3 and 4, both measures decreased significantly. Group 2 showed no change in shoulder fROM over the first three blocks and a progressive increase in peak shoulder elevation over all blocks. Then, when switching from VR to RW between blocks 3 and 4, their shoulder fROM increased significantly. Group 1 increased elbow fROM between blocks 1 and 2, stabilized between blocks 2 and 3, and then increased significantly again when changing from RW to VR between blocks 3 and 4. Conversely, Group 2 decreased elbow fROM between blocks 1 and 2, stabilized between blocks 2 and 3, and then decreased significantly again when changing from VR to RW between blocks 3 and 4. SPM analyses provided further insight into these changing movement patterns, showing more elbow flexion in block 4 as compared to block 3 between 22 and 72% of movement in Group 1 **[Fig. 6.8 a]** and between 0 and 20% of movement in Group 2 **[Fig. 6.8 b].** The traces of elbow angle over movement phase for Group 1 show a relatively straight elbow throughout the movement in RW with a more exaggerated flexion of the elbow during the mid-phase of movement in VR. The same traces for Group 2 show the elbow beginning in a more flexed position in RW and a commensurate amount of flexion during mid- and end-phase of movement in RW and VR. Although the statistical comparison is not made, it is also interesting to observe that the patterns in elbow motion for both blocks 3 and 4 in Group 2 are similar to that of block 4 in Group 1. Together these results show that when familiarized with the task in RW, a shift toward increased mid-phase elbow flexion occurs with the change to a VR environment, and when familiarized with the task in VR, mid-phase elbow flexion occurs in both environments. Other studies of upper limb kinematics in real and virtual settings do not show consistent results. Some studies have shown no differences (Arlati et

al., 2022; Levin et al., 2015a) while others also see a shift to the elbow-focused movements strategy (Drew et al., 2020) or greater joint excursions overall (Thomas et al., 2016) in VR. The current study indicates that environment does affect movement strategy at the shoulder and elbow, and that environment in which task familiarization occurs affects movement strategies upon the transition between environments.

4.3 Kinetics

Upon transitioning to VR, the biceps brachii [**Fig. 6.9**] and anterior deltoid [**Fig. 6.10**] muscles peaked later and more frequently than they did during task performance in the RW. Conversely, upon transitioning to the RW, the biceps brachii, anterior deltoid, and upper trapezius [**Fig. 6.11**] peaked earlier and less frequently than they did during task performance in VR. Additionally, the transition to the RW from VR was accompanied with higher activation peaks in the biceps brachii and anterior deltoid muscles. These timing and activation patterns agree with the kinematics measures discussed previously. In the RW, a shoulder-focused movement strategy is employed with less contribution from movement at the elbow joint. Therefore, the biceps brachii, anterior deltoid, and upper trapezius muscles all activate early to lift the entire arm from the resting position and begin moving it toward the target, peaking around 43%, 67%, and 54% of movement, respectively. In VR, and in RW following task familiarization in VR, elbow flexion beginning around 20% of movement brought the load of the forearm closer to the arm, reducing the moment on the shoulder. Around 80% of movement, the elbow is nearly fully extended again, increasing the moment on the shoulder. Peak amplitude of all three muscles occurs during this period of simultaneous shoulder

elevation and elbow extension with the biceps brachii peaking around 53%, anterior deltoid around 73%, and upper trapezius around 58% of movement. The increased amplitude peaks in VR are congruent with the increased endpoint velocity peaks in the kinematic measures. Together these are representative of movement smoothness, as a peak in the EMG signal is indicative of a burst of electrical activity in the muscle that subsides quickly. These bursts in muscles associated with movement at joints controlling the endpoint position would ultimately lead to less smooth endpoint movement as well.

5. Conclusions

While immersive VR systems show great promise in terms of accessibility and customization for applications in many fields including healthcare, there is reason to carefully consider the appropriateness of using these virtual environments for training purposes. Along with previous fMRI and movement research (Beck et al., 2010; Bourdin et al., 2019; Drew et al., 2020; Gonzalez-Franco et al., 2019; Harris et al., 2019; Wright, 2014), the current study calls in to question the translation of motor skills between virtual and real environments. This study examined upper limb kinematics and kinetics when switching between VR and RW environments during a visually cued, reaching to target movement and came to the following conclusions: After performing three blocks of the task in RW, upon transitioning to VR participants demonstrated: a) slower responses to visual targets and slower overall movements toward the targets b) an elbow as opposed to shoulder-focused movement strategy; and c) less smooth muscular control and endpoint movements. After performing three blocks of the task in VR, upon transitioning to RW participants demonstrated: a) faster responses to visual targets and faster overall

movements toward the targets b) a shoulder as opposed to elbow-focused movement strategy; and c) more smooth muscular control and endpoint movements. In line with the initial hypothesis, regardless of the environment in which the task was initially performed, a change in environment led to changes in kinematic and kinetic measures.

Overall, it appears that becoming familiar with a task in the RW, then taking that task in to the VR will result in worse performance in VR as compared to RW. However, the opposite pattern is true when familiarization occurs in VR, and the task is subsequently performed in the RW. These results support two conflicting ideas. First, performance changes upon the transition between environments. This may be viewed negatively if the goal is to train someone how to perform a task in a specific way that needs to be maintained between environments (e.g., training a surgical technique). Second, the improvement of performance when switching to RW after task familiarization in VR may support the use of virtual environments for training skills to be performed in real environments. Further studies into the long-term effects of training environment and the effects of environment on neural circuitry are important to eventually determining the safety and usefulness of VR systems.

CHAPTER VII

CONCLUDING SUMMARY

1. Summary of Results and Findings

This dissertation aims to understand upper limb movement in both virtual and real-world environments. The rapid advancement of virtual and mixed reality technologies has led to their widespread adoption in various industries, including several areas within the medical field. These systems have tremendous potential to control the user's sensory field while simultaneously capturing their response to the virtual environment. Harnessing these capabilities has emerged as a popular avenue of research for movement and behavioral training. Before deploying virtual applications to modify or augment behavior, it is important to understand how humans are affected by the virtual presentation of sensory information.

The body of work presented in this dissertation contributes to that understanding in several key ways. First, it validates sensors which are integrated in an immersive VR system (the HTC VIVE) for the collection of position and orientation data. Second, it explores the roles of vision and proprioception in movement within a virtual environment. Lastly, it compares movements in VR and RW environments and the effects of transitioning between environments. As a whole, the studies outlined in this dissertation contribute to the broader base of motor control, offering insights to inform the design and implementation of effective protocols and applications in both real and virtual settings. The sections below provide an overview of the main outcomes from each topic area.

1.1 Sensor Validation

Chapters II and III of this dissertation provide evidence that the HTC VIVE sensors are reliable and accurate tools for the collection of position and orientation data, as compared to industry gold standard systems. During static testing, the error measurements of both VIVE sensors were low, as indicated by mean rotational errors below 0.4° and mean translational errors below 3 mm. Drift over a 10 second period was higher from both VIVE sensors than from the gold-standard, but was still relatively low, falling below 0.1° for rotational components and 0.35 mm for translational components. During dynamic rotational testing, no differences were seen between speeds, sections of the room, or configurations of the lighthouse and sensors. Comparisons between the gold-standard system and VIVE tracker resulted in mean r-squared values of 0.99, mean RSME of 1.1°, and a mean absolute error of 0.23°. These measures of accuracy and reliability are promising and support the use of these systems for the collection of larger ranges of human movement. Applications which require extreme precision, such as the study of surgical techniques, may want to consider other systems. These measures should be regularly reevaluated as sensing and computing technology improves.

1.2 Vision and Proprioception in VR

Chapter IV of this dissertation shows how joint position matching is affected by alterations to visuoproprioceptive congruency in a VR environment. Building on findings from the previous two chapters, the VIVE tracker was used to estimate arm position and orientation. Accuracy and consistency of position matching were tested under conditions where the participant had either a true visual representation of their upper limb, no visual

representation of their upper limb, or visual representation of their upper limb which was offset from the proprioceptive representation. While removing visual representation of the limb did not alter accuracy or consistency, offsetting limb representation resulted in decreased accuracy but unaltered consistency. This suggests that in the absence of visual input proprioceptive information in combination with information from prior experience is sufficient for accurate and reliable completion of movement. However, when there is a mismatch between visual and proprioceptive signals, the inaccurate visual signal takes precedence over the accurate proprioceptive signal. These findings underlie the importance of visual information in movement planning and execution and confirm their importance within a VR environment.

1.3 Virtual and Real-Worlds

Chapters V and VI of this dissertation show how kinematic and kinetic characteristics of reaching movements differ between real and virtual environments, and that the differences are effected by order of exposure to environment. As compared to the RW, movements in VR were slower, more delayed in their initiation, employed more movement at the elbow, exhibited more peaks in EMG amplitude, and the EMG signal peaked later in the movement. When task familiarization occurred in the RW, performance in the above-mentioned metrics decreased upon switching to VR. However, when familiarization occurred in VR, performance improved upon switching to the RW. These results show that performance does change when switching between environments, but that the order of environment matters. Given these findings, it is important to

carefully consider whether current VR technology is appropriate depending on the intended use case.

2. Recommendations for Future Work

With virtual and other extended reality systems rapidly improving, the options for future work in this area is ever expanding. Keeping up with the technological progress in this area is an entire area of work in itself. As the computing power and methodologies used to operate these systems continues to expand, they will proliferate many areas of scientific investigation. A few key areas of interest that are related to this work are outlined here.

Tracking human characteristics is a key feature of rapid development in VR and other XR technologies. This dissertation focuses on the capability of the HTC VIVE surface sensors to track 6-degree of freedom movement of body segments. However, systems are immerging that have the capability to track eye movement, facial expressions, hand gestures, and objects in the external environment. The technology used in this dissertation employs a combination of optical and inertial sensors to estimate position and orientation, but camera-based markerless tracking is on a steep incline. Continuing to validate the accuracy and reliability of tracking capabilities from immerging systems is important to their continued use for scientific investigation.

This work examined some kinematic and kinetic outcomes from upper limb movements in virtual and real environments. From these outcomes, inferences about movement planning and cortical processes can be made. However, to provide a deeper understanding of how the brain is processing virtual visual cues, more direct

measurements should be taken. Using BOLD or electrical measurement systems in concert with virtual visual environments can provide important insights into the neural circuitry involved in the processing of virtual sensory signals. Additionally, examining all of these metrics using different movement paradigms is important in expanding the general knowledge base regarding movement in VR.

While this work did examine the effect of familiarization environment on movement outcomes, it did not employ any training practice paradigm to investigate learning. Future work should create an intentional framework for skill-based learning in both environments and consider the consequences on skill performance when switching environments. This is very important in the context of clinical investigations or any training application. A deep understanding of the relationship between environments in the context of skill acquisition and transfer is essential in protecting vulnerable populations.

REFERENCES CITED

Amasay, T., Karduna, A., 2013. Patient's Body Size Influences Dental Hygienist Shoulder Kinematics. IIE Trans. Occup. Ergon. Hum. Factors 1, 153–165. https://doi.org/10.1080/21577323.2013.787956

Arlati, S., Keijsers, N., Paolini, G., Ferrigno, G., Sacco, M., 2022. Kinematics of aimed movements in ecological immersive virtual reality: a comparative study with real world. Virtual Real. 26, 885–901.

Bagesteiro, L.B., Sarlegna, F.R., Sainburg, R.L., 2006. Differential influence of vision and proprioception on control of movement distance. Exp. Brain Res. 171, 358–370. https://doi.org/10.1007/s00221-005-0272-y

Barden, J.M., Balyk, R., James Raso, V., Moreau, M., Bagnall, K., 2005. Repetitive pointing to remembered proprioceptive targets improves 3D hand positioning accuracy. Hum. Mov. Sci. 24, 184–205. https://doi.org/10.1016/j.humov.2005.03.004

Beck, L., Wolter, M., Mungard, N.F., Vohn, R., Staedtgen, M., Kuhlen, T., Sturm, W., 2010. Evaluation of spatial processing in virtual reality using functional magnetic resonance imaging (fMRI). Cyberpsychology, Behav. Soc. Netw. 13, 211–215. https://doi.org/10.1089/cyber.2008.0343

Berkinblit, M.B., Fookson, O.I., Smetanin, B., Adamovich, S. V, Poizner, H., 1995. The interaction of visual and proprioceptive inputs in pointing to actual and remembered targets. Exp. brain Res. 107, 326–30.

Birkfellner, W., Watzinger, F., Wanschitz, F., Ewers, R., Bergmann, H., 1998. Calibration of tracking systems in a surgical environment. IEEE Trans. Med. Imaging 17, 737–42. https://doi.org/10.1109/42.736028

Block, H.J., Bastian, A.J., 2011. Sensory weighting and realignment: independent compensatory processes. J. Neurophysiol. 106, 59–70. https://doi.org/10.1152/jn.00641.2010.

Block, H.J., Bastian, A.J., 2010. Sensory Reweighting in Targeted Reaching: Effects of Conscious Effort, Error History, and Target Salience. J. Neurophysiol. 103, 206–217. https://doi.org/10.1152/jn.90961.2008

Blouin, J., Bard, C., Teasdale, N., Paillard, J., Fleury, M., Forget, R., Lamarre, Y., 1993. Reference systems for coding spatial information in normal subjects and a deafferented patient. Exp. Brain Res. 93, 324–331.

Bourdin, P., Martini, M., Sanchez-Vives, M. V., 2019. Altered visual feedback from an embodied avatar unconsciously influences movement amplitude and muscle activity. Sci. Rep. 9, 1–9. https://doi.org/10.1038/s41598-019-56034-5

Bruno, N., Bernardis, P., Gentilucci, M., 2008. Visually guided pointing, the Muïler-Lyer illusion, and the functional interpretation of the dorsal-ventral split: Conclusions from 33 independent studies. Neurosci. Biobehav. Rev. 32, 423–437. https://doi.org/10.1016/j.neubiorev.2007.08.006

Burgess, C.R., Livneh, Y., Ramesh, R.N., Andermann, M.L., 2018. Gating of visual processing by physiological need. Curr. Opin. Neurobiol. 49, 16–23. https://doi.org/10.1016/j.conb.2017.10.020

Caola, B., Montalti, M., Zanini, A., Leadbetter, A., Martini, M., 2018. The Bodily Illusion in Adverse Conditions: Virtual Arm Ownership During Visuomotor Mismatch. Perception 47, 477–491. https://doi.org/10.1177/0301006618758211

Cheng, D.T., Luis, M., Tremblay, L., 2008. Randomizing visual feedback in manual aiming: Reminiscence of the previous trial condition and prior knowledge of feedback availability. Exp. Brain Res. 189, 403–410. https://doi.org/10.1007/s00221-008-1436-3

Cipresso, P., Giglioli, I.A.C., Raya, M.A., Riva, G., 2018. The past, present, and future of virtual and augmented reality research: A network and cluster analysis of the literature. Front. Psychol. 9, 1–20. https://doi.org/10.3389/fpsyg.2018.02086

Cortes, G., Argelaguet, F., Marchand, E., Lécuyer, A., 2018. Virtual shadows for real humans in a cave: Influence on virtual embodiment and 3D interaction, Proceedings - SAP 2018: ACM Symposium on Applied Perception. https://doi.org/10.1145/3225153.3225165

Cruse, H., Dean, J., Heuer, H., Scmidt, R., 1990. Utilization of sensory information for motor control, in: Neumann, O., Prinz, W. (Eds.), Relationships between Perception and Action. Springer-Verlag, Berlin, pp. 43–79.

Cruz-Neira, C., Sandin, D.J., DeFanti, T.A., Kenyon, R. V., Hart, J.C., 1992. The CAVE: audio visual experience automatic virtual environment, in: Communications of the ACM. p. 64.

Dadarlat, M.C., O, J.E., Sabes, P.N., 2015. A learning-based approach to artificial sensory feedback leads to optimal integration. Nat. Neurosci. 18, 138–146. https://doi.org/10.1038/nn.3883

Darling, W.G., Miller, G.F., 1993. Transformations between visual and kinesthetic coordinate systems in reaches to remembered object locations and orientations. Exp. brain Res. 93, 534–547.

Drew, S.A., Awad, M.F., Armendariz, J.A., Gabay, B., Lachica, I.J., Hinkel-Lipsker, J.W., 2020. The Trade-Off of Virtual Reality Training for Dart Throwing: A Facilitation of Perceptual-Motor Learning With a Detriment to Performance. Front. Sport. Act. Living 2, 1–14. https://doi.org/10.3389/fspor.2020.00059

Edwards, E.S., Liang-Lin, Y., King, J.H., Karduna, A.R., 2016. Joint position sense – There's an app for that. J. Biomech. 49, 3529–3533. https://doi.org/10.1016/j.jbiomech.2016.07.033

Egger, J., Gall, M., Wallner, J., Boechat, P., Hann, A., Li, X., Chen, X., Schmalstieg, D., 2017. HTC Vive MeVisLab integration via OpenVR for medical applications. PLoS One 12, 1–14. https://doi.org/10.1371/journal.pone.0173972

Enoka, R.M., 2002. Sensory Receptor, in: Neuromechanics of Human Movement. pp. 232–239.

Erickson, R.I.C., Karduna, A.R., 2012. Three-dimensional repositioning tasks show differences in joint position sense between active and passive shoulder motion. J. Orthop. Res. 30, 787–792. https://doi.org/10.1002/jor.22007

Ernst, M.O., Banks, M.S., 2002. Humans integrate visual and haptic information in a statistically optimal fashion. Nature 415, 429–433. https://doi.org/10.1038/415429a

Ettinger, L., Shapiro, M., Karduna, A., 2014. Subacromial Injection Results in Further Scapular Dyskinesis. Orthop. J. Sport. Med. 2, 1–7. https://doi.org/10.1177/2325967114544104

Faisal, A.A., Luc, S.P.J., Wolpert, D.M., 2008. Noise in the nervous system. Nat. Rev. Neurosci. 9, 292–303. https://doi.org/10.1037/h0023240

Fisk, J.D., Goodale, M.A., 1985. The organization of eye and limb movements during unrestricted reaching to targets in contralateral and ipsilateral visual space. Exp. Brain Res. 60, 159–178. https://doi.org/10.1007/BF00237028

Frantz, D., Wiles, Andrew Donald, Kirsch, Stefan Reinhard, Frantz, D.D., Wiles, A D, Leis, S.E., Kirsch, S R, 2003. Accuracy assessment protocols for electromagnetic tracking systems. Phys. Med. Biol. Phys. Med. Biol 48, 2241–2251. https://doi.org/10.1088/0031-9155/48/14/314

Ghez, C., Gordon, J., Ghilardi, M.F., 1995. Impairments of Reaching Movements in Patients Without Proprioception . II . Effects of Visual Information on Accuracy. J. Neurophysiol. 73, 361–371.

Goble, D.J., 2010. Proprioceptive Acuity Assessment Via Joint Position Matching: From Basic Science to General Practice. Phys. Ther. 90, 1176–1184. https://doi.org/10.2522/ptj.20090399

Gonzalez-Franco, M., Abtahi, P., Steed, A., 2019. Individual differences in embodied distance estimation in virtual reality. 26th IEEE Conf. Virtual Real. 3D User Interfaces, VR 2019 - Proc. 941–943. https://doi.org/10.1109/VR.2019.8798348

Goodale, M.A., 2011. Transforming vision into action. Vision Res. 51, 1567–1587. https://doi.org/10.1016/j.visres.2010.07.027

Goodale, M.A., Pelisson, D., Prablanc, C., 1986. Large adjustments in visually guided reaching do not depend on vision of the hand or perception of target displacement. Nature 320, 748–750. https://doi.org/10.1038/320748a0

Goodale, M.A., Westwood, D.A., 2004. An evolving view of duplex vision: Separate but interacting cortical pathways for perception and action. Curr. Opin. Neurobiol. 14, 203–211. https://doi.org/10.1016/j.conb.2004.03.002

Goodman, R., Tremblay, L., 2018. Using proprioception to control ongoing actions: dominance of vision or altered proprioceptive weighing? Exp. Brain Res. 236, 1897–1910. https://doi.org/10.1007/s00221-018-5258-7

Guillaud, E., Simoneau, M., Blouin, J., 2011. Prediction of the body rotation-induced torques on the arm during reaching movements: Evidence from a proprioceptively deafferented subject. Neuropsychologia 49, 2055–2059. https://doi.org/10.1016/j.neuropsychologia.2011.03.035

Han, J., Waddington, G., Adams, R., Anson, J., Liu, Y., 2016. Assessing proprioception: A critical review of methods. J. Sport Heal. Sci. 5, 80–90. https://doi.org/10.1016/j.jshs.2014.10.004

Harris, C.M., Wolpert, D.M., 1998. Signal-dependent noise determines motor planning. Nature 394, 780–784.

Harris, D.J., Bird, J.M., Smart, P.A., Wilson, M.R., Vine, S.J., 2020. A Framework for the Testing and Validation of Simulated Environments in Experimentation and Training. Front. Psychol. 11, 1–10. https://doi.org/10.3389/fpsyg.2020.00605

Harris, D.J., Buckingham, G., Wilson, M.R., Vine, S.J., 2019. Virtually the same? How impaired sensory information in virtual reality may disrupt vision for action. Exp. Brain Res. 237, 2761–2766. https://doi.org/10.1007/s00221-019-05642-8

Helms Tillery, S., Sainburg, R.L., 2012. Multisensory Integration for Motor Control and Adaptation. J. Mot. Behav. 44, 389–390. https://doi.org/10.1080/00222895.2012.747306

Hillier, S., Immink, M., Thewlis, D., 2015. Assessing Proprioception: A Systematic Review of Possibilities. Neurorehabil. Neural Repair 29, 933–949. https://doi.org/10.1177/1545968315573055

Holmes, N.P., Spence, C., 2005. Visual bias of unseen hand position with a mirror: Spatial and temporal factors. Exp. Brain Res. 1666, 489–497. https://doi.org/10.1007/s00221-005-2389-4

htc VIVE User Guide, 2016. https://doi.org/10.4337/9781782545583.00006

Hussain, N., Murphy, M.A., Sunnerhagen, K.S., 2018. Upper limb kinematics in stroke and healthy controls using target-to-target task in virtual reality. Front. Neurol. 9, 1–9. https://doi.org/10.3389/fneur.2018.00300

Ikbali Afsar, S., Mirzayev, I., Umit Yemisci, O., Cosar Saracgil, S.N., 2018. Virtual Reality in Upper Extremity Rehabilitation of Stroke Patients: A Randomized Controlled Trial. J. Stroke Cerebrovasc. Dis. 27, 3473–3478. https://doi.org/10.1016/j.jstrokecerebrovasdis.2018.08.007

Janeh, O., Fründt, O., Schönwald, B., Gulberti, A., Buhmann, C., Gerloff, C., Steinicke, F., Pötter-Nerger, M., 2019. Gait Training in Virtual Reality: Short-Term Effects of Different Virtual Manipulation Techniques in Parkinson's Disease. Cells 8, 419. https://doi.org/10.3390/cells8050419

Jankowska, E., 1992. Interneuronal relay in spinal pathways from proprioceptors, Progress in Neurobiology.

Jiang, W., Jiang, H., Stein, B.E., 2001. Two Corticotectual Areas Facilitate Multisensory Orientation Behavior. J. Cogn. Neurosci. 14, 1240–1255.

Johansson, H., Silfvenius, H., 1977. Axon-collateral activation by dorsal spinocerebellar tract fibres of group I relay cells of nucleus z in the cat medulla oblongata. J. Physiol. 265, 341–369.

Jost, T.A., Drewelow, G., Koziol, S., Rylander, J., 2019. A quantitative method for evaluation of 6 degree of freedom virtual reality systems. J. Biomech. 97, 109379. https://doi.org/10.1016/j.jbiomech.2019.109379

Juan, M.C., Elexpuru, J., Dias, P., Sousa, B., Paula, S., 2022. Immersive virtual reality for upper limb rehabilitation : comparing hand and controller interaction. Virtual Real. https://doi.org/10.1007/s10055-022-00722-7

Kahol, K., Leyba, M.J., Deka, M., Deka, V., Mayes, S., Smith, M., Ferrara, J.J., Panchanathan, S., 2008. Effect of fatigue on psychomotor and cognitive skills. Am. J. Surg. 195, 195–204. https://doi.org/10.1016/J.AMJSURG.2007.10.004

Kahol, K., Satava, R.M., Ferrara, J., Smith, M.L., 2009. Effect of Short-Term Pretrial Practice on Surgical Proficiency in Simulated Environments: A Randomized Trial of the "Preoperative Warm-Up" Effect. J. Am. Coll. Surg. 208, 255–268. https://doi.org/10.1016/J.JAMCOLLSURG.2008.09.029

Keshner, E.A., Weiss, P.T., Geifman, D., Raban, D., 2019. Tracking the evolution of virtual reality applications to rehabilitation as a field of study. J. Neuroeng. Rehabil. 16, 1–15. https://doi.org/10.1186/s12984-019-0552-6

Kilteni, K., Groten, R., Slater, M., 2012. The Sense of Embodiment in virtual reality. Presence Teleoperators Virtual Environ. 21, 373–387. https://doi.org/10.1162/PRES_a_00124

King, J., Harding, E., Karduna, A., 2013. The Shoulder and Elbow Joints and Right and Left Sides Demonstrate Similar Joint Position Sense. J. Mot. Behav. 45, 479–486.

Körding, K.P., Wolpert, D.M., 2006. Bayesian decision theory in sensorimotor control. TRENDS Cogn. Sci. 10, 319–326. https://doi.org/10.1016/j.tics.2006.05.003

Kwon, Y.W., Pinto, V.J., Yoon, J., Frankle, M.A., Dunning, P.E., Sheikhzadeh, A., 2012. Kinematic analysis of dynamic shoulder motion in patients with reverse total shoulder arthroplasty. J. Shoulder Elb. Surg. 21, 1184–1190. https://doi.org/10.1016/J.JSE.2011.07.031

Landgren, S., Silfvenius, H., 1971. Nucleus Z, The medullary relay in the projection path to the cerebral cortex of group I muscle afferents from the cat's hind limb. J. Physiol. 218, 551–571.

Lebel, K., Boissy, P., Hamel, M., Duval, C., 2013. Inertial measures of motion for clinical biomechanics: Comparative assessment of accuracy under controlled conditions - Effect of velocity. PLoS One 8. https://doi.org/10.1371/journal.pone.0079945

Lei, Y., Wang, J., 2018. The effect of proprioceptive acuity variability on motor adaptation in older adults. Exp. Brain Res. 236, 599–608. https://doi.org/10.1007/s00221-017-5150-x

Levin, M.F., Magdalon, E.C., Michaelsen, S.M., Quevedo, A.A.F., 2015a. Quality of Grasping and the Role of Haptics in a 3-D Immersive Virtual Reality Environment in Individuals With Stroke. IEEE Trans. Neural Syst. Rehabil. Eng. 23, 1047–1055. https://doi.org/10.1109/TNSRE.2014.2387412

Levin, M.F., Weiss, P.L., Keshner, E.A., 2015b. Emergence of Virtual Reality as a Tool for Upper Limb Rehabilitation: Incorporation of Motor Control and Motor Learning Principles. Phys. Ther. 95, 415–425. https://doi.org/10.2522/ptj.20130579

Lin, Y.-L., Karduna, A., 2016. Exercises focusing on rotator cuff and scapular muscles do not improve shoulder joint position sense in healthy subjects. Hum. Mov. Sci. 49, 248–257. https://doi.org/10.1016/j.humov.2016.06.016

Martindale, J., 2018. Oculus Rift vs. HTC Vive Spec Comparison [WWW Document]. Digit. Trends. URL https://www.digitaltrends.com/virtual-reality/oculus-rift-vs-htc-vive/ (accessed 9.3.18).

Matthews, P.B.C., 1982. Where does Sherrington's "muscular sense" originate? Muscles, joints, corollary discharges? Ann Rev Neurosci 5, 189–218.

Mekbib, D.B., Han, J., Zhang, L., Fang, S., Jiang, H., Zhu, J., Roe, A.W., Xu, D., 2020. Virtual reality therapy for upper limb rehabilitation in patients with stroke: a meta-analysis of randomized clinical trials. Brain Inj. 34, 456–465. https://doi.org/10.1080/02699052.2020.1725126

Meredith, M.A., Stein, B.E., 1986. Visual, auditory, and somatosensory convergence on cells in superior colliculus results in multisensory integration. J. Neurophysiol. 56, 640–62. https://doi.org/10.1152/jn.1986.56.3.640

Mineiro, J., Buckingham, G., 2023. O hand, where art thou? Mapping hand location across the visual field during common activities. Exp. Brain Res. 241, 1227–1239. https://doi.org/10.1007/s00221-023-06597-7

Mocap for VR - Vicon Reality | VICON [WWW Document], n.d. URL https://www.vicon.com/motion-capture/vicon-reality (accessed 9.3.18).

Mori, M., Macdorman, K.F., 2017. The Uncanny Valley: The Original Essay by Masahiro Mori, IEEE Spectrum.

Nafis, C., Jensen, V., Beauregard, L., Anderson, P., 2006. Method for estimating dynamic EM tracking accuracy of Surgical Navigation tools.

Niehorster, D.C., Li, L., Lappe, M., 2017. The Accuracy and Precision of Position and Orientation Tracking in the HTC Vive Virtual Reality System for Scientific Research. Iperception. 8. https://doi.org/10.1177/2041669517708205

Nierula, B., Spanlang, B., Martini, M., Borrell, M., Nikulin, V. V., Sanchez-Vives, M. V., 2019. Agency and responsibility over virtual movements controlled through different paradigms of brain−computer interface. J. Physiol. 0, 1–16. https://doi.org/10.1113/JP278167

Nyland, J.A., Caborn, D.N.M., Johnson, D.L., 1998. The human glenohumeral joint: A proprioceptive and stability alliance. Knee Surgery, Sport. Traumatol. Arthrosc. 6, 50–61. https://doi.org/10.1007/s001670050072

Oldfield, R.C., 1971. The assessment and analysis of handedness: the Edinburgh inventory. Neuropsychologia 9, 97–113.

OptiTrack - Motion Capture for Virtual Reality [WWW Document], 2018. URL https://optitrack.com/motion-capture-virtual-reality/ (accessed 9.3.18).

Ott, T., Nieder, A., 2019. Feature Review Dopamine and Cognitive Control in Prefrontal Cortex. Trends Cogn. Sci. 23. https://doi.org/10.1016/j.tics.2018.12.006

Pataky, T.C., 2012. One-dimensional statistical parametric mapping in Python. Comput. Methods Biomech. Biomed. Engin. 15, 295–301. https://doi.org/10.1080/10255842.2010.527837

Polhemus, 2012. LIBERTY™ USER MANUAL.

Pritchard, S.C., Zopf, R., Polito, V., Kaplan, D.M., Williams, M.A., 2016. Non-hierarchical influence of visual form, touch, and position cues on embodiment, agency, and presence in virtual reality. Front. Psychol. 7, 1–14. https://doi.org/10.3389/fpsyg.2016.01649

Proske, U., Gandevia, S.C., 2012. The Proprioceptive Senses: Their Roles in Signaling Body Shape, Body Position and Movement, and Muscle Force. Physiol. Rev. 92, 1651–1697. https://doi.org/10.1152/physrev.00048.2011.-This

Proske, U., Gandevia, S.C., 2009. The kinaesthetic senses. J. Physiol. 587, 4139–4146. https://doi.org/10.1113/jphysiol.2009.175372

Rickards, C., Cody, Frederick W J, Cody, F W J, 1997. Proprioceptive control of wrist movements in Parkinson's disease Reduced muscle vibration-induced errors. Brain 120, 977–990.

Riemann, B.L., Lephart, S.M., 2002a. The Sensorimotor System, Part I: The Physiologic Basis of Functional Joint Stability. J. Athl. Train. 37, 71–79.

Riemann, B.L., Lephart, S.M., 2002b. The Sensorimotor System, Part II: The Role of Proprioception in Motor Control and Functional Joint Stability. J. Athl. Train. 3737, 80–84.

Roll, J.P., Vedel, J.P., Ribot, E., 1989. Alteration of proprioceptive messages induced by tendon vibration in man: a microneurographic study. Exp. brain Res. 76, 213–222.

Rossetti, Y., Desmurget, M., Prablanc, C., 1995. Vectorial coding of movement: vision, proprioception, or both? J. Neurophysiol. 74, 457–463.

Sainburg, R.L., Lateiner, J.E., Latash, M.L., Bagesteiro, L.B., 2003. Effects of Altering Initial Position on Movement Direction and Extent. J. Neurophysiol. 89, 401–415. https://doi.org/10.1152/jn.00243.2002

Sansone, L.G., Stanzani, R., Job, M., Battista, S., Signori, A., Testa, M., 2022. Robustness and static-positional accuracy of the SteamVR 1.0 virtual reality tracking system. Virtual Real. 26, 903–924. https://doi.org/10.1007/s10055-021-00584-5

Sarlegna, F.R., Malfait, N., Bringoux, L., Bourdin, C., Vercher, J.L., 2010. Force-field adaptation without proprioception: Can vision be used to model limb dynamics? Neuropsychologia 48, 60–67. https://doi.org/10.1016/j.neuropsychologia.2009.08.011

Sarlegna, F.R., Sainburg, R.L., 2009. The roles of vision and proprioception in the planning of reaching movements., in: Springer (Ed.), Progress in Motor Control. Boston, MA, pp. 317–335. https://doi.org/10.1007/978-0-387-77064-2_16

Sarlegna, F.R., Sainburg, R.L., 2007. The effect of target modality on visual and proprioceptive contributions to the control of movement distance. Exp. Brain Res. 176, 267–280. https://doi.org/10.1007/s00221-006-0613-5

Seidler, R.D., Bernard, J.A., Burutolu, T.B., Fling, B.W., Gordon, M.T., Gwin, J.T., Kwak, Y., Lipps, D.B., 2010. Motor control and aging: Links to age-related brain structural, functional, and biochemical effects. Neurosci. Biobehav. Rev. 34, 721–733. https://doi.org/10.1016/j.neubiorev.2009.10.005

Seiss, E., Praamstra, P., Hesse, C.W., Rickards, H., 2003. Proprioceptive sensory function in Parkinson's disease and Huntington's disease: Evidence from proprioception-related EEG potentials. Exp. Brain Res. 148, 308–319. https://doi.org/10.1007/s00221-002-1291-6

Sergio, L.E., Scott, S.H., 1998. Hand and joint paths during reaching movements with and without vision. Exp. Brain Res. 122, 157–164. https://doi.org/10.1007/s002210050503

Shomstein, S., 2012. Cognitive functions of the posterior parietal cortex: Top-down and bottom-up attentional control. Front. Integr. Neurosci. 6, 1–7. https://doi.org/10.3389/fnint.2012.00038

Soares, I., Sousa, R.B., Petry, M., Moreira, A.P., 2021. Accuracy and repeatability tests on hololens 2 and htc vive. Multimodal Technol. Interact. 5, 1–14. https://doi.org/10.3390/mti5080047

Sober, S.J., Sabes, P.N., 2005. Flexible strategies for sensory integration during motor planning. Nat. Neurosci. 8, 490–497. https://doi.org/10.1038/nn1427

Sober, S.J., Sabes, P.N., 2003. Multisensory Integration during Motor Planning. J. Neurosci. 23, 6982–6992. https://doi.org/citeulike-article-id:409345

Soechting, J.F., Flanders, M., 1989. Errors in pointing are due to approximations in sensorimotor transformations. J. Neurophysiol. 62, 595–608. https://doi.org/10.1152/jn.1989.62.2.595

Spitzley, K.A., Karduna, A.R., 2022. Joint Position Accuracy Is Influenced by Visuoproprioceptive Congruency in Virtual Reality. J. Mot. Behav. 54, 92–101. https://doi.org/10.1080/00222895.2021.1916425

Spitzley, K.A., Karduna, A.R., 2019. Feasibility of using a fully immersive virtual reality system for kinematic data collection. J. Biomech. 87, 172–176. https://doi.org/10.1016/j.jbiomech.2019.02.015

Spoor, C.W.;, Veldpaus, F.E., 1980. Rigid body motion calculated from spatial co-ordinates of markers. J. Biomech. 13, 391–393. https://doi.org/10.1016/0021-9290(80)90020-2

Stein, B.E., Stanford, T.R., Rowland, B.A., 2009. The Neural Basis of Multisensory Integration in the Midbrain: Its Organization and Maturation. Hear. Res. 258, 4–15. https://doi.org/10.1016/j.bmcl.2009.08.098

Stein, B.E., Wallace, M.W., Stanford, T.R., Jiang, W., 2002. Cortex governs multisensory integration in the midbrain. Neuroscientist 8, 306–314. https://doi.org/10.1177/107385840200800406

Suprak, D.N., Osternig, L.R., van Donkelaar, P., Karduna, A.R., 2006. Shoulder Joint Position Sense Improves with Elevation Angle in a Novel, Unconstrained Task. J. Orthop. Res. 24, 559–568. https://doi.org/https://doi.org/10.1002/jor.20095

Sutherland, I.E., 1968. A head-mounted three dimensional display, in: Proceedings of the December 9-11, 1968, Fall Joint Computer Conference, Part I. Association for Computing Machinery, pp. 757–764. https://doi.org/10.1016/0033-5894(75)90039-3

Thomas, J.S., France, C.R., Leitkam, S.T., Applegate, M.E., Pidcoe, P.E., Walkowski, S., 2016. Effects of real-world versus virtual environments on joint excursions in full-body reaching tasks. IEEE J. Transl. Eng. Heal. Med. 4, 1–8. https://doi.org/10.1109/JTEHM.2016.2623787

van Beers, R.J., Sittig, A.C., Denier van der Gon, jan J., 1999. Integration of Proprioceptive and Visual Position-Information: An Experimentally Supported Model. J. Neurophysiol. 81, 1355–1364.

van Beers, R.J., Sittig, A.C., Denier Van Der Gon, J.J., 1996. How humans combine simultaneous proprioceptive and visual position information. Exp. brain Res. 111, 253–261. https://doi.org/10.1007/BF00227302

van Beers, R.J., Wolpert, D.M., Haggard, P., 2002. When Feeling Is More Important Than Seeing in Sensorimotor Adaptation, Current Biology. https://doi.org/10.1016/S0960-9822(02)00836-9

Van Der Kooij, K., Brenner, E., van Beers, R.J., Schot, W.D., Smeets, J.B.J., 2013. Alignment to natural and imposed mismatches between the senses. J. Neurophysiol. 109, 1890–1899. https://doi.org/10.1152/jn.00845.2012.

Verhoef, B.E., Vogels, R., Janssen, P., 2016. Binocular depth processing in the ventral visual pathway. Philos. Trans. R. Soc. B Biol. Sci. 371. https://doi.org/10.1098/rstb.2015.0259

Waked, I.S., Eid, M.M., 2019. Virtual reality: A non-pharmacological complementary strategy facilitating Physical Therapy procedures for adolescent burned patients Physical Therapy and Rehabilitation. Phys. Ther. Rehabil. 6, 2055–2386. https://doi.org/10.7243/2055-2386-6-1

Wall, P., Noordenbos, W., 1977. Sensory functions which remain in man after complete transection of dorsal columns. Brain 100, 641–653.

Weiss, P.H., Marshall, J.C., Wunderlich, G., Tellmann, L., Halligan, P.W., Freund, H.J., Zilles, K., Fink, G.R., 2000. Neural consequences of acting in near versus far space: A physiological basis for clinical dissociations. Brain 123, 2531–2541. https://doi.org/10.1093/brain/123.12.2531

Welch, R.B., Warren, D.H., 1986. Intersensory interactions, in: Boff, K.R., Kaufman, L., Thomas, J.P. (Eds.), Handbook of Perception and Human Performance. John Wiley & Sons, New York, pp. 1–36.

Wenk, N., Penalver-Andres, J., Buetler, K.A., Nef, T., Müri, R.M., Marchal-Crespo, L., 2021. Effect of immersive visualization technologies on cognitive load, motivation, usability, and embodiment. Virtual Real. https://doi.org/10.1007/s10055-021-00565-8

Wohlgenannt, I., Simons, A., Sti, S., 2020. Virtual Reality. Bus. Inf. Syst. Eng. 62, 455–461.

Wolpert, D.M., Diedrichsen, J., Flanagan, J.R., 2011. Principles of sensorimotor learning. Nat. Rev. Neurosci. 12. https://doi.org/10.1038/nrn3112

Wolpert, D.M., Ghahramani, Z., Jordan, M.I., 1995. An Internal Model for Sensorimotor Integration. Science (80-.). 29, 1880–1882.

Wright, G.W., 2014. Using virtual reality to augment perception, enhance sensorimotor adaptation, and change our minds. Front. Syst. Neurosci. https://doi.org/10.3389/fnsys.2014.00056

Wright, W.G., 2013. Using virtual reality to induce cross-axis adaptation of postural control: Implications for rehabilitation, in: 2013 International Conference on Virtual Rehabilitation. pp. 289–294. https://doi.org/10.1109/ICVR.2013.6662095

Wurtz, R.H., 1996. Vision for the Control of Movement. Invest. Ophthalmol. Vis. Sci. 37, 2131–2145.

Zuckerman, J.D., Gallagher, M.A., Lehman, C., Kraushaar, B.S., Choueka, J., 1999. Normal shouluder proprioception and effect of lidocaine injection. J. shoulder Elb. Surg. 8, 11–16.